Thermal monitoring for the control of packed bed adsorption chromatography

Yang, Mengyan

Award date:
1993

Awarding institution:
University of Bath

THERMAL MONITORING FOR THE CONTROL OF PACKED BED ADSORPTION CHROMATOGRAPHY

Submitted by Mengyan Yang

for the degree of PhD

of the University of Bath

1993

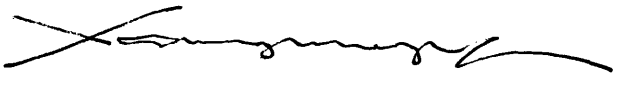

ProQuest LLC
789 East Eisenhower Parkway
P.O. Box 1346
Ann Arbor, MI 48106-1346

ACKNOWLEDGEMENTS

I would like to thank my supervisor Dr. John Hubble for his professional advice, support, and kind encouragement. My thanks are extended to both Dr. Richard Rathbone and Mr. A.D. Lockett for their useful advice and support.

My thanks are also due to the Chemical Engineering School as a whole for providing a warm environment in which to work, and its technical staff in particular for their efficient help. Also Dr. Fang Ming's helpful discussion is acknowledged.

Finally, the generous financial support provided by the SERC (grant No. GR/F71294) is gratefully acknowledged.

ABSTRACT

This thesis describes a detection technique for use in monitoring and control of packed bed adsorption chromatography. This technique is based on following temperature changes resulting from heats of adsorption. Although a similar approach has been previously described for use with pressure swing adsorption (PSA) systems, the small magnitude of thermal changes encountered in liquid based separations generates significantly greater technical problems which have inhibited similar development in this area. To overcome these problems a thermal sensing system comprising a series of thermistors placed in a packed bed was developed. Results for the ion exchange based adsorption of aspartic acid are presented and show that thermal monitoring can be successfully applied to liquid based adsorption processes, offering a practical alternative to existing methods of column monitoring.

Thermal responses to aspartic acid uptake on both beaded and perfusive DEAE based resins were investigated. The results show that the thermal response coincides with the adsorption front, such that the saturation front in the column can be inferred from the thermal response profile. A linear correlation in terms of elution volume and the sensor position was proposed to predict the occurrence of the breakthrough.

To understand the relationship between thermal response and adsorption saturation, a theoretical model of heat and mass transfer in a packed bed was developed. Simulation results show that the model can efficiently describe the packed bed adsorption process used. This model provided a basis for the application of the Kalman filter technique, which allows *in situ* estimation and prediction. With a Kalman filter the concentration wave within the bed can be well traced, and in addition variations in bed capacity can be determined as the column ages.

Artificial neural network techniques were also applied to thermal monitoring systems. Trained with a limited number of samples the networks effectively recognised the functional relationship between thermal signals and the concentration profile at the bed outlet, and then were used to predict the breakthrough profile using on-line thermal signals. The neural network technique requires no detailed understanding of the adsorption process and should be applicable to any thermal monitoring system capable of providing detectable signals. A comparison between the performance of the Kalman filter and neural network is given.

CONTENTS

CHAPTER. 1 INTRODUCTION 1

1.1 Packed bed adsorption chromatography in downstream processes 1

1.2 Basic concepts and theories of adsorption chromatography 2

1.2.1 Adsorption equilibrium and kinetics 2

1.2.2 Theories of adsorption chromatography 3

1.2.3 Breakthrough curve and bed capacity 7

1.3.4 Adsorption heat 8

1.3 Process control implications 9

CHAPTER. 2 ON-LINE MONITORING AND CONTROL PROTOCOLS FOR PACKED BED ADSORPTION PROCESSES 12

2.1 Packed column chromatography cycle 12

2.2 Control of cyclic operation and related problems 15

2.2.1 Control of cyclic operation 15

2.2.2 Column capacity deterioration 17

2.2.3 Optimum control criteria 19

2.3 On-line monitoring methods for packed bed adsorption processes ... 20

2.3.1 General monitoring methods 20

2.3.2 Biosensors 22

2.3.3 Liquid chromatography 23

2.3.4 On-line thermal monitoring methods 24

2.4 On-line thermal monitoring and control protocols for packed bed adsorption processes 24

2.4.1 Application of thermal monitoring in packed bed processes 24

2.4.2 Feasibility of thermal monitoring of packed bed liquid adsorption chromatography 25

CHAPTER.3 STATE ESTIMATION TECHNIQUES 27

3.1 General on-line state estimation problems 27

3.1.1 Basic considerations 27

3.1.2 General state estimation problem 28

3.2 Kalman filter approach 29

3.2.1 Brief historical perspective 29

3.2.2 Kalman filter theory 30

3.2.3 Application of Kalman filters in chemical engineering processes . 35

3.3 Artificial neural network (ANN) approach to state estimation 38

3.3.1 Difficulties in process modelling 38

3.3.2 Concept of artificial neural networks 39

3.3.3 Brief historical perspective 40

3.3.4 Application of ANNs in chemical and biochemical processes ... 41

3.3.5 Feedforward neural networks 44

3.3.6 Network training- Backpropagation learning topology 47

CHAPTER. 4 EXPERIMENTAL RIG DESIGN AND PERFORMANCE CHARACTERISTICS 54

4.1 Thermal sensors 54

4.1.1 Essential properties of thermal sensors used for process monitoring 54

4.1.2 Thermal and electrical properties of semi-conductor thermistors 55

4.1.3 Thermistor circuit and its output characteristic 57

4.2 Experimental rig design 59

4.2.1 System outline and devices 59

4.2.2 Column installation 61

4.2.3 Reference thermistors- external and internal references 62

4.2.4 Wheatstone bridge 64

4.2.5 Automatic data collection and processing system 64

4.3 Base line stability 66

4.3.1 Base line noise characteristics 66

4.3.2 Effect of temperature fluctuations of the water bath 67

4.3.3 Effect of feed flow rate 69

4.3.4 Effect of thermistor thermal characteristics 71

4.3.5 Effect of the excitation voltage 72

4.3.6 Comparison of base line performances between the external and "in-bed" reference system 73

4.3.7 Other effects 74

4.4 Selection of thermistors 74

4.4.1 Stability to flow rate change 74

4.4.2 Long term stability of thermistor insulation 75

4.4.3 Selection criteria 76

CHAPTER. 5 EXPERIMENTAL AND THEORETICAL INVESTIGATION OF THERMAL MONITORING ADSORPTION CHROMATOGRAPHY 78

5.1 Selection of adsorption systems 78

5.2 Materials, column packing, and concentration monitoring techniques 79

5.3 Measurement of adsorption parameters 81

5.4 Experiment methods 85

5.4.1 Point heat source tests 85

5.4.2 Thermal monitoring adsorption experiments 85

5.5 Theory of heat transfer in packed beds 89

5.5.1 General considerations 89

5.5.2 Heat transfer in packed beds with liquid flow 90

5.5.3 Mathematical description of the adsorption process 92

5.5.4 Overall heat conductivity and heat transfer coefficient 95

5.5.5 Estimation of the heat of adsorption 96

5.6 Thermal responses in packed beds- results 97

5.6.1 Temperature profiles in point heat source tests 98

5.6.2 Thermal responses to aspartic acid uptake on ion exchangers ... 99

5.6.3 Protein adsorption systems 105

5.6.4 Adsorption heat 106

5.6.5 Comparison of performances between in-bed and external reference systems 107

5.7 Influences of operational conditions 107

5.7.1 Operational temperature 107

5.7.2 Flow rate and feed concentration 108

5.7.3 Buffer 110

5.8 Relationship between thermal responses and the adsorption front ... 111

5.8.1 Coincidence of thermal response and adsorption front movement 111

5.8.2 A linear correlation for elution volume ratio 113

5.9 Comparison of experimental results with the theory 115

5.9.1 Parameter determination 115

5.9.2 Simulation results 115

5.10 Prediction of breakthrough and optimization of thermistor position 119

5.10.1 Breakthrough prediction 119

5.10.2 Optimization of thermistor position 120

5.11 The main factors on which the feasibility of the method depends ... 121

CHAPTER. 6 ON-LINE BREAKTHROUGH ESTIMATION USING THERMAL MEASUREMENT- APPLICATION OF KALMAN FILTERS 122

6.1 Two key problems in application of EKFs for state estimation 122

6.2 State space model for the thermal monitoring packed bed adsorption system 123

6.2.1 Simplified six stage heat and mass transfer model with fixed parameters 123

6.2.2 Extended state space model for the EKF 126

6.2.3 Measurement formulation 128

6.3 Formulation of the EKF 129

6.4 Simulation studies using fixed parameters 130

6.5 Real time estimation of state variables and parameters 134

6.5.1 State estimation using the EKF with known parameters 134

6.5.2 State estimation using the EKF with unknown parameters 137

6.5.3 Estimation under unthermostatted condition 139

6.5.4 Estimation when a mixed feed solution is used 140

6.6 The problem of model mismatch 141

6.7 Error covariance matrix 143

CHAPTER. 7 ON-LINE BREAKTHROUGH ESTIMATION AND PREDICTION USING THERMAL SIGNALS- APPLICATION OF NEURAL NETWORKS 144

7.1 Basic considerations 144

7.2 Use of networks for breakthrough estimation 145

7.2.1 Input and target vectors and the network structure 145

7.2.2 Sample sets for network training 146

7.2.3 Training convergency and the network performance 148

7.2.4 Comparison of the network estimation with the experimental

measurements 152

7.2.5 Use of a network to capture the system dynamic behaviour 154

7.2.6 Real time use of the trained network 156

7.3 Long term prediction of the breakthrough using dynamic networks .. 157

7.3.1 Network approach to long term prediction 157

7.3.2 Training sample set assembly 158

7.3.3 Training fits 160

7.3.4 Tests of network predictions 162

CHAPTER. 8 DISCUSSION AND CONCLUSION 165

8.1 Feasibility of the thermal monitoring method 165

8.2 Choice of reference sensors 166

8.3 Advantage and limitation of the EKF approach 167

8.3.1 Comparison with the empirical correlation approach 167

8.3.2 Potential for use in process optimisation 168

8.3.3 More understanding of the system and the process 168

8.3.4 Limitation of the EKF approach 169

8.4 Artificial neural networks- a robust approach to state estimation and prediction problems 170

8.4.1 Robust approach to state estimation 170

8.4.2 Comparison with Kalman filter 171

8.5 Conclusion 172

8.5.1 A generic and simple approach to packed bed process monitoring 172

8.5.2 The model based technique enhanced thermal monitoring and control approach 173

NOTATION 176

REFERENCES 178

APPENDIX 192

1 The correlation between concentration and UV absorbence 192

2. **Programs used in this thesis** 192

"heat transfer" 192

"sub-stage model 195

"sub-diffusion" 196

"multlog" 196

"neural net" 204

3. **Publications and presentations of the results contained in this thesis** .. 207

Publications 207

Presentations 207

CHAPTER. 1 INTRODUCTION

1.1 Packed bed adsorption chromatography in downstream processes

There are five main types of liquid chromatography: ion-exchange, affinity, gel filtration, hydrophobic interaction, and reverse-phase. Adsorption based chromatography techniques are of particular importance in the downstream processing of biological materials, as they offer the potential for both selective recovery and significant concentration in a single process step. At present ion exchange and affinity adsorption chromatography are the most commonly used.

Ion-exchange chromatography separates molecules according to electrical charge difference, and usually uses an aqueous solution as its mobile phase. Compared with other methods, such as solvent extraction, in which some organic solvents may be used, ion-exchange chromatography offers the advantages of operation simplicity and reduced chemical hazards. This makes it well suited for separation processing of biological products. The widespread use of ion-exchange chromatography has been highlighted in a study of published purification protocols which found that ion-exchangers were used in 75% of all purifications (Bonnerjea *et al.* 1986). The importance of this technique is also highlighted by the growing demand for biological materials worldwide. Amino acids, which are mainly produced by means of fermentation, and are commonly recovered using ion-exchange chromatography, represent a significant and increasing market. For

example, the worldwide annual output of gluconic acid had already reached 50000 tonnes by the 1980's (Milsom and Meers, 1985).

Affinity chromatography separates substances by means of selective adsorption which is based on a specific affinity between the ligand and substrate. Affinity chromatography, unlike ion-exchange which can be traced back many years (Helfferich, 1986), is a recently developed separation technique. It was introduced by Campbell *et al* in 1951, and was not widely applied until the late 1960's (Cuatrecasas *et al.* 1969). Because of its high selectivity, affinity separation can result in very high degree of purification being achieved in a single step process, and has been increasingly applied to downstream processing of high value biochemical products.

1.2 Basic concepts and theories of adsorption chromatography

1.2.1 Adsorption equilibrium and kinetics

Compared with the theory of adsorption of gases on solid surfaces, the theory describing adsorption from solution is much less developed. Theoretical models for the adsorption of gases on solid surfaces are often cited to describe adsorption phenomena in liquid-solid systems even though the parameters may lose some of their physical meaning. The equation to describe the adsorption interaction can be written as:

$$\frac{dq}{dt} = k_1 C(q_{max} - q) - k_2 q \qquad (1\text{-}1)$$

where q_{max} is the maximum resin capacity, k_1 and k_2, adsorption and desorption constant, C and q, adsorbate concentration in mobile and immobile phase. The net adsorption rate becomes equal to zero when adsorption equilibrium is established, and the following Langmuir isotherm is obtained

$$q = \frac{q_{max} C}{\frac{k_2}{k_1} + C} \qquad (1\text{-}2)$$

Eq. 1-2 can be used to calculate q_{max}, and the dissociation constant, $K_d = k_2/k_1$ from experimental isotherm data.

It should be noted that equation. Eq. 1-2 was initially developed for the description of the single step kinetics of surface adsorption, however it is commonly used to describe the overall rate of adsorption.

1.2.2 Theories of adsorption chromatography

Packed bed chromatography can be described as a distributed parameter process, in which concentration is a function of both time and position. Theories have been developed to describe column performance, and a comprehensive review can be found in Yang and Tsao (1982). The theories can be divided into two categories namely, the plate and the rate theories. These are briefly discussed below.

Plate theory

Plate theory was first introduced by Martin and Synge (1941) as the equilibrium stage model, which was later refined by Said (1956). This model depicts the column as a succession of well mixed equilibrium stages. By assuming that equilibrium is always attained between the two phases in each stage the process can be treated as a series of ideally mixed flow contactors. Assuming a linear isotherm, the material balance equations obtained can be solved analytically, which results in a pulse with a Poisson distribution moving along the column if the sample injected is of very small size.

The plate theory has proved useful in the analysis of zone migration, spreading, and resolution in elution development. It can also be applied to model the adsorption front breakthrough. The most obvious shortcoming of this original plate theory is its inability to predict the number of stages or effective plate height, and the failure to provide information as how a change in operating conditions will affect the column performance consequently. The number of stages must be experimentally determined before any calculation can be made and the optimum operating condition can only be found by trial and error (Yang and Tsao, 1982).

Rate theories

The rate theories comprise a series of mass balance equations together with appropriate boundary and initial conditions. Based on the continuous flow of carrier fluid through the column, finite rates of mass transfer, and a certain

isotherm or adsorption kinetics, the equation of mass balance in the mobile phase can thus be formulated as:

$$\frac{\partial C}{\partial t} = D_x \frac{\partial^2 C}{\partial x^2} - v\frac{\partial C}{\partial x} - R \qquad (1\text{-}3)$$

where D_x is the axial dispersion coefficient, v is the linear flow velocity, R is the rate of interface mass transfer and x and t are the space and time coordinates respectively.

The rate theories have long been studied, and a number of models have been developed. The diversity of the models in the literature stems from the variation in the rate equations for interface mass transfer, *ie.* in the formation of the term, R in Eq.1-3.

The mechanism of adsorbate uptake consists of transport through the liquid film surrounding the adsorbent particles, diffusion within particle pores and the surface adsorption itself. Therefore the overall rate may be controlled by one or a combination of the steps. If the surface adsorption rate is slow compared to the mass transfer rate, so that the concentration is the same inside and outside the particles, then the overall rate equation will take the form of Eq. 1-1. If the film diffusion is a rate controlling step, the concentration inside the particles will be constant, and the overall rate equation becomes:

$$R = k_f a (C - C_i) \qquad (1\text{-}4)$$

where k_f is the film diffusion coefficient, a is the interface area per unit interstitial void volume of the bed, and C_i is the concentration inside the particles. In most practical cases the overall rate is often controlled by the pore diffusion step, and the rate equation in these cases will be discussed later.

Simplified and empirical rate equations

The rate theory models are mathematically rigorous, however they are often too difficult to be solved analytically or even numerically. These mathematical difficulties result from the complexity and non-linearity of the term, R. Therefore a wide range of simplified, empirical rate equations have been proposed, a typical example takes the form of Eq.1-1, which has been widely used (Liapis,1989; Chase, 1984; Cowan, 1986). This empirical rate equation is derived by treating the adsorption process as a chemical reaction and using the mass reaction law. It should be noted that parameters in such an equation are not actually constant and their physical significance has little in common with those of a true chemical reaction.

Hubble (1989) proposed a simple discrete stage model, considering each stage as a well-mixed tank with adsorption proceeding for resident time of the fluid in the stage. Although this model is essentially a plate model, dividing the column into a series of stages, it eliminates the need for an equilibrium assumption by using a simplified rate equation in the same form of Eq.1-1 to describe the adsorption

process. Concentrations in each stage in both mobile and immobile phases can by analytically calculated at each time step. This greatly reduces the computing effort.

1.2.3 Breakthrough curve and bed capacity

During loading of a packed bed the adsorbate uptake will take place until the whole bed is in equilibrium with the input solution, consequently the level of adsorbate in the bed output will rise from initially zero until it is equal to the concentration of the input. A plot of the level of adsorbate in the bed output against the loading time is the so-called breakthrough curve, which will usually have the form shown in Fig. 1-1.

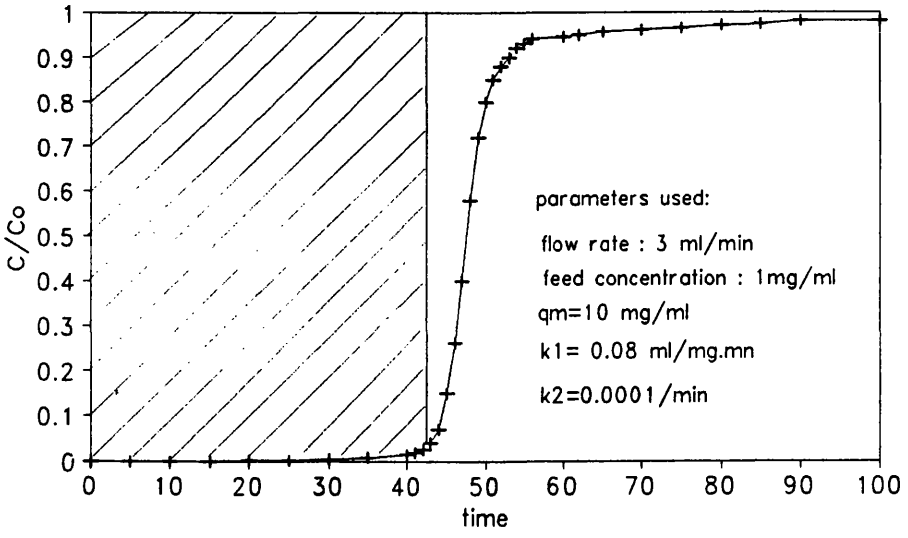

Fig.1-1 Breakthrough curve

simulated using the stage model which is described in Chapter. 5

For any loading breakthrough curve it is possible to calculate the total amount of adsorbate uptake, *ie.* saturation or total bed capacity, q_t (Slater, 1991). In practice loading a bed is often terminated at a time when the breakthrough concentration reaches a specified value. The amount of adsorbate uptake at this time gives the operating bed capacity, q_{op}, which can be represented by the shaded area in Fig.1-1. Clearly any factors which affect the shape of a breakthrough curve have an effect on the operating bed capacity. q_{op} is largely dependent on the resin characteristics such as the maximum. resin capacity, $q_{max.}$, as well as operational conditions, such as feed concentration and flow rate (Samuelson, 1963).

1.2.4 Adsorption heat

Small heat evolutions are usually observed when ion-exchange occurs, and standard enthalpy changes are of the order of 4-10 kJ/mole (Helfferich, 1962). Groszek (1988) studied heats of adsorption of NaCl and $CaCl_2$ onto Amberlite using a flow microcalorimeter. He reported the heats of adsorption in such systems to be in the range 4.2-23.7 J/g. However, ion-exchange may be followed by other process with considerable enthalpy changes. Cation exchange of a resin in H^+ form with a base such as NaOH is a typical example. In this case ion-exchange is followed by a neutralization of H^+ and OH^- with a considerable heat liberation (57.2 kJ/mole). In affinity adsorption systems enzymes with their corresponding ligands show values of the order of 40 kJ/mole. It is these thermal effects of adsorption processes that provide a basis for the development of an *in situ* technique for monitoring of the process performance.

1.3 Process control implications

Given the high value of many of the new generation of biochemical products, optimisation of adsorption chromatography in terms of fractional product recovery becomes extremely important. In practice, one of the major problems is predicting when a desirable operating capacity will be reached, so that excess adsorbate is not lost during loading and washing stages, and optimum separation performance is achieved. To solve this performance optimization problem two parallel approaches *ie.* model prediction and process monitoring have been investigated.

Model based prediction and its limitation

Although most reported theoretical studies have been aimed at improving our understanding of chromatographic processes (Slater, 1991), a few have contributed to performance prediction. Tsou and Graham (1985) applied a two-film model to predict BSA breakthrough in a DEAE Sephadex packed bed. With the information obtained in small column experiments Cowan *et al.* (1986) used the FACSIMILE code to solve a set of differential equations to predict the performance of column separation of aspartic acid using Duolite A162 anion exchanger.

In spite of a number of reports on the good performance obtained using such model based approaches, their application is largely restricted to specific systems under very limited conditions. This problem has been discussed by Chase (1986) who concludes that, although modelling of column performance can form the

basis for a prediction of adsorbate breakthrough, experimental variations and decline of adsorbent capacity with repeated use limit the accuracy of this approach. Ideally, on-line sensors are required to produce a continuous reading of the product level.

In situ or off line sensing

Many sensor programmes have been developed which detect the breakthrough using on-line or off-line detectors and in bioprocessing application of these detectors can be quite complex. However, specific sensors are difficult to use where multicomponent adsorption is occuring. For example the specific enzyme based sensors, which are sometimes used to detect complex molecules, are sensitive to contamination and thermal degradation, and may give an unpredictably false reading as a result of un-monitored deterioration. Ideally what is needed is a more generally applicable technique which is robust, cheap, and which can follow the extent of adsorption at positions within the bed.

Incorporation of in situ sensing with state estimation techniques

In this thesis, after a brief review of monitoring and control techniques, the use of a thermal monitoring systems is considered for the control of packed bed adsorption chromatography, and an automatic thermal monitoring chromatography system, together with state estimation and prediction *ie.* the Kalman filter and neural network techniques is described. Thermal sensors, which are generic, cheap and reliable, provide *in situ* information to a state estimator, which is operated in parallel with the adsorption chromatography system. With

such *in situ* information the state estimator tunes itself to trace the adsorption process and produce key signals for control.

CHAPTER. 2 ON-LINE MONITORING AND CONTROL PROTOCOLS FOR PACKED BED ADSORPTION PROCESSES

2.1 Packed column chromatography cycle

Packed bed adsorptive separations, including those which are ion-exchange or affinity based, are normally carried out repetitively in a cyclic manner, with each cycle consisting of a adsorption or loading stage, followed by a wash, elution and finally regeneration stage prior to next cycle. A brief discussion of each stage is given below.

Adsorption (loading) stage

Initially the adsorbent, resin, is contacted with a multi-component crude mixture, and during this adsorption stage only the components for which the resin is selective will be bound to the resin. The output of the bed will initially contain no adsorbate but as the bed capacity becomes progressively saturated, the level of adsorbate in the output will rise until it is equal to that at the inlet. This response gives the so-called breakthrough curve. Once the outlet concentration reaches the input value the resin will be at equilibrium with the input stream and no further binding will occur. In practice loading of the bed is unlikely to be continued until full breakthrough occurs, but stopped at a preset extent. Therefore the position and shape of a breakthrough curve will strongly determine the performance of a packed column. This can be demonstrated by Fig. 2-1, in which the shaded areas represent the loading amounts for different performances

respectively. Clearly, overloading the bed due to incorrect control may result in considerably loss of valuable products.

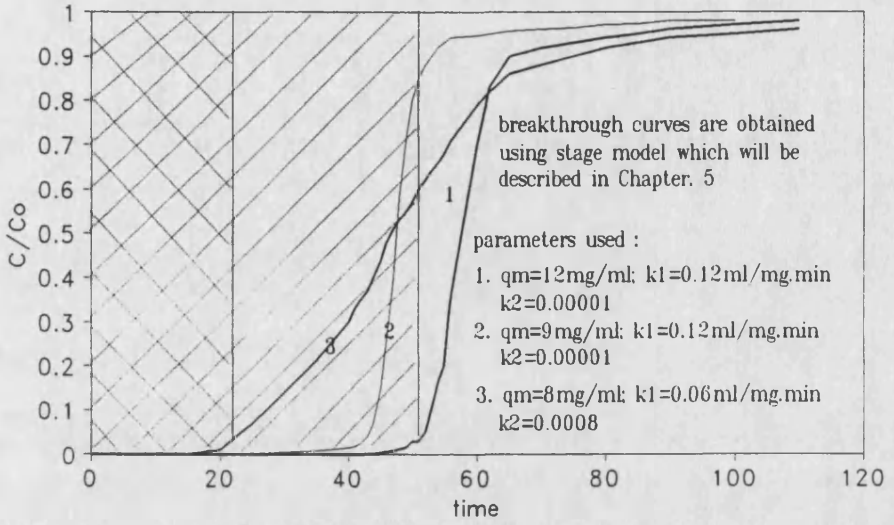

Fig. 2-1 The effect of the shape and position of breakthrough curves on column performance

Washing stage

The resin is washed immediately after the loading stage to remove unbound contaminants. Washing is achieved by passing buffer through the bed until the level of contaminants in the outlet has fallen below a predetermined level. Contaminants present in both mobile and fixed phases must be removed during this stage. To remove the contaminants which are not adsorbed, but present within the void of the bed or diffused into the pores, a maximum of three bed volume wash will be required according to Arnold *et al.* (1985). Whilst to remove contaminants which are non-specifically bound to the resin, up to eight bed

volumes may be required (Arve and Liapis, 1978). It is recognised (Graves and Wu. 1979; Wankat, 1974; Chase, 1984) that the washing procedure may cause valuable products to be lost. The extent of product loss depends on the dissociation constant. For a system with a dissociation constant of less then 10^{-5} M the product loss during the washing stage will be negligible. Above this value the product loss is likely to be significant (Graves and Wu, 1974).

Elution stage

Ideally, the adsorbate should be eluted at high concentration in a small volume of solution. For an ion-exchange system the selectively adsorbed product is removed from the resin during the elution stage by adjustment of either the pH or ionic strength of the buffer, and eluting until no further products are released. For an affinity system, the elution requires the complete dissociation of the adsorbate-adsorbent complex. The elution can be carried out by ligand competition, *ie.* using free ligands in the buffer to compete with those in the support resin for binding to the adsorbate. If the soluble ligand is in vast excess, the adsorbate will partition exclusively into the mobile phase which is then separated from the adsorbent. However, this method can sometimes prove expensive and usually time consuming. Another approach is co-substrate elution, using a biospecific eluent to substitute the bound substrate. Other elution methods including ionic strength alteration, solvent changes, temperature changes, buffer and pH changes, chaotropic reagents, and electrophoretic elution, are also used. A detailed description of the practical applications of these techniques is given in Dean *et al.* (1985)

Regeneration and re-equilibrium stage

As a column is operated in a repetitive manner, a slow build up of contamination may occur. This may result in the loss of adsorption capacity, and even column blockage. To prevent this build-up, column regeneration is necessary. Washing with a high salt concentration buffer is often used to remove weakly bound contaminants, and high concentrations of NaOH can be used to remove more strongly bound contaminants. After regeneration the resin is re-equilibrated with an appropriate buffer, and is ready for a further cycle of operation. Despite the effort of regeneration contaminant build-up is inevitable during long term repeated use, and column capacity will eventually be inevitably reduced.

2.2 Control of packed bed chromatography and related problems

2.2.1 Control of the cyclic operation

The effective control of packed column separations requires the accurate determination of the appropriate duration for each stage. This is accomplished by manual or automatic switching of a set of multi-way valves to regulate the application of liquid streams to the bed (feed streams, eluents, regenerants, re-equilibrants, *etc.*) and the collection of liquid from the bed (product, waste, unabsorbed material).

Anderson *et al.*, (1975) described a program-controlled affinity chromatography system which was a typical example of an early developed automatic control system. In their approach, valve switching actions were programmed by

mechanical resetable clocks and cam-operating units. The input stream volume was controlled by programming the length of the loading stage duration which was achieved through a rotary timer driven by either a one or two hour clock. Other stage durations were controlled in the same manner. The timer adjustments are made during the first few cycles. Monitoring of the product level was carried out by fixed wavelength detectors. It should be noted that the information obtained by the monitor was not directly used to trigger the timers. In later systems the clock driven timers were replaced by micro processors (Eveleigh, 1982). These systems were easy to operate and could produce consistent results, however they required a constant input concentration, a criterion which may not be met in some applications. The conditions pertaining during extended, repeated use of a separation would not always be invariant. Under such circumstances the use of a constant time period for the adsorption stage in each cycle could result in under or over-utilisation of the available bed capacity. Clearly, a high degree of flexibility in sequence control is desirable.

Chase (1984) described a microcomputer based system for adsorption control. The system received analogue information from monitoring instruments, such as spectrophotometers and pH meters, and used this information to determine the duration of various sequences. Durations of some stages were not difficult to determine. The washing stage, for example, could be continued until the level of contaminants, as detected by monitoring the optical density of the output stream, fell below a preset value. Information obtained by monitoring pH and ionic strength could be easily used to control the duration of a simple re-equilibration

or regeneration step. Control of the duration of the elution stage was not difficult as the product was the only component present by this stage. However monitoring the level of a particular component in fluid streams for control of the duration of the loading procedure was not so straightforward because of the presence of additional components, often in vast excess, to the product.

2.2.2 Column capacity deterioration

The adsorption performance of a packed column is highly dependent on the column adsorption capacity. Under repeated use a packed column will gradually lose its adsorption capacity. There are a number of factors which can lead to column deterioration:

a) Incomplete elution of adsorbate during each cycle of operation causes loss of bed capacity (Eveleigh and Levy, 1977). Also the slow build-up of non-specifically bound contaminants that are neither removed during washing nor regeneration stages will eventually give rise to loss of capacity.

b) Loss of active sites in the resin resulting in a reduction of the bed capacity. Leakage of affinity ligands from the resin may cause significant loss of bed capacity.

c) Changes in the mechanical or chemical properties of the resin may significantly affect the practical performance of the bed. For example a decrease in mechanical stability can result in compaction of compressible resin beads, thus resulting in a decrease in flow rate through the bed.

In any assessment of performance, neglecting the column deterioration will lead to inappropriate operation, resulting in overloading of the bed and hence loss of potentially valuable products. The effect of a continuous loss of a small percentage of the bed capacity with each cycle of operation is shown in Fig. 2-2. If the loading of the bed is stopped at a time, A, which is considerably before the initial capacity of the bed is totally saturated, the column process can be operated for many cycles without any noticeable affect on the adsorption performance. If loading is terminated at a time, B, nearer the position of exhaustion of the initial capacity, the adsorption performance would be seen to deteriorate with usage, and the amount of the adsorbate passing through the bed without being adsorbed will increase. The former situation is merely inefficient, prolonging the necessary overall processing time, whereas the later situation may well give rise to actual loss of product or the need to recycle product containing column effluent.

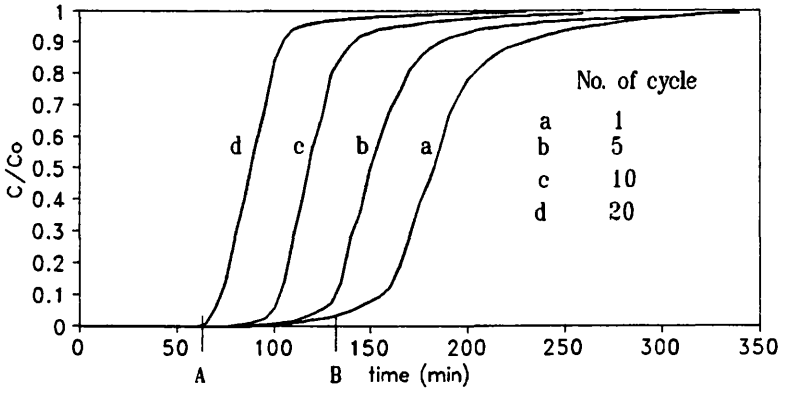

Fig.2-2 Reduction of packed bedperformance with the number of repeated cycles of operation

A 2% loss of the bed capacity is assumed to occur per cycle
The simulation was carried out using the stage model which is described in Chapter. 5

In order to use the column more efficiently Chase (1986) proposed a control approach in which model simulation plays a central role. Results from simulation studies, together with off-line assay information about the input stream, enables the duration and/or flow rate of the critical loading phase to be determined. In a similar manner, provided the bed capacity deterioration is known as a function of time or cycle number from previous experience, appropriate changes can be made in advance to the durations of the different stages of the separation protocol. Although the above method may be satisfactory in some situations, it is not suited for total automated, unattended operation. In this case he suggested that a more efficient mode of operation could be achieved by using an interactive form of control in which the performance of the bed is monitored during the run by analyzing the concentrations of adsorbate in the bed outlet and inlet streams. The information of adsorbate breakthrough obtained on-line would enable the duration of the loading stage to be efficiently regulated.

2.2.3 Optimum Control criteria

The control criteria are determined by a number of factors including product, operation, and resin costs. Maximum product purity (Chase, 1984) is, of course, an important criterion for control. If the product is of high value, minimisation of product loss will be also a criterion. Other criteria could be maximum use of bed capacity, or maximum process throughput. The optimum control is aimed at an appropriate compromise between these criteria which leads to the most

profitable operating conditions.

It is understood that the loading stage in each cycle is critical for separation performance. Loading a bed until close to breakthrough, which is a typical operating procedure, allows the bed capacity to be fully utilized. While a partial loading strategy proposed by Dantigny *et al.* (1991) offers the advantage of potential optimisation of the process with respect to a number of different criteria. The idea of the partial loading approach is that by stoping adsorption before all capacity is saturated, unbound product and also material removed in the upper region of the column during the washing stage can be reabsorbed in the lower regions of the column, so that product loss can be minimised. For effective implementation this strategy requires the determination of the position of the saturation front within the column. This highlights the need for continuous, *in situ* monitoring techniques.

To summarise, it is highly desirable that the movement of adsorption front within the bed is comprehensively monitored on-line to allow compensation for changes in bed capacity.

2.3 On-line monitoring methods for packed bed adsorption processes

2.3.1 General monitoring methods

Traditionally, chemical process monitoring is performed by measurements of physical and/or chemical characteristics such as temperature, pH, optical

absorbence, or electric conductance. Many techniques have been developed for chemical process monitoring, including optical, chemical or electrochemical, chromatographic, thermal, dielectric, and conductive. A comprehensive review of measurement techniques is beyond the scope of this thesis, but a brief summary of the measurement methods, which are applicable to chemical processes, is outlined below.

Optical devices, such as UV and IR spectrophotometers, are widely used in chemical process monitoring, because they do not consume or contaminate samples, and they are easily installed for on-line use. UV detectors are often used to monitor the product level in the column outlet streams (Chase, 1986). They are, however sensitive to contaminant substances present at even ppm levels. Specific chemical analysis can be used, but this is usually both sample and time consuming, and is difficult to use on-line. Electrochemical techniques, such as ion selective electrodes (Albery, *et al.* 1986, Boitieux *et al* 1979, 1981) are specific to their target substances. They offer high sensitivity and selectivity to some specific substance, but this may limit their generic application. Dielectric and conductive techniques have been recently applied to this field and are generic for any substances which make a contribution to the dielectric constant or conductance of systems (Kell, 1987). Dielectric and conductive instruments are commercially available, and have been applied to biomass monitoring (Markx, *et al.* 1991). Dielectric and conductometric measurement is often considered to be relatively non-specific, and the measured data is not always easily interpreted, because it results from the contributions of all substances present in the system.

2.3.2 Biosensors

In the last two decades the development of enzyme immobilization techniques has led to the development of bioanalytical devices in which the sensing enzymes are placed in close proximity to the actual measuring component, the transducer. A number of examples of such a combination of enzyme and transducer have been reported, in particular, the concepts of enzyme electrodes and enzyme thermistors (Guilbault, 1976). Enzyme thermistor devices (Mosbach *et al.*, 1981, Mosbach, 1991) are, in principle, microcalorimeters, with which the thermal effects of enzyme catalyzed reaction can be registered. These devices are usually based on highly sophisticated heat calibration and temperature control units and have been reported to be sensitive to changes of the order of $1x10^{-3}$°C (Danielsson and Mosbach 1988). Because of the enzyme catalysis feature, enzyme thermistors are highly sensitive and specific to a particular substrate. This high specificity, which makes them attractive, however limits the application of any individual enzyme sensor to a limited range of compounds. Mandenius and Danielsson (1988) reported an approach to monitoring and control of sucrose hydrolysis using enzyme thermistors, in which they had to use two thermistor devices to monitor the levels of sucrose and glucose respectively.

Another significant limitation to on-line use of enzyme thermistors is that enzymes are sensitive to bio-contaminants. If used on-line, the sensor device must allow automatic treatment of samples. This is a serious problem (Enfors and Cleland, 1988) which remains largely unsolved, and make it difficult to use enzyme thermistors in continuous flow-through conditions.

2.2.3 Liquid chromatography

Automatic liquid chromatography is a powerful analytical and separation technique, and is widely used in process monitoring. Chase (1986) described an on-line approach for use in column breakthrough monitoring. A small scale automatic liquid chromatography system was used to analyze protein samples which were repeatedly sampled from the column exit stream. In this automatic chromatography system, the proteins were resolved by a rapid chromatographic process and the peak of optical absorbency at 280 nm in the chromatogram, corresponding to the protein of interest, is identified. This peak was then integrated to find its area and, using previous calibration data, the amount of that protein in the sampled volume could be determined.

A possible disadvantage of this approach is that information on the level of the particular protein is only updated intermittently after every analysis cycle of the chromatograph, thus a monitoring time lag is inevitable. The time lag, normally a few minutes, may be very short compared to the duration of individual stages employed in packed bed affinity separations. However, this delay could be critical in the control of ion-exchange separations where high flow rates may be applicable (Fang *et al*, 1991.).

Another possible problem is that rapid chromatographic separation might not always be able to resolve the component of interest in the presence of contaminants.

2.3.4 On-line thermal monitoring methods

Thermal techniques have been developed by several industrial groups, and by instrumentation groups for calorimetric or thermal sensor devices (Litz, 1983, 1987; Regenass, 1985; Schnelle, *et al.* 1986; Wu, 1985). With these devices temperature changes or heat production, which are often an accompanying phenomenon of a chemical process, can be easily registered continuously on-line, and thus the process can be monitored. Practical applications of thermal monitoring techniques reported in the literature are mainly in the field of batch reaction systems. Thermal sensors, such as thermocouple and thermistors are usually simple to use and generic in measurement. In general thermal measurements offer the advantage of high sensitivity, rapid response, and high reliability. Although thermal monitoring is non-specific to a particular reaction process, the specificity arises from the choice of catalysts in chemical reaction processes, or the choice of the packed materials and the operational conditions in adsorption processes. For example, in ion-exchange adsorption processes selective adsorption of a particular kind of amino acid in the feed can be achieved by the appropriate choice of the resin and the pH value. Therefore thermal monitoring, if used, would be specific to such an amino acid adsorption process.

2.4 On-line thermal monitoring for the control of packed bed adsorption process

2.4.1 Application of thermal monitoring in packed bed process

Despite widespread application of thermal monitoring in chemical processes, there are very few reports dealing with this application in packed bed processes.

Matz and Knaebel (1987) described an approach of temperature front sensing for feed step control in a pressure swing adsorption (PSA) process which was used for gas separation. They used simple instruments, *e.g.*, thermocouples to sense the temperature change resulting from the heat of adsorption at a series of sections within a column packed with active carbon. In their case the temperature changes observed were reported to be in the range of 5-45°C. Analysis of the progression of thermal profiles, which were related to the concentration profiles, provided a means for controlling the duration of steps in a pressure swing adsorption cycle. They declared that deactivation of adsorbent caused by impurities in the bed could be accounted for by thermal sensing, as the amount of heat of adsorption on a deactivated bed was relatively small. Accordingly, details of the feed control algorithm could be modified to adapt to such foreseeable conditions.

2.4.2 Feasibility of thermal monitoring of packed bed liquid adsorption process

A measurable thermal effect and an applicable mapping protocol for use in correlating thermal signals to concentration variables are the two factors that the thermal monitoring method rests on.

Measurable thermal response to adsorption uptake

The approach of temperature front sensing for PSA control takes advantage of the large temperature changes in the column. Such temperature changes are probably due to the relatively large heats of adsorption and low heat capacity of the bed. For liquid adsorption chromatography high voidage resins are usually

used as packing materials, and the input streams are almost always aqueous solutions, therefore the heat capacity of the bed is likely to be close to that of water. Furthermore the adsorbate concentration in input streams is usually low, for example, a raw solution with higher than 10 g/l of protein or amino acid is unlikely in any practical situation. Thus the consequent heat evolution of the adsorption process is expected to be relatively low. Whether such a small thermal effect in a packed bed is detectable or not can be assessed by comparison with that of the process in enzyme thermistor devices. Fulton *et al.* (1976) reported that urea in a solution down to 0.01 mmol/l (0.6 mg/l) could be detected by using a enzyme thermistor analyzer. The heat of urea hydrolysis catalyzed by urease was reported to be 6.6 kJ/mol (Brown, 1969). Whilst literature (Helfferich, 1962) reports suggest that the heats of adsorption for low molecular weight compounds on ion-exchange resins are of the order of $-\Delta H$, 5-10 kJ/mol. This suggests that such thermal effects can be detected by using a sensing device similar to the enzyme thermistor analyzer.

Mapping measurable thermal signals to target variables

Clearly, thermal monitoring is not a direct measurement of the variable whose value is of interest, *ie.* the adsorbate concentration in a column. However, such a target variable can be inferred or mapped from thermal measurements. A successful example has been presented by Matz and Knaebel (1987) with a PSA process. A detailed discussion will be given in the next chapter.

CHAPTER. 3 STATE ESTIMATION TECHNIQUES

3.1 The general on-line state estimation problem

3.1.1 Basic consideration

Difficulties in direct measurement of concentration variables give rise to the problem of how to achieve a reliable estimation of such variables using the available on-line measurements. In practice problems of this type are encountered in many fields of engineering, especially biochemical engineering, as it is commonly the case that the variable of interest is not directly measurable but it is observable through the measurement of other state. The simplest approach to this problem is to establish a correlation between primary process variables and the measurable secondary process variables, whilst ignoring measurement errors, noise, *etc.* More elegant methods typically use a prior knowledge in the form of mathematical process model to interpret available measurement data. Thus, more reliable information can be drawn from the process. The process model is simulated in real-time on a microcomputer, and some corrective action has to be taken in order to achieve convergence of the model and process states. This is done by feeding back the difference between the real measurement and simulated variables. Then an estimate for the real process state is provided by the model. These methods are classified as "model based" techniques, and are comprehensively reviewed by Gilles (1987). They have attracted increasing interest during the past decade, which can be seen in the recent special issue of *Chemical Engineering Science* (1992) dealing with model based techniques. This

chapter begins with an introduction to the basic features of the general estimation problem, followed by the theory of Kalman filters and a brief review of applications of Kalman filters in the field of chemical engineering. Then the neural network approach to state estimation is discussed, and a review of its application is given.

3.1.2 General state estimation problem

The state of a system can be described by the values of a set of variables x_i, called state variables (Brogan, 1991). Then the state can be represented by a m component state vector **X**, belonging to a m-dimensional vector space called state space. For simplicity a linear system is considered. The state estimation problem then can be generally stated as follows: if the m dimension state vector $\mathbf{X}(x_1, x_2,.....x_m)$ of a dynamic system satisfies the following linear equation

$$\boldsymbol{X}(n) = \boldsymbol{A}\boldsymbol{X}(n-1) + Bu(n-1) + \boldsymbol{W}(n-1) \qquad (3\text{-}1)$$

where u is a non-random input for control (not necessarily involved in all processes), and W is the random disturbance. The estimation problem is how to develop an algorithm for determining the state **X**(n) at time step n from the observation of the output **Y** (a p-dimensional vector) of the system, given that the relationship between the measurements and the state variables is as follows

$$\boldsymbol{Y}(n) = \boldsymbol{C}\boldsymbol{X}(n) + \boldsymbol{V}(n) \qquad (3\text{-}2)$$

where p is the number of measurements, usually $p<m$, and **V** is a p dimension random error vector.

Because of the error **V** in the measurement, the "true" value of **X** can never be found, but in practice an acceptable estimate may be obtained. In the presence of the random noise **W**(n) and **V**(n), the estimation problem must be understood in the sense of finding an estimate $\overline{\mathbf{X}}$ of the state **X** such that the uncertainty, or the variance , of the estimation error is minimized. The process of constructing $\overline{\mathbf{X}}$ is called filtering because it essentially requires the extracting of a signal from the background noise. A significant feature of a well designed filter is that even though the number of measurements is less than the number of state variables it is possible to estimate all the state variables provided that each state variable influences at least one measurement.

Demands on state estimation have lead to the development of model based estimation techniques and the theory of estimation. A comprehensive review of the development of model based estimation techniques will not be attempted, but can be found elsewhere (Gilles 1987). However one of the most commonly used methods, the Kalman filter, and its application in chemical engineering is briefly discussed in this section.

3.2 Kalman Filter approach

3.2.1 A brief historical perspective

Mathematicians and control engineers had previously tried to solve the estimation problem using complicated mathematical techniques, which required a huge computing capacity to solve a large set of equations. This inhibited the practical use of the real-time estimation. To overcome this difficulty, R.E. Kalman (1960) proposed a new filter. His contribution was to construct a recursive algorithm to solve the estimation problem for linear processes with independent additive Gaussian white noise on both states and outputs. The recursive algorithm of the Kalman filter greatly decreases the computational effort at each time step. Moreover by using a Kalman filter the whole state space can be reconstructed based on the noise corrupted measurements, that is, the variables which are not even directly reflected in the measurements made on the system can be estimated. These features consequently make real-time estimation a practical proposition. Since then the modern estimation and control theory has been rapidly developed and put to wide use. The Kalman filter theory has been extended to nonlinear systems (Jazwinski, 1970) to provide a sub-optimal filter with the same structure as that used for linear systems. At first Kalman filters were mainly employed in the areas of military and aerospace science, however they have increasingly received attention from chemical engineers since 1970.

3.2.2 Kalman Filter Theory

The theory of the Kalman filtering is too involved to go in detail, and can be found in a number of textbooks (Jazwinski, 1970; Bozic, 1979; Lewis, 1986), Here only a brief presentation of the theory is given below.

Firstly a linear process as described by Eqs. 3-1 and 3-2 is considered. Assuming W(n) and V(n) to be independent white noise time series with zero mean, the following equations in respect of covariance matrices for W(n) and V(n) can apply

$$cov[W(i),W(j)]=E[W(i)W^T(j)]=Q(i)\delta_{i,j},\quad i=0,1,2... \tag{3-3}$$

$$cov[V(i),V(j)]=E[V(i)V^T(j)]=R(i)\delta_{i,j},\quad i=0,1,2... \tag{3-4}$$

$$cov[w(i),V(j)]=cov[v(i),w(j)]=0 \tag{3-5}$$

where Q(i) and R(i) are mxm and pxp semi-positive determined matrix respectively. Also assuming the initial state of the system to be a random vector which is independent from W(n) and V(n), similar relationships apply

$$E[X(0)]=0 \tag{3-6}$$

$$E[X(0)X^T(0)]=P(0) \tag{3-7}$$

$$E[X(0)W^T(n)]=0 \tag{3-8}$$

$$E[X(0)V^T(0)]=0 \tag{3-9}$$

The filter design is to seek the optimal estimation of $\overline{X}$ in such a way that the error of estimation is minimised. It is normal to choose the mean error square

$$E(n)=E[(X(n)-\overline{X}(n))^T(X(n)-\overline{X}(n))] \tag{3-10}$$

as the minimisation criterion. The corrective action is taken by the following filter formula to minimise E(n).

$$\bar{X}(n)=A\bar{X}(n-1)+K(n)[Y(n)-CA\bar{X}(n-1)] \tag{3-11}$$

where $\bar{X}$(n-1) is the estimate of **X** at time n-1, and **K**(n) is the filter gain. For simplicity the system input u(n) is not considered, however the final formulation to be derived will be the same. Given the initial estimate of **X**(0), the estimate of X(n) can be iteratively obtained by using (3-11). The question left is how to determine the filter gain **K**(n) for the purpose of minimising E(n). In order to derive K(n) the error covariance matrix is defined by

$$P(n)=E[(X(n)-\bar{X}(n))(X(n)-\bar{X}(n))^T] \tag{3-12}$$

where the sum of the elements in the diagonal of the matrix is called the trace and defined as **tr**(n), and evidently **tr**(n)=E(n). The estimate error of the filter is where the sum of the elements in the diagonal of the matrix is called the trace and defined as **tr**(n), and clearly, **tr**(n)=E(n). The estimate error of the filter is

$$X(n)-\bar{X}(n)=AX(n-1)+W(n-1)-A\bar{X}(n-1)-K(n)[Y(n)-CA\bar{X}(n-1)]$$

(3-13)

Substituting (3-1) in this equation, and rearranging gives

$$X(n)-\bar{X}(n)=[I-K(n)C][A(X(n-1)-\bar{X}(n-1))+W(n-1)]-K(n)V(n)$$

(3-14)

where **I** is the identity matrix. For simplicity let the estimated error be represented by

$$Er(n)=X(n)-\overline{X}(n) \tag{3-15}$$

substituting (3-14) in (3-12), the following is obtained

$$\begin{aligned}
&P(n)=E[Er(n)Er^{T}(n)]= \\
&=[[(I-K(n)C)(AEr(n-1)+W(n-1))-K(n)V(n)] \\
&\quad [(I-K(n)C)(AEr(n-1)+W(n-1)-K(n)V(n)]^{T}]= \\
&=[I-K(n)C]AE[Er(n-1)Er^{T}(n-1)]A^{T}[I-K(n)C]^{T}+ \\
&\quad +[I-K(n)C]E[W(n-1)W^{T}(n-1)][I-K(n)C]^{T}+ \\
&\quad +K(n)E[V(n)V^{T}(n)]K^{T}(n)= \\
&=[I-K(n)C][AP(n-1)A^{T}+Q][I-K(n)C]^{T}+K(n)RK^{T}(n)
\end{aligned} \tag{3-16}$$

Introduce

$$P1(n)=AP(n-1)A^{T}+Q \tag{3-17}$$

and substituting (3-17) in (3-16), P(n) becomes

$$\begin{aligned}
&P(n)=[I-K(n)C]P1(n)[I-K(n)C]^{T}+K(n)RK^{T}(n)= \\
&=P1(n)-K(n)CP1(n)-P1(n)CK^{T}(n)+K(n)[CP1(n)C^{T}+R]K^{T}(n)
\end{aligned}$$

(3-18)

Where $CP(n)C^{T} + R$ is a non negative symmetric square matrix, therefore it can be represented by

$$S(n)S^{T}(n)=CP1(n)C^{T}+R \tag{3-19}$$

and $S^{T}(n)$ can be written as

$$S^{T}(n)=P1(n)C^{T} \tag{3-20}$$

Substituting Eqs. 3-19 and 3-20 in Eq. 3-18, P(n) becomes

$$P1(n)=P1(n)-K(n)S(n)-S^T(n)K^T(n)+K(n)S(n)S^T(n)K^T(n)=$$
$$=P1(n)+[K(n)S(n)-I][K(n)S(n)-I]^T-I \tag{3-21}$$

In order to minimise the trace of **P**(n), thus to minimize the mean square of the estimate error, the following relationship should be introduced

$$K(n)S(n)=I, \quad \textit{that is,}$$
$$K(n)=S^{-1}(n)=S^T(n)[S(n)S^T(n)]^{-1} \tag{3-22}$$

Substituting Eqs. 3-19 and 3-20 in Eq. 3-22, the iterative formula for the filter gain is obtained

$$K(n)=P1(n)C^T[CP1(n)+R]^{-1} \tag{3-23}$$

Substituting **I**=**K**(n)**S**(n)=**K**(n)**C**P1(n) in (3-21), **P**(n) becomes

$$P(n)=[I-K(n)C]P1(n) \tag{3-24}$$

Hence the all the iterative formulae (Eqs. 3-17, 3-23, and 3-24) have been obtained. Given the initial error covariance P(0), the Kalman Gain K(n) can be iteratively calculated. Fig. 3-1 shows the recursive algorithm of the Kalman filter. Because of the iterating feature of the formulae only current data of the states, K(n), P1(n), and P(n) need to be stored, so that the computing effort is not a big burden, and the state estimation can be obtained in real time. The algorithm is derived for a linear system, however it can be extended to a non-linear system by using a linearisation topology, which will be presented with the real case study later.

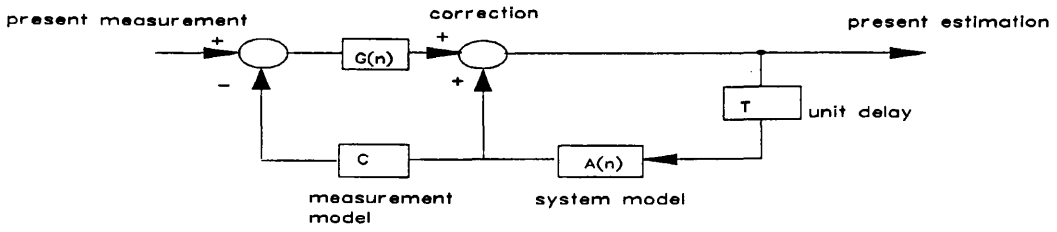

Fig. 3−1 Kalman filter estimator

3.2.3 Application of Kalman filters in chemical engineering processes

A number of reports on process applications of Kalman filters can be seen in the literature. They can be classified as two main areas, batch/semi-batch reactors and fixed bed systems.

Batch/semi-batch reactors

Lynch and Ramirez (1975) applied a Kalman filter to a stirred tank reactor for state estimation. A similar effort was made for optimal control of a polymerization process by Schuler and Suzhen (1985), and Schuler and Papadopoulou (1986). In their studies perfect models were assumed, and effects of unaccounted disturbances or model mismatch were not considered. Dimitratos *et al.* (1989) applied the EKF to a seeded semi-batch emulsion vinyl acetate/n-butyl acrylate copolymerization reactor, again not accounting for the effects of model mismatch. MacGregor *et al.* (1986) used the EKF to infer state properties in a batch polystyrene latex reactor, in which a reactive impurity is initially

unknown. To compensate for the unknown impurity level a impurity state was introduced. Ramirez (1987) applied a Kalman filter to a batch beer fermentation problem. The EKF they used was based on a determinant model, and was combined with a sequential parameter estimator to account for the model mismatch. Stephanopoulos and San (1984a, 1984b) proposed a strategy for state estimation and filtering in batch, semi-batch and continuous bioreactors using the EKF with very simplified, semi-empirical models. In their strategy the growth parameters, which suffer from poorly defined disturbances, were included in the filter to account for the all possible observed responses. They successfully applied this approach to a semi-batch fermentation reactor over a wide range of the operating conditions.

Fixed bed processes

The use of Kalman filters for state estimation in fixed bed systems is more complex, as these systems belong to the class of distributed-parameter systems, i.e. their state variables (temperature, concentration at fixed and mobile phases) are functions of both time and spatial coordinates.

Although it is highly desirable to know all the states at each location for the purpose of monitoring and control, it is almost impossible to measure all the state variables at artificially specified locations. This highlights the state estimation problem. For the fixed bed processes the estimation problems can be classified into two areas, one is the estimation of steady-state profiles, the other, the estimation of the system dynamic behaviour.

For a reactor at steady state, only the spatial profiles of the state variables are required to be reconstructed. Kuruoglu and co-workers (1982, 1985) applied the EKF to a packed-tube reactor for ethylbenzene dehydrogenation, and obtained estimates of the steady-state temperature and concentration profiles. Canavas (1984) used the EKF for a similar reactor in the presence of severe model parameter errors. By including the unknown model parameters in the state vector reliable estimates of state variables and model parameters, such as heat transfer coefficient, and frequency factors of the reaction kinetics were obtained.

For packed bed adsorption processes the main concern is never the steady state estimation as the process never reaches its steady state at loading and elution stages. To estimate the dynamic bed behaviour the filter design is largely based on the axial discretization of the packed bed. This results in a relatively high computation effort as the number of the model equations depends on the number of the spatial grid points. In order to achieve a realistic computing effort some authors (Cinar 1984, Soliman and Ray 1979) solved the filter equations off-line at a nominal steady state and used steady state gains, i.e. "suboptimal" gains for the filter implementation. For technical application simplified models based on reliable assumptions offer the advantage of reducing the computational burden. Sørensen *et al.* (1980) employed a simplified linearized model of a tubular catalytic reactor converting hydrogen to water, and investigated the filter performance. Ajinkya and co-workers (1974) and Kuruoglu *et al.* (1981, 1985) applied filter techniques to estimate the activity profiles of decaying catalyst in a packed bed. In their studies they considered the estimation of time varying

parameters as well as optimization of sensor location in the catalyst bed.

It can be seen that model mismatch and unknown parameter variations were simply ignored in the early studies, but these problems have been addressed in later work. Great efforts have been made to compensate for the effects of the model mismatch resulting from the model simplification and unknown disturbances. This has led to significant performance improvement and improved applicability for a range of applications.

3.3 Artificial Neural Network (ANN) approach to state estimation

3.3.1 Difficulties in process modelling

The processing of stochastic or imprecise information is becoming more important in the fields of process engineering, process design and simulation, process supervision, control and estimation, and process fault detection and diagnosis. Currently model based techniques are often employed to tackle such tasks. These models are dependent upon quantitative knowledge derived from experience, or specified in terms of a set of differential equations, or a loosely integrated combination of both. This approach can provide an acceptable description of the process, however it is prone to failure arising from the model mismatch and the intrinsic nonlinearity of many process systems. It is usually the case that establishing the model equations is a complex and time consuming exercise, moreover the required parameter determination is not easy. Some parameters are even impossible to determine from an understanding of their physical

meaning alone. For example, to determine pore diffusion coefficients one has to employ an optimization algorithm in an iterative series of simulations. In such a case the practical utility of a physically defined parameter is limited. In addition the validity of such models will be highly dependent on the operational conditions, for example a film diffusion may apply at low, but not high flow rate. These difficulties have forced engineers to seek alternative strategies of process modelling, as a result so-called black-box methods have attracted increasing interest. Recently, there has been a rapid upsurge in interest in the application of artificial neural networks for process description.

3.3.2 The basic idea of artificial neural networks

The idea of using artificial neural networks as a potential solution strategy for problems which require complex data analysis is not new. In fact the field of neural computation is as old as digital computation itself. Neural network research can be traced back to the 1940s, when the paper by Hebb (1949) on modelling of neurons and on learning first appeared. Since then, scientists have been attempting to realise the "real" neural structure of the human brain, and to develop algorithmic equivalents of the human learning process. The principal motivation behind this research is the desire to achieve the sophisticated level of information processing displayed by the brain. However, the structure of the human brain is extremely complex, with approximately 10^{11} neurons and between 10^{14} and 10^{15} synapses (the connections between neurons). Whilst the function of single neurons is relatively well understood, their collective role within the conglomeration of cerebral elements is much less clear and the subject of avid

postulation (Francis 1989). Consequently, the architecture of an artificial neural network is based upon a primitive understanding of the function of the biological neural system. A neural network is composed of units that have some of the properties of the biological neurons. That is, each unit has many inputs, some of which excite it and some of which inhibit it. However attempts never have been made to emulate exactly the immensely distributed structure of the human brain because of the limitations of the current computer hardware technology. Hence, artificial neural networks attempt to capture and utilise the neuron connection philosophy on a more modest and manageable manner, instead of accurately model the intricacies of the human cerebral functions.

3.3.3 A brief historical perspective

The investigation of artificial neural networks (ANN) has a somewhat chequered history. Widrow's ADALINE (1960) and Rosenblatt's publication on the perceptron (1962) sparked a great deal of interest initially. However, in 1969 the text, Perceptron, was published by Minsky and Papert, which showed that the linear neural networks which had received so much attention were severely limited in the problems they could solve. It also speculated that the study of multilayered nets would be a "sterile" area. Although this speculation was proved later to be incorrect, this text led to a great loss of interest in neural computation until the early 1980s. At that time Rumelhart (1986) proposed the error back-propagating learning algorithm which can be applied to nets involving hidden layers. This led to a resurgence of ANN research, and interest in the field has been growing rapidly ever since. A comprehensive review of the neural network

studies can be found in Widrow *et al.*(1990).

The introduction of the hidden layer together with the backpropagation learning, or training algorithm offers the network the ability to self-organize. In other words the network can develop an "internal representation" of the system features through a "learning" process. This self-organizing ability, together with the neuron processing function, gives ANNs their powerful signal processing capability. A properly trained ANN can recognise the functional relationship between the input and output vectors. In this state it can be used for process modelling, state estimation, and prediction. All of these problems have been encountered in the study of the thermal monitoring of packed bed adsorption process. Although these problems can be solved by using the EKF techniques, which have been described in the last section, a neural network offers the advantage of simplicity and greater reliability. In this study the purpose of using ANNs is not only to illustrate the applicability of modelling techniques to the system concerned, but also to seek the most effective prediction algorithm for relating signals derived from thermal monitoring to the position of the breakthrough front.

In this section a brief review of the application of ANNs in chemical and biochemical processes is presented, then the feed forward network topology and the backpropagation training approach are discussed.

3.3.4 Application of ANNs in chemical and biochemical processes-a brief review

ANNs have been widely applied to the fields of electronic and information

engineering, image analysis and visual recognition, speech recognition, and the reading of handprinted numbers are some of the successful applications. To review the studies of ANNs in all of the fields is of course far beyond the scope of this thesis. However at present, there is a strong and growing interest in ANN application in various areas of chemical engineering. This can be seen in the recent special issue of *Computers & Chemical Engineering* dealing with neural networks (1992 Vol. 16, No.4). These applications can be grouped into two broad categories: (i) modelling, estimating and control, (ii) pattern recognition and process fault diagnosis. Here the first category is mainly addressed as it is more closely related to the topic of this thesis.

A number of ANN applications in the modelling of chemical and biochemical processes have been reported in the literature. Hoskins and Himmelblau (1988) illustrated an ANN approach to knowledge representation in chemical engineering, and demonstrated the ability of neural network models to learn and adapt themselves to different statistical distributions of inputs involving non-linear mapping and to spontaneously generalize, thus allowing the classification of similar inputs not used in the network training. Bhat *et al.* (1989a, 1989b) utilized the ANN technique to characterise successfully two non-linear chemical systems as well as to interpret biosensor data. Bhat and McAvoy (1990) developed a backpropagation network for dynamic modelling and control of a stirred tank reactor. Birky *et al.* (1989) utilised a neural network to solve the design problems of the distillation control. Thibault *et al.* (1990) used the neural network technique for prediction of fermentation variables, and showed that neural

networks could rival other prediction techniques. Hudson *et al* (1990) developed a dynamic ANN to analyze the time series from electrochemical reactions. Willis *et al.* (1991) demonstrated that a neural network estimator could give reliable prediction of the target biomass concentration in a mycelial fermentation system from directly measured data including dilution rate, and carbon dioxide evolution rate. They also demonstrated that significant improvements in process regulation could be achieved by using a neural network control approach. DiMassimo *et al.* (1992) applied a network model to estimate the biomass concentration in the penicillin fermentation process. Hernandez and Arkun (1992) studied the stability of neural network models as well as the stability of the model's inverse, thus providing a background within which to study the neural network-based control algorithms. Hoskins and Himmelblau (1992) described a network architecture for process control, and explained how the weights on the connections in the network can be adjusted to yield the desired control action. Su and McAvoy (1992) applied recurrent neural networks for long-term prediction of chemical processes. It may be worth mentioning the application of ANNs to the field of software sensors. The use of so-called software sensors enables the easily measured information to be more effectively utilised to estimate the target states of a system. Montague *et al.* (1992) demonstrate how software sensors based on neural networks can be formulated.

Studies involving applications of neural network techniques to chemical engineering processes have only been reported over the past 5 years, however, applications of these techniques have already covered a broad area of chemical

engineering, and the great potential of these techniques has been highlighted by many authors. Despite the variety of application of ANNs, there are still few literature reports dealing with their application to packed bed adsorption processes.

3.3.5 Feedforward Neural network

Basic structure

A typical neural network, as shown in Fig. 3-2, consists of 3 or more separate regions, specifically a input layer, output layer, and one or more hidden layers. The number of nodes, called neurons, in both input and output layers depends on the respective number of inputs and outputs being considered. In contrast, the number of neurons in each hidden layer will be specified by the user . Similarly the number of hidden layers may be varied according to the system complexity. It is the hidden layer structure that essentially defines the topology of a feedforward ANN.

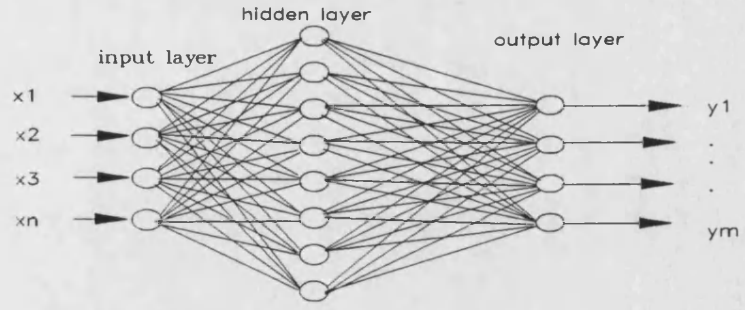

Fig. 3-2 Feedforward artificial neural network

The neurons in the input layer provide a means by which scaled data (usually scaled to the range of 0-1) is introduced into the network. The data is fed forward through the network via the connections between hidden layers to the output layer. Each connection acts as a weight to modify the strength of the signal being transferred. In the hidden and output layers each neuron firstly acts as a summing junction for the weighted signals:

$$S_j=\sum_{i=0}^{N} w_{i,j}x_i \tag{3-25}$$

where $w_{i,j}$ is the weight representing the connection strength between neuron i and neuron j. Then each neuron transfers the summation through a sigmoidal processing function:

$$y_j=\frac{1}{1+\exp(-S_j)} \tag{3-26}$$

where y_j is the output of node j, and also an element of the inputs to the output layer node. The response characteristics are shown in Fig. 3-3. It is not necessary to use the specific function described. In practice any sigmoid function with a bounded derivative can be used, for example, the tanh function is an acceptable alternative (Rummelhart *et al.* 1986)

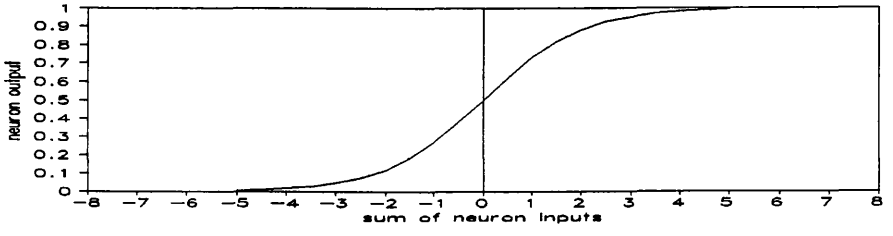

Fig. 3−3 Sigmoidal function

Topology Selection

Although an artificial neural network can be regarded as a black box model, the construction of an ANN for a given process depends on the understanding of the process to a certain degree. To construct an ANN shown in Fig. 3-2 the following system parameters must be specified:

1) the number of network inputs and outputs. The choice is primarily based upon an engineering understanding of the problem. As seen with linear identification techniques, redundancy of information due to highly correlated inputs may lead to a poor resulting model. Therefore it is necessary to minimise correlated inputs to the network.

2) the number of hidden layers. With regard to the choice of the number of hidden layers the information provided in the literature to date is conflicting. Some authors (*e.g.* Cybenko 1989) postulated that two hidden layers were sufficient to model any continuous non-linearity, while others (Hornik *et al.* 1989) claimed that one hidden layer was sufficient. In practice the decision is often empirical, that is, if the use of one hidden layer is unsuccessful then additional layers can be included. Research aimed at optimisation of the network structure for a given model is still ongoing. For example, Bhat and McAvoy (1992) proposed a neural network stripping algorithm called StripNet for determining the optimum network topology.

3) the number of neurons in each hidden layer. The choice here is also often

heuristic, however a number of more structued methods have been proposed. For example Wang *et al.* (1992) employed an approach that assessed redundancy through analysis of hidden layer neuron outputs.

These factors indicate that methods used for the construction of an ANN are not fully refined. Nevertheless, in many cases the use of a trial and error approach can rapidly lead to a topology which gives an acceptable representation of system behaviour.

3.3.6 Network training-backpropagation learning topology

Once the structure of an ANN has been specified, the network weights must be determined. This is realised through a training or learning procedure. There have been many attempts to design self-organizing neural networks. The aim is to find an effective synaptic modification rule that will allow an arbitrarily connected neural network to develop an internal structure that is appropriate for a particular task. The task is specified by giving the desired data vector of the output neurons for each state vector of the input neurons, *i.e.* the target. If the input neurons are directly connected to the output neurons it is relatively easy to find learning rules that iteratively adjust the relative strengths of the connections, *i.e.* the weights, so as to progressively reduce the difference between the actual and desired output vectors. These were the cases in the early stage of the neural network studies, unfortunately little progress was achieved at that stage because of the imperfect structure of such networks. For example even a simple task, the detection of symmetry, cannot be implemented by a simple connection of input

to the output neurons.

The introduction of an intermediate, hidden layer, led to an astonishing progress in ANN studies. However, learning becomes both more attractive and more difficult when hidden neurons were introduced. This is because the desired state vectors of hidden neurons are not specified by the task. The learning procedure must decide under what circumstances the hidden neurons should be active in order to help achieve the desired input-output behaviour. This amounts to deciding what these neurons should represent. In other words, the question for many years was: how does a neuron deeply embedded within a network "know" to what extent the outcome of an overall action was attributable to its state? This problem was first addressed in 1962 by Rosenblatt (1962), but it was not until 1983 that the practical solution was first provided by Rumelhart, and refined in a series of papers over the next three years (Rumelhart and J.M. McClelland 1986; Rumelhart *et al.* 1986). The method they developed is the backpropagation leaning procedure, of which a brief review is presented below.

As described above, the input signals are processed by the neurons through Eqs. 3-25 and 3-26, and finally output vectors are produced at the output neurons. The aim of the learning procedure is to find a set of weights which ensures that for each input vector the output vector produced by the network is the same as, or sufficiently close to, the desired output vector. If there is a fixed, finite set of input-output cases, the total error in the performance of the network with a particular set of weights can be computed by comparing the actual and desired

output vector for each case. The total error, E, is defined as

$$E=\frac{1}{2}\sum\sum(\hat{y}_{j,k}-y_{j,k})^2 \tag{3-27}$$

where j is an index over cases (input-output pairs), k is an index over output neurons, $\hat{y}$ is the actual state of an output neuron and y is its desired state. To minimize E using a gradient descent method it is necessary to compute the partial derivative of E with respect to each weight in the network. This is simply the sum of the partial derivative for each of the input-output cases. For a given case, the partial derivative of the error with respect to each weight is computed through a backward pass through which the derivatives are propagated from the output layer back to the input layer.

The backward pass starts by computing $\partial E/\partial\hat{y}$ for each of the output neurons. Differentiating Eq. 3-27 for a particular case, j, and suppressing the index i gives

$$\frac{\partial E}{\partial\hat{y}_j}=\hat{y}_j-y_j \tag{3-28}$$

To calculate $\partial E/\partial s_j$ the chain rule is applied

$$\frac{\partial E}{\partial s_j}=\frac{\partial E}{\partial y_j}\frac{\partial y_j}{\partial s_j} \tag{3-29}$$

Differentiating Eq. 3-26 to get the value of the last term in the above equation and substituting gives

$$\frac{\partial E}{\partial s_j}=\frac{\partial E}{\partial y_j}y_j(1-y_j) \tag{3-30}$$

as defined in Eq. 3-25, s_j is a linear function of the states of the input neurons. It is also a linear function of the weights on the connections, so it is not difficult to calculate how the error will be affected by changing these states and weights. For a weight $w_{j,i}$, from i to j the derivative is

$$\frac{\partial E}{\partial w_{j,i}} = \frac{\partial E}{\partial s_j}\frac{\partial s_j}{\partial w_{j,i}} = \frac{\partial E}{\partial s_j} y_j \tag{3-31}$$

and for the output of neuron i the contribution to $\partial E/\partial \hat{y}_j$ resulting from the effect of i on j is simply

$$\frac{\partial E}{\partial s_j}\frac{\partial E}{\partial y_i} = \frac{\partial E}{\partial s_j} w_{j,i} \tag{3-32}$$

so taking into account all the connections emanating from neuron i the following equation is given

$$\frac{\partial E}{\partial y_i} = \sum \frac{\partial E}{\partial s_j} w_{j,i} \tag{3-33}$$

where the sum is for all j. It has been seen so far how $\partial E/\partial y$ may be calculated for any neuron in the penultimate layer given $\partial E/\partial y$ for all neurons in the last layer. The procedure can be therefore repeated to calculate this term for successive earlier layers, then to calculate $\partial E/\partial w$ for all weights.

One way of using $\partial E/\partial w$ is to change the weights after every input-output case. This has the advantage that no separate memory is required for the derivatives. An alternative scheme is to accumulate the derivatives over all the input-output cases. The simplest version of gradient descent is to change each weight by an

amount proportional to the accumulated derivatives

$$\Delta w = -\mu \Sigma \frac{\partial E}{\partial w} \tag{3-34}$$

where the sum is for all cases (input-output pairs). This method is simple and can easily be implemented on a personal computer, although it does not converge as rapidly as methods using the second derivatives. Some improvements have been made to accelerate the convergence. One of them is to use the current gradient to modify the velocity of the point in weight space instead of its position (Rumelhart *et al.* 1986)

$$\Delta w(t) = \mu \frac{\partial E}{\partial w(t)} + \alpha \Delta w(t-1) \tag{3-35}$$

where t is increased by 1 for each sweep through the whole set of input-output cases, and α is an exponential decay factor between 0 and 1 that determines the relative contribution of the current gradient and earlier gradient to the weight change.

The network training procedure is summarised as follows. It is first set up with small random connection weights. A particular input vector is then given to the network, which produces the output vector in the output layer. Meanwhile for the particular input vector the network is provided with a desired output vector, or target vector, which is used to make a comparison and thus to calculate the error. The error signals are used to adjust the weights of the connections to the output

layer, then this information is back-propagated to the hidden layer to adjust the weights of all the connections between the hidden layer and the input layer. The most common strategy for the adjustment is based on gradient descent. This means that the algorithm used makes a small adjustment to the strength of each connection, in such a way that each alteration reduces the total error in the performance of the network. Applied repeatedly, this necessarily leads to a minimum in the total error. It is well known that such methods run the risk of being trapped in a local minimum, which may be far above the global minimum. However this rarely happens with neural networks, probably because of the many neurons involved and because of their graded response. Moreover the absolute global minimum is usually not required, only a sufficiently close approximation (Francis 1989).

Some alternative approaches for network training have been proposed. Willis *et al.* (1991) cited an attractive algorithm proposed by Bremermann and Anderson (1989). In their approach the weight adjustments occur in a random order, and the weight changes follow a multivariate Gaussian distribution with zero mean. In fact, the weights are adjusted by adding Gaussian distributed random values to old ones. The new weights will not be accepted unless the resulting prediction error is smaller than that recorded using the old ones. The procedure is repeated until the reduction in error is negligible. They claimed that the proposed technique was 'neurobiologically more plausible'. This algorithm is similar to so called bacterial chemotaxis, and thus the procedure is referred to as the chemotaxis algorithm. In general this approach is flexible and ease to use, and

more efficient when large networks are used (Willis *et al.*, 1991), while the back-error propagation algorithm is superior for simple network structures (Bremermann and Anderson 1989). In this study back error propagation will be concentrated upon, because of its widespread popularity, and the relatively small networks required.

Dynamic neural networks

The neural networks described above perform a non-linear mapping between inputs and outputs. Dynamics are not inherently included within their structures, whereas in many practical cases dynamic relationships exist between the system state variables. In this study, there are a number of dynamic relationships between the temperature and the concentration variables in the column, so that networks which are able to handle system dynamics will be required. The system dynamics can be simply introduced by making use of time histories of the data for the network training and prediction, and elegant approaches have been developed by some researchers (Su *et al.*, 1992).

CHAPTER. 4 EXPERIMENTAL RIG DESIGN AND PERFORMANCE CHARACTERISTICS

4.1 Thermal sensors

4.1.1 Essential properties of thermal sensors used for process monitoring

Thermal sensors used for chemical process monitoring must ideally possess a number of properties:

a) High sensitivity to temperature change

b) Low response time

c) Unique response to temperature change

d) Appropriate size to allow accessibility to the system

e) High stability to the chemical media

f) High long term stability

In practice a compromise may be made amongst these properties for a given application. The most commonly used thermal sensors are thermocouples and thermistors. Thermocouples give an electric potential response to temperature without the need of a driving power. Matz *et al.* (1987) used thermocouples to follow the temperature change within an active carbon packed bed. However the sensitivity limitation of thermocouples precludes their use with very small temperature signals. Thermistors are thermally sensitive resistors whose primary function is to exhibit a change in electrical resistance with a change in body temperature. Of the various types of thermistors available semiconductor

thermistors are the most sensitive, offering large negative temperature coefficients. Semiconductor thermistors in a mini-bead glass coated form offer low response times, good accessibility to an adsorption column, and high chemical stability. Thus they are well suited for thermal monitoring systems.

4.1.2 Thermal and electric properties of semiconductor thermistors

Three important characteristics which specify a thermistor's response behaviour are briefly reviewed below, while more detailed discussion can be found in Sapoff (1972).

Zero-power resistance temperature characteristics

When a thermistor is operated at a power level which is sufficiently low so as to produce negligible self-heating, its resistance is referred to as the Zero-Power resistance. The Zero-power resistance temperature characteristic is the relationship between the zero-power resistance of a thermistor and its body temperature. This characteristic may be expressed as

$$R_T = R_0 \exp\left[\frac{\beta}{T} - \frac{\beta}{T_0}\right] \qquad (4\text{-}1)$$

where R_T and R_0 are the zero-power resistance of the thermistor at temperature, T, at a reference temperature, T_0, respectively, β is the material constant of the thermistor. Although β increases slightly with increasing temperature, it may by assumed to be constant over a limited temperature span of 10 to 20 K.

Power dissipation characteristics.

When a thermistor is operated under a limited voltage, the power dissipated can be derived from the heat balance, taking the form of

$$P=\delta(T-T_a)+C\frac{dT}{dt} \qquad (4\text{-}2)$$

where C is the heat capacity of the thermistor, δ is the dissipation constant of the thermistor and is defined as the ratio, at a specified ambient temperature, T_a, of the change in power dissipation in a thermistor to the resultant body temperature change. Since the term $\delta(T\text{-}T_a)$, in Eq. 4-2, is the rate at which heat is transferred away from the thermistor, it is seen that the dissipation constant must be dependent upon the thermal conductivity and the flow rate of the medium surrounding the thermistor, the heat loss due to free convection in a still medium, the rate of heat conduction through the thermistor leads to its mount, and the heat loss due to radiation. Hence the dissipation constant, δ, is not a true constant and will be dependent on operating conditions.

At steady state, *ie.* at a condition of thermal equilibrium ($dT/dt=0$), the dissipation constant simply represents the amount of power required to raise the temperature of the thermistor 1 K above its ambient temperature. This is usually provided by the manufacturer for specified conditions.

Time constant

Under Zero-power conditions Eq. 4-2 becomes

$$\frac{dT}{dt} = -\frac{\delta}{C}(T - T_a) \tag{4-3}$$

which is, in fact, a mathematical statement of Newton's Law of Cooling, and its solution can be writen

$$T = T_a + (T_i - T_a)\exp(-t/\tau) \tag{4-4}$$

where T_i is the initial temperature and $\tau = C/\delta$ is the thermal time constant of the thermistor. The time constant may be expressed in terms of the time required for the thermistor at zero power to change 63% of the difference between its initial temperature value and that of a new imposed temperature environment.

The characteristics data for the thermistors used in this study are listed in Table. 4-1.

Table. 4-1 Characteristic data of thermistors

thermistor	RS micro*	RS151-142	RS151-158	YSI44106
resistance at 25°C (kΩ)	1	4.7	47	10
dissipation constant (mW/°C)	0.1	0.75	0.75	8
time constant (sec)	<0.5	5	5	2.5
β (K)	2910	3340	3940	3650
β tolerance %	-	±3	±3	±0.2

* in micro bead form

4.1.3 Thermistor circuit and its output characteristics

To detect the resistance change of a thermistor a Wheastone bridge together with a power source is required. A typical circuit for thermistors is shown in Fig. 4-1.

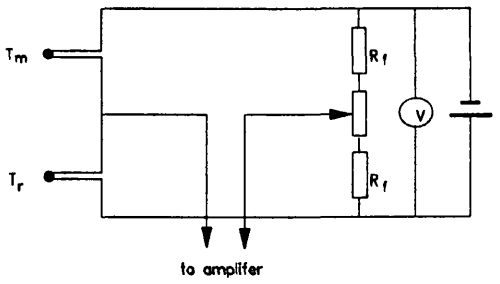

Fig. 4-1 Wheatstone bridge

T_m T_r measurement and reference thermistor

R_f resistance with low temperature coefficient

For a given resistant change, the output of the bridge circuit can be expressed as (see Hubble 1986)

$$dv=\left(\frac{R_m}{R_m+R_r}-\frac{R_m+dR}{R_m+R_r+dR}\right)V \tag{4-5}$$

where V is the bridge excitation voltage, and dR is the resistance change of the measuring thermistor. In most cases the temperature at the measuring point is very close to that at the reference point, hence $R_m=R_r$ approximately applies. Taking this approximation, Eq. 4-5 becomes

$$dv=\left(\frac{1}{2}-\frac{1+\frac{dR}{R_m}}{2+\frac{dR}{R_m}}\right)V=-\frac{1}{2}\left(\frac{dlnR}{2+dlnR}\right)V \tag{4-6}$$

In view of very small value of dlnR, the above equation can approximated by

$$dv=-0.25V\,d\ln R \tag{4-7}$$

where dlnR can be derived from Eq. 4-1, and takes the following form

$$d\ln R = -\frac{\beta}{T^2} dT \qquad (4\text{-}8)$$

Substituting Eq. 4-8 in Eq. 4-7, the output of thermistor bridge can be finally expressed as

$$dv = \frac{\beta}{4T^2} V dT \qquad (4\text{-}9)$$

This equation shows that the thermistor bridge output gives a linear response to temperature change provided that the temperature changes is sufficiently small, 0.1°C for instance. It also shows that the sensitivity of the thermistor bridge system is proportional to the excitation voltage. This suggests that the use of a high excitation voltage is favoured. However high excitation voltages result in high power dissipation from the thermistor according to the relation $W = V^2/R$. This in turn results in a large difference in temperature between the thermistor body and the medium, thus the temperature distribution becomes highly uneven and potentially unstable. In practice a compromise must be made to maximise sensitivety within an acceptable power dissipation range.

4.2 Apparatus for the thermal monitoring column system

4.2.1 System outline and devices

The outline of the thermal monitoring liquid chromatography system developed in this work is shown in Fig. 4-2. A peristaltic pump (Minipulse 2, Gilson,France) drives the liquid flow via a 6-way automatic control valve, through a coil heat exchanger, and on to the column. A UV detector, LKB2238 LKB-Produkter AB

Sweden, set at either 280 or 205nm, is used to monitor the adsorbate concentration at the column outlet. Meanwhile signals resulting from temperature changes within the column are sensed by thermistor-Wheatstone bridges, and are fed to a microcomputer via a pre-amplifier analog/digital convertor. Both thermal and UV signals are processed by the computer. A complete operating cycle, including loading, washing, eluting, and regenerating, can be automatically carried out under computer control. A programme, including signal processing and valve control, which was based on the PC-Labcard software (Intercole, Eastleigh, Hants, UK) and written in Quick Basic (Microsoft, 1988) is listed in the Appendix, coded as "multlog".

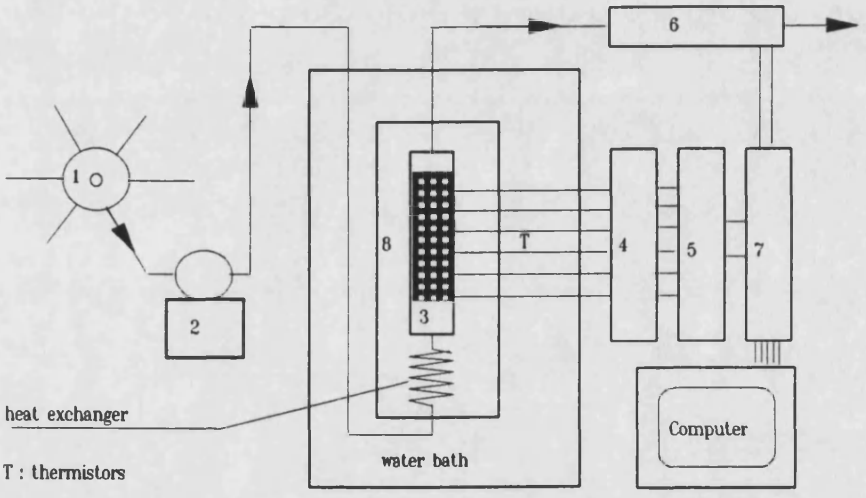

1. 6 way valve; 2. pump; 3. column; 4. Weatstone bridge; 5. PCL 889 card
6, LKB-2238 UV detector ; 7, PCL-818 A/D card ; 8, jacket

Fig.4-2 Thermal monitoring liquid chromatography system

The six-way electrical-magnetic valve is a product of NR research Incorprated, Italy, and was purchased from Alpha Controls Ltd, Lover, Buckinghamshire, UK. The relay card for the valve operation was made "in house" by the School's workshop. Other devices will be described in later sections.

4.2.2 Column installation

A borosilicate Pyrex glass column (150 x 25 mm O.D. length adjustable; Omnifit Limited, modified by the addition of 8 side pipes in the University glass-shop) was placed in a plexiglass jacket (200 x 85 mm I.D.) filled with either water or air. The column together with its jacket is placed in a water bath (400 x 300 mm). The jacket design has been proved to be an effective means of reducing short period thermal disturbances resulting from water turbulence. In the thermostatted water bath, temperature within the jacket can be maintained at a given set point with a fluctuation less than 0.001 °C. The column with 6 thermistors mounted is shown in Fig. 4-3. The miniature bead thermistors (RS151-142 4.7 kΩ or RS 151-158, 47 kΩ, RS Data library, 1990) were sealed with epoxy in glass tubes of 3mm O.D and 40mm length. The sealed thermistors then were aged in water for at least 4 days, whilst the insulation resistance was monitored. Only thermistors whose insulation resistance was greater than 100 MΩ were chosen to be mounted into the column. A 1kΩ resistor was also mounted as a point heat source in the column for calibration experiments. YSI44106 (10 kΩ) thermistors were also used in later research.

RS thermistors were purchased from RS Components Ltd, Corby Northants, UK. YSI44106 thermistors were purchased from Yellow Springs Instrument Incorporated, Yellow Springs, Ohio, USA.

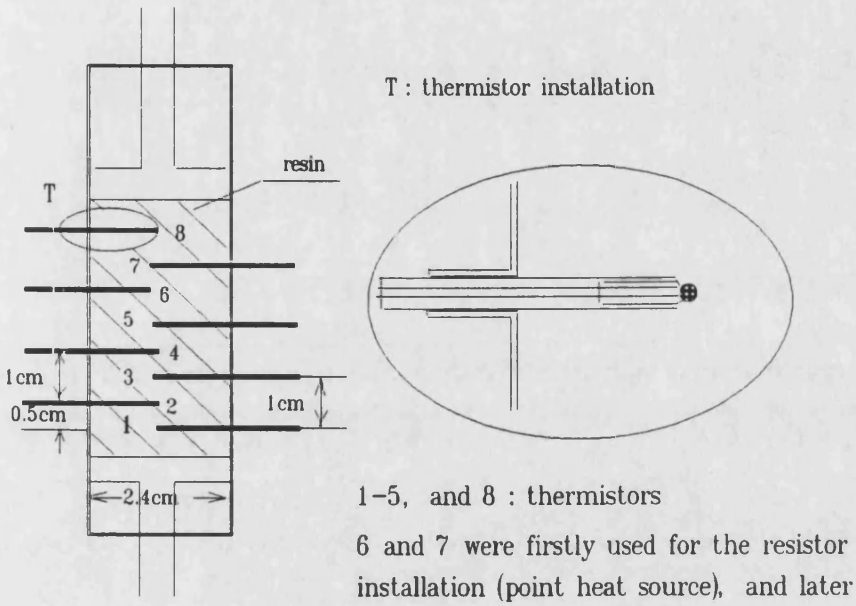

Fig. 4-3 Column with thermistors mounted

4.2.3 Reference thermistors-external and "in bed" reference

In a preliminary survey temperature monitoring was attempted by using one thermistor as a measuring arm in the Wheatstone bridge of which the other three arms were of fixed resistance. However the results obtained showed that this arrangement was incapable of eliminating time dependent baseline drift even when the system was maintained in an accurately thermostatted bath. Drift levels were observed to be ±0.5 mV within 4 hours, precluding the use of this simple

circuit. Efforts were therefore turned to the use of reference thermistors in the bridges.

External reference thermistors

Initially, reference thermistors were mounted in such a way that their temperature was unlikely be disturbed by the effect of water turbulence in the external bath. An aluminium ring, shown in Fig. 4-4, 6.5cm in diameter, 1.2cm in thickness, was used as a support for the reference thermistors. The high thermal conductivity of aluminium and the heat capacity of the ring give an even temperature such that all the reference thermistors are in a similar environment. The reference thermistors were mounted in this aluminium ring which was fixed around the upper regin of the column. Therefore thermal signals sensed by a thermistor bridge actually refer to the temperature difference between the vicinity of the sensing thermistors and the aluminium ring. This sensor arrangement gave much improved baseline stability and was used for preliminary studies.

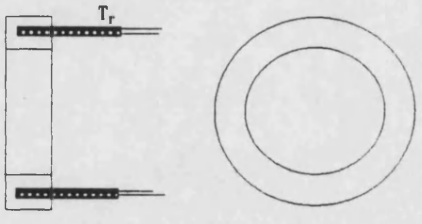

T_r reference thermistor

Fig. 4-4 Aluminium ring for mounting reference thermistors

"In bed" reference thermistors

Subsequent refinements to the above approach were carried out by using "in bed" reference thermistors. Consequently, "in bed" differential thermal signals sensed by such a thermistor bridge are referred to as the temperature difference between the two positions where the sensing-reference thermistor pair is located. The codes, (thermistor pair) 1-3 *(et al)* used in later chapters mean that thermistors 1 and 3 are used as sensing and reference thermistors respectively. It would be expected that "in bed" differential thermal sensing is more tolerant to the thermal "noise" caused by the room temperature and flow rate fluctuations.

4.2.3 Wheatstone bridge

A Wheatstone bridge circuit (see Fig. 4-1) was used to output signals from each sensor/reference pair to the computer data collection system. The bridges were driven by a laboratory power supply. The resistances comprising the two static arms of the bridge were of low temperature coefficient. A 4.7 kΩ potentiometer was included to allow adjustment of output level. Through a theoretical analysis (Hubble, 1986), based on the quoted characteristics of the thermistor used, a response of 3.15 mV per 0.1K should be obtained for an excitation voltage of 3.5 V. The bridges were made "in house" using components purchased from RS.

4.2.4 Automatic data collection and processing system

The data logging and analysis system consists of an OPUS PCXS 386sx microcomputer, a high performance data acquisition card, PCL-818, providing 16 analog input channels, and 16 digital output channels (with 12 bit resolution at

100 KHz). The card was used for both analog/digital converting, and to provide a digital triggering input source to the automatic control valve gear. In view of the very low output level of the thermistor bridge, a pre-amplifier was required to amplify the signal output to match the input range (minimum ±0.5 V) of the PCL-818. card. A PCL-889 board was used for this purpose, providing 16 input channels, and having a programmable gain ranging from 0.5 to 1000. Signals coming from thermistor bridges were input to the amplifier, where they were amplified, then fed to an input channel on the PCL-818 card. Whilst signals output by the UV detector were directly input to another PCL-818 input channel. Table. 4-2 shows the calibration performance of the system obtained with a reference voltage source. Both Cards were purchased from Intercole, Eastleigh, Hants, UK.

Table.4-2 Survey of the performance of the PCL-889-
PCL-818 data acquisition system

input (mv)	output (mv)		
gain*	100	200	1000
0.0000	-0.2284	-0.1016	-0.0214
0.0400	-	-	0.0196
0.1000	-0.1285	0.0006	0.0800
0.1400	-	-	0.1208
0.2000	-0.0027	0.1913	0.1821
0.3000	0.0774	-	0.2836
0.4000	0.1781	-	0.3847

* refers to PCL-889 gain, input range of PCL-818 was set to be ±0.5 V.

It can be seen from Table.4.2 that there appear to be offsets. However the relative output level of the system with respect to a zero input is highly precise (±1 %).

4.3 Baseline stability

4.3.1 Baseline noise characteristics

Because of the inevitability of noise in any sensing system, enhanced performance of a sensor system may be achieved in two ways: improving system performance to reduce the noise level, or alternatively filtering the noise. This requires a comprehensive understanding of the noise characteristics and the factors which determine these.

Baseline

Because of the heat dissipation characteristics of the thermistors, thermal equilibrium between thermistors and their surroundings is never fully reached. However a steady state temperature distribution which is not time varying can be achieved. This steady state will specify the thermistor bridge zero output, *ie.* the baseline. Any factor which disturbs the steady state will make a contribution to the baseline noise.

Long term and short term noise

Baseline variations can be characterised into short term noise, and long term noise. In this context short term noise was measured in terms of baseline fluctuation within a sampling period used in experiments, *e.g.* 1 min. Long term noise was considered to result from a temperature field redistribution process, and is measured in terms of the maximum baseline drift within a period covering

a stage of the system operation, *e.g.* 2 hours for the loading stage. A series of observations was carried out to investigate the baseline stability and the factors which affect the noise level. The thermistor at position 2 (refer to Fig. 4-3) was chosen as the observing sensor.

4.3.2 Effect of temperature fluctuation of the water bath

Water bath TE-8A and W28

Two water baths were used for temperature control. The first was a cylinder tank with a TE-8A thermoregulator made by Techne Limited (Cambridge), which gives temperature stability of ±0.01°C, The second, W28, purchased from Grant Instruments Limited (Cambridge), gives significantly improved performance (temperature stability ±0.004°C). To assess the effect of temperature fluctuations of the water bath on the thermistor bridge baseline, sensor output was monitored in the absence of column flow. Figs. 4-5a and 4-5b show the baseline obtained using external reference thermistors in each water bath. Using a thermistor bridge driving voltage of 3.5 V, the short term noise was observed to be in the range of ±0.01 mV using the first water bath, and of ±0.005 mV using the second, which correspond to temperature fluctuations of ±0.0004 °C and ±0.0002 °C respectively. Whilst the long term noise was seen to be ±0.1 mV (±0.003 °C) using the first water bath and ±0.02 mV (±0.0006 °C) using the second water bath.

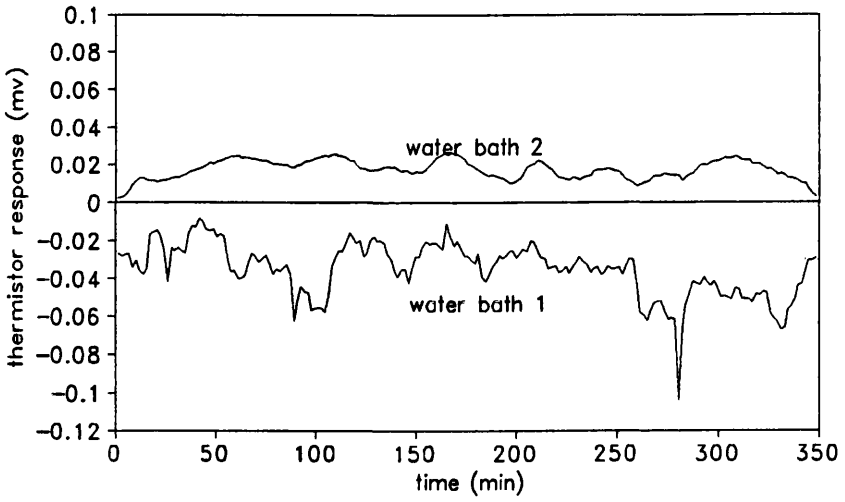

Fig.4-5a Long term baseline stability

manufacturer stated performance :
water bath 1, +0.01 °C ; water bath 2, +0.004° C

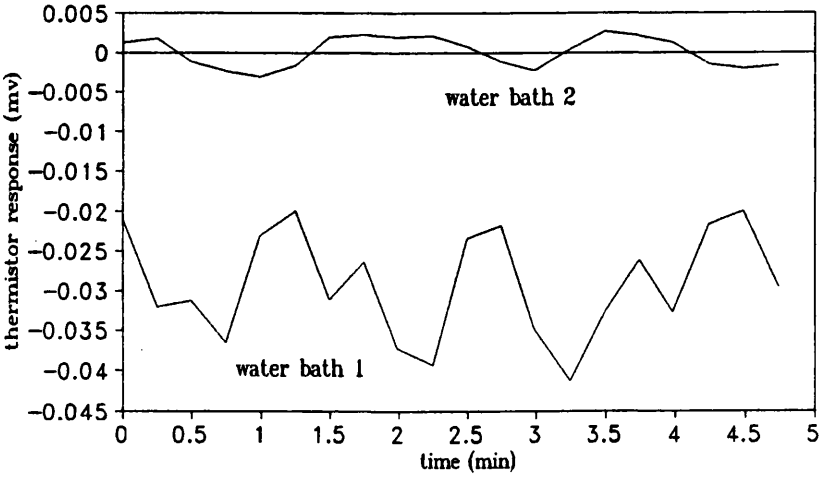

Fig.4-5b Short term baselinestability
water bath as used in Fig.4-5a

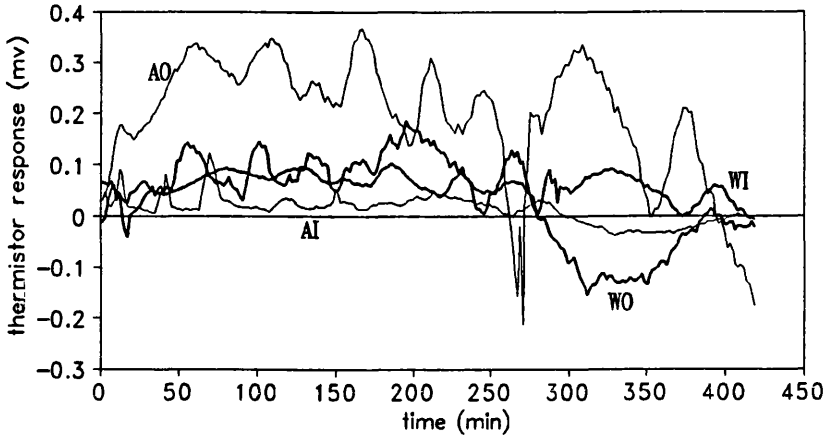

Fig. 4-5c Long term baseline using unthermostatted water bath or air bath

AO, AI : outside and "in bed " reference system in an air jacket

WO, WI : outside and "in bed" reference system in a water bath

Unthermostatted bath or air bath

A system which can be operated with an unthermostatted water bath or even with a simple air filled jacket offers significant practical advantages over more complex systems requiring complex temperature control. Baselines obtained by using both external and "in bed" reference thermistors in an unthermostatted water bath and a air filled jacket conditions are shown in Fig. 4-5c. In these cases room temperature fluctuations were more obviously reflected in the baseline response for the system with external reference thermistors.

4.3.3 Effect of flow rate

Because of the heat dissipation of the thermistors, the liquid flow will inevitably affect the temperature field around the thermistors. This can be seen from Eq.

4-2. The noise levels resulting from different flow rates are given in Tables. 4-3a and 4-3b.

Table. 4-3a Noise level at different flow rates (external reference)

flow rate (ml/min)	short term (±mV, 1 min) bath 1	bath 2	long term (±mV, 2h) bath 1	bath 2
0.56	0.024	0.008	0.11	0.05
1.1	0.031	0.010	0.12	0.06
2.4	0.034	0.014	0.12	0.07
5.6	0.041	0.021	0.17	0.12
8.8	0.045	0.024	0.18	0.14

Table. 4-3b Noise level at different flow rates ("in bed" reference, water bath 2)

flow rate (ml/min)	short term (±mV, 1 min)	long term (±mV, 2 hours)
5.6	0.018	0.09
8.4	0.022	0.12
16.2	0.025	0.13
24.5	0.036	0.15

It is seen that the long term noise level is highly dependent on the flow rate used, and that the advantages of a highly precise temperature controlled water bath are less significant at high flow rates. This can be explained by the fact that temperature fluctuations in the liquid reservoir can be introduced to the column by the liquid flow, and this effect will be magnified at high flow rates where there will be less time for feed temperature equilibrium to be reached. This argument

is supported by the fact that fluctuations of the room temperature, on which the reservoir temperature depends, affect the baseline noise level.

4.3.4 Effect of thermistor thermal characteristics

The instability of thermistor characteristics will, theoretically, make a contribution to the baseline noise, and this is specified by thermistor manufacturers. The stability of the thermistors was extensively studied at the National Bureau of Standards (Wood *et al.* 1978), and their conclusion was that many bead thermistors have drift rates at the level of only 1 mK per 100 days at temperature up to 60°C. Therefore the deterioration of thermistor performance is unlikely to be a major source of noise in this study.

The heat dissipation, which affects the temperature field distribution, is highly dependent on the thermistor resistance given a constant driving voltage, as discussed in secion 4.1. This dependence will consequently result in a relation between the noise level of the thermistor response baseline and thermistor resistance. Tables. 4-4 and 4-5 list the noise levels, with the different thermistors used.

Table. 4-4 Short term noise levels obtained with different thermistors

thermistor type resistance (kΩ)	RS micro 1	RS151-142 4.7	RS151-158 47	YSI44106 10
noise level(±mV) at flow rate, 1 ml/min	0.168	0.031	0.016	0.014
noise level(±mV) at flow rate, 4 ml/min	0.169	0.042	0.017	0.015

Table.4-5 Long term noise levels obtained with different thermistors

thermistor type resistance (kΩ)	RS micro 1	RS151-142 4.7	RS151-158 47	YSI44106 10
noise level(±mV) at flow rate, 1 ml/min	0.27	0.162	0.145	0.141
noise level(±mV) at flow rate, 4 ml/min	0.32	0.185	0.152	0.154

Data listed in the above two tables were obtained using a driving voltage of 3.5 V, and in water bath 1, except those with YSI44106, which were obtained in water bath 2.

Not surprisingly the results show that, driven at same voltage, the thermistor with low resistance gives a higher noise level baseline as it produces more heat and consequently increases its temperature to a high level in respect to its vicinity, resulting in an unstable temperature distribution.

4.3.5 Effect of excitation voltage

In section 4.1.3 the two effects of excitation voltage have been briefly discussed. The advantage of high sensitivity offered by using high excitation voltages may be illustrated by Eq. 4-9. Whilst more details of the other effect of excitation voltage can be seen in Fig. 4-6. This figure shows that for each type of thermistor there is a critical region of excitation voltage, above which the noise level sharply increases. Therefore the voltage used in any practical sensing situation should be below this critical region.

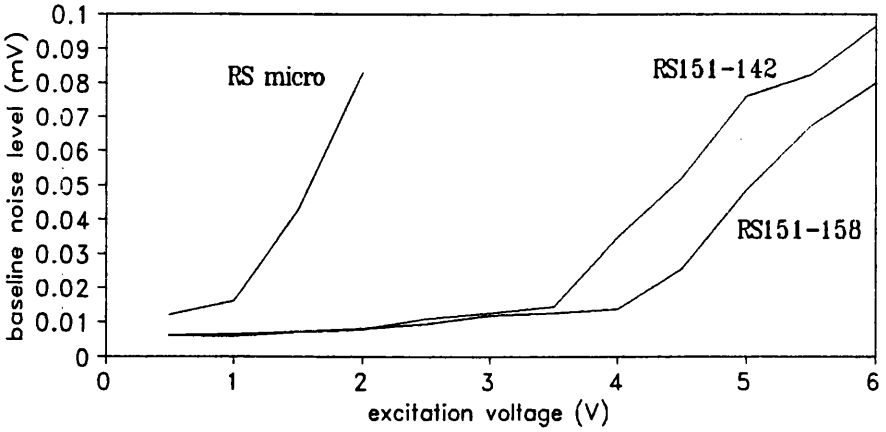

Fig.4-6 Effect of excitation voltage on baseline stability

4.3.6 Comparison of baseline performance between external and internal reference systems

The main advantage offered by a sensing system with internal reference thermistors is a higher tolerance to thermal "noise" under unthermostatted conditions, which can be seen in Fig. 4-5c. The slightly improved performance of the internal reference system with a high performance water bath can be seen by comparison of Table. 4-3b with Table. 4-3a, however in this case the advantage is not so significant as that under the unthermostatted conditions.

4.3.6 Other effects

It was found that sunlight impiging on the column may disturb the thermistor system and give rise to an unstable baseline. To reduce this disturbance the water bath was shielded from direct sunlight with a reflective cover.

4.4 Selection of thermistors

4.4.1 Stability to flow rate change

Because of the heat dissipation effect a small change in flow rate will give rise to a shift of baseline output from the thermistor bridge from its original level to a new level via a transient state. This effect can be illustrated by the stability to flow rate change, and is expressed in terms of the baseline shift as a function of flow rate. Baseline stability to the flow rate for each type of thermistor is shown in Table. 4-6, which also shows the transient time. Clearly thermistors with high resistance offer the advantage of higher stability in the presence of flow rate changes.

Table. 4-6 Baseline stability in the presence of flow rate changes (outside bed reference, excitation voltage: 3.5V)

Thermistor	dissipation power (mW)*	transient time (min)	stability to flow rate (mV/ml*min)
RS micro (1 kΩ)	12.2	11.1	7
RS151-142 (4.7 kΩ)	2.6	4.2	4.5
RS151-158 (47 kΩ)	0.26	2.8	2.7
YSI44106 (10 kΩ)	1.22	3.3	3.6

4.4.2 Long term stability of thermistor sealing

It has been observed that the insulation of thermistors deteriorates with immersion time. This deterioration seems unavoidable, as thermistors are placed in a solution. An example of the deterioration of thermistor insulation is shown in Fig. 4-7.

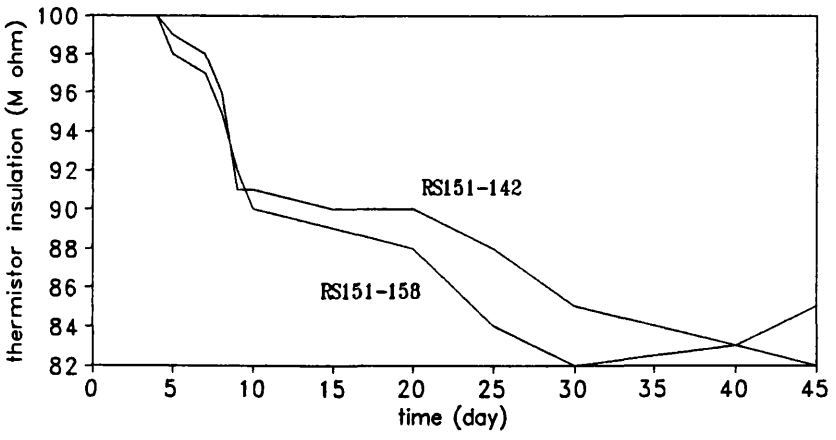

Fig. 4-7 Deterioration of thermistor insulation

The deterioration of insulation severely disturbs the sensor performance, as can be seen in Fig. 4-8 which shows the relation between baseline noise level and the thermistor insulation deterioration period. The baseline of the sensor system using high resistance thermistors suffers more from the deterioration of thermistor insulation than that using low resistance thermistors. This can be explained with the help of the diagram shown in Fig. 4-9. The effective resistance of the insulation will make its contribution to the bridge measuring arms. This contribution will be more significant when higher resistance thermistors are used

as bridge arms. Fig. 4-8 also shows that there is a critical region for each type of thermistors above which the noise level sharply increases. By locating the critical region in this time scale a life time for each type of thermistor can be defined. From this point of view the life time of higher resistance thermistors is shorter than that of those with lower resistance, for example, the life time of RS151-142 is 24 days, and of RS151-158, 7 days.

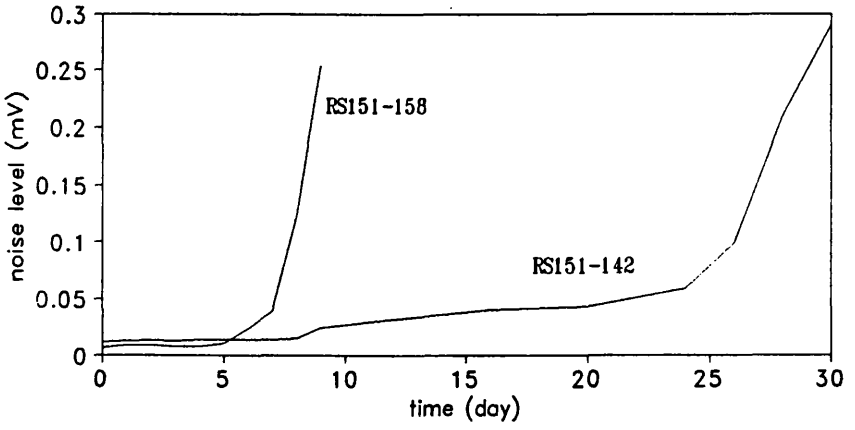

Fig. 4-8 The effect of insulation deterioration on background noise

4.4.3 Selection of criteria

The results shown in section 4.3.4 and the analysis of thermistor bridge output characteristics in section 4.1.3 indicate that thermistors with higher resistance might be excited with higher voltages, therefore giving a higher sensitivity, and the heat dissipation effect would be much less than that in the case using low resistance thermistors, excited with a similar voltage. Furthermore high resistance thermistors offer higher stability to varying flow rate, which is significant, as flow rate fluctuation is unavoidable in practice. These factors favour the use of higher

resistance thermistors. However the converse is here when the operational life time is considered in the light of these factors. Taking both factors into account, RSMicro was rejected, and RS151-142 and YIS44106 were selected for use. YSI44106 is a high precision thermistor, offering the advantage of a precise match between sensing and reference thermistors, and is provided in a teflon covered form making the installation much easier. However this type of thermistor is approximately ten times the cost of the RS151-142, which is an important practical consideration.

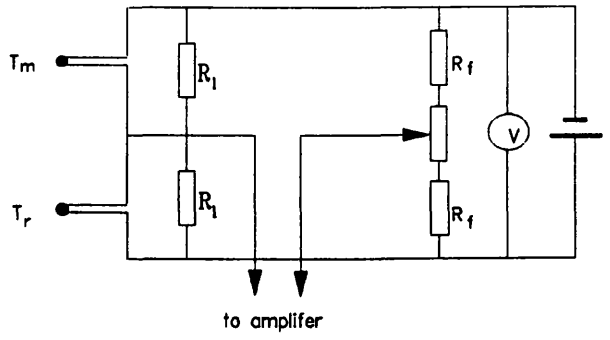

Fig.4-9 Equivalent circuit of leak resistance

T_m T_r measurement and reference thermistor

R_l equivalent leak resistance

CHAPTER. 5 EXPERIMENTAL AND THEORETICAL INVESTIGATION OF THERMAL MONOTORING ADSORPTION CHROMATOGRAPHY

5.1 Selection of adsorption systems

Initial work was aimed at developing the monitoring system using ion exchange based separations in order to take advantage of the larger thermal changes arising from their higher binding capacity. The adsorption of an amino acid, aspartic acid, onto a weak anion exchanger, DEAE based resin, was selected for preliminary investigation. This is an example of a simple system with adsorption of a single component, and as such is ideal for preliminary evaluation of thermal monitoring. Ion exchange has the additional advantage of being the most widely used adsorption separation in the fermentation industry. Interactions of the type used here have been widely reported, for example ion exchange adsorption of aspartic acid (Chibata *ea al.*, 1985), lactic acid (Srivastava, 1992), gluconic acid, and itaconic acid (Hirose *ea al.*, 1985).

Two types of resin were used. One was a DEAE based beaded resin, which has been widely used for a number of years. The other, DEAE based perfusive resin Productiv™ was developed in the School of Chemical Engineering at Bath University, and has been recent commercialised by BPS (Biotechnology Process Services, Mountjoy Research Centre, Durham, UK). This is a novel sponge based perfusive resin allowing significantly higher flow rates to be used. The purpose of using a perfusive resin is to assess the influence of a number of factors including

flow rate, bed voidage, and the structure of the adsorbent, over a wider range of conditions than could be obtained using a beaded resin alone.

For affinity systems, because of the high molecular weight of the substrate (usually protein with molecular weight of more than 15000 g/mole), very low molar concentrations of the feed stock will be expected in practice. This, together with the lower capacities of affinity resins, will result in very small rates of adsorbate uptake, and thus much smaller thermal signals, even though the reported data (Mosbach and Danielsson 1981) suggests that in the case of protein adsorption, larger heats of adsorption should be observed for a given number of moles of adsorbed material. The available performance data (Mosbach and Danielsson 1981; Chase 1984) and the relatively low molecular weight of the adsorbate (13930 g/mole) suggest that lysozyme-Cibacron Blue Sepharose™ represents a suitable model system for initial studies.

5.2 Materials, column packing, and concentration monitoring method

Materials

L-Aspartic acid, minimum assay 99% pure, was purchased from BDH Chemicals Ltd (Poole, Dorset, UK). Chemicals for buffer solutions were also purchased from BDH.

Lysozyme (from hen egg white) and BSA were purchased from Fluka Chemika-Biochemika (Buchs, Switzerland).

DEAE based resin in beaded form was produced by Waitaki International Biosciences, New Zealand. The particle size of the resin is in the range of 250-425 μm. DEAE based resin in sponge sheet form, trade mark Productiv™, was purchased from BPS (Durham, UK).

Cibacron Blue-Sepharose™-CL6B was denoted by Dr. A. Booth (1992), School of Chemical Engineering, Bath University.

Column packing

Spherical particle resin (wet weight 14 g) was first suspended in 0.5 M NaOH and stirred for 4 hours to allow the resin to transfer to OH^- form completely before washing with distilled water until the pH equalled 7. The resin and water mixture was gradually poured into the column shown in Chapter. 4, and a bed of about 4 cm height in the column of 2.4 cm OD was formed by the free settling of resin particles. The water content of the resin settled in the column was 89% as measured in terms of the dry resin weight per unit volume of the settled bed.

To pack the Productiv™ resin, the semi-dry sponge sheets were cut into disks of 24 mm diameter, and then fitted into the column. The water content of the bed was estimated to be greater than 92%.

Glass beads (0.2 mm diameter) were used to fill the pre-bed and post-bed volumes, and to adjust the bed position in the column, so that the first thermistor was located at the bed start for the external reference thermistor system, and at

0.5 cm from the bed start for the "in bed" reference system (refer to Fig.4-3 for column details).

Concentration monitoring method

Aspartic acid concentration was monitored using a UV detector set at 205 nm. A polynomial correlation, which was obtained by calibration using standard amino acid analysis method (Moore, 1968) was used to relate the UV absorbance to the concentration (the correlation is given in the Appendix). UV monitoring is limited with respect to the concentration range which can be followed, however it provides a simple approach to *in-situ* concentration monitoring when used in conjunction with off-line standard analysis.

Lysozyme and BSA concentrations were monitored using a UV detector set at 280 nm. UV absorbance was correlated to concentration using a simple linear calibration relationship.

5.3 Measurement of adsorption parameters

Batch experiments were carried out in order to obtain the adsorption equilibrium and kinetic parameters which are necessary for modelling the overall thermal processes within the column. The rig used for this purpose was based on that described by Cowan *et al.* (1986) and is shown in Fig. 5-1.

Isotherm measurement

A suspension of resin was allowed to settle in a measuring cylinder and its volume measured. A mass of this resin equal to 1 ml settled volume was added to 20 ml of 2.5 mM tris buffer pH 7.2 in a beaker maintained at a preset temperature. A given volume of adsorbate solution with a known concentration was added to the beaker. The solution was then recycled until the UV response became constant. The amount of aspartic acid uptake was calculated from the initial and final concentrations and volumes. Adsorption isotherms obtained are shown in Fig. 5-2 for aspartic acid-DEAE ion exchanger, and in Fig. 5-3 for lysozyme-Cibacron Blue Sepharose™. Langmuir fits for the adsorption isotherms are also shown in Figs. 5-2 and 5-3.

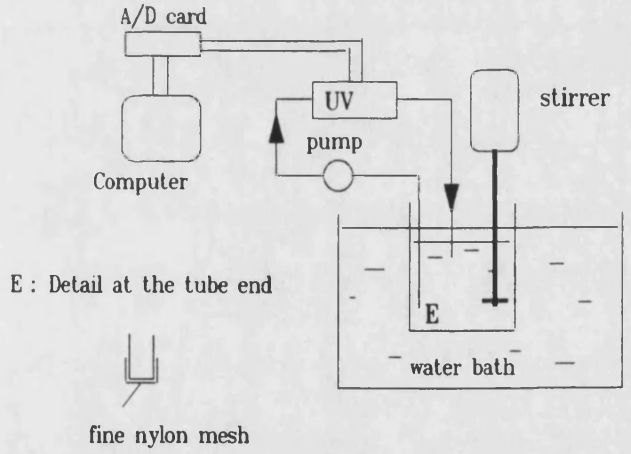

Fig. 5-1 Rig for adsorption isotherm and kinetics measurements

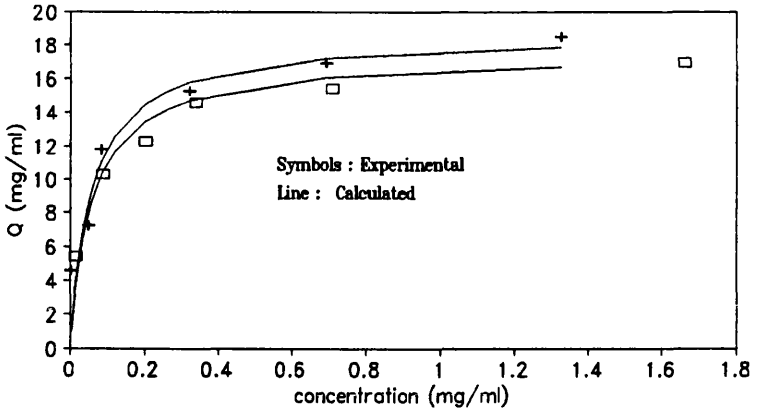

Fig. 5-2 Adsorption isotherms
Aspartic acid- DEAE based beaded resin

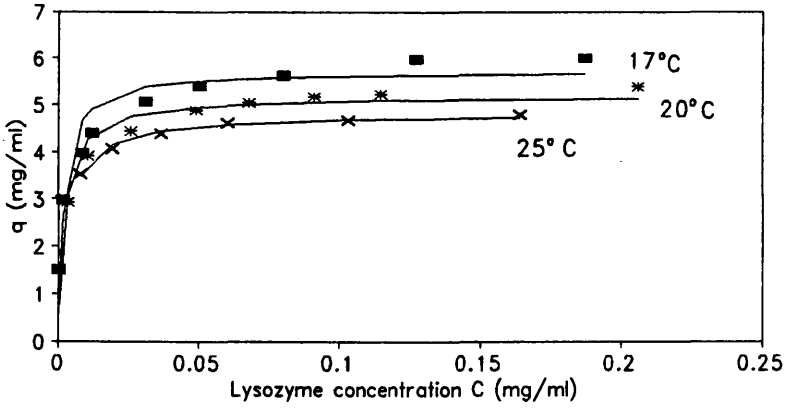

Fig. 5-3 Adsorption isotherms
Lysozyme-Cibacron Blue Sepharose

Adsorption kinetics measurement

Adsorption kinetics were measured using a modification of the above technique.

A known volume of the resin was added to a solution containing a given amount

of adsorbate while the mixture was stirred rapidly. The solution was rapidly recycled, and adsorbate concentration was monitored from changes in UV absorbance. A typical plot of adsorbate concentration against the time is shown in Fig. 5-4. Adsorption rate was calculated from each initial gradient in those concentration-time curves in view of a negligible initial desorption rate relating to a very small initial adsorption amount (refer Eq. 1-1). The "best estimates" of the Langmuir equilibrium (refer to Eq.1-2) and kinetic parameters obtained using a least squares criteria are shown in Tables. 5-1a and 5-1b.

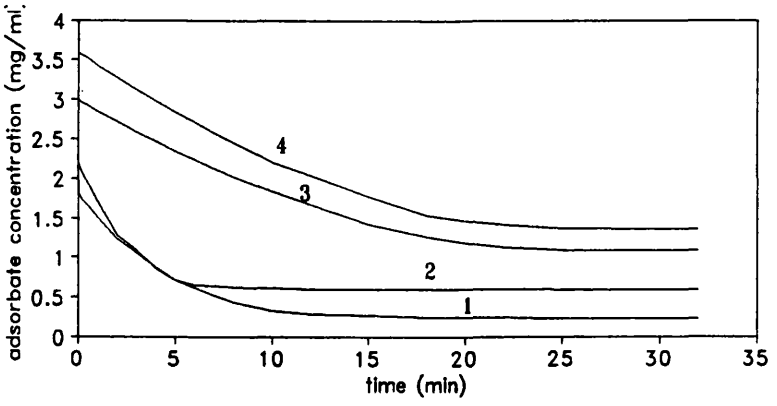

Fig.5-4 Plots of adsorbate concentration in solution aganist time

1 and 2 : aspartic acid- DEAE based ion-exchager at 10 and 20 C

3 and 4 : lysozyme- Cibacron Blue sepharose at 17 and 20 C

Table. 5-1a Adsorption paraments of aspartic acid-DEAE ion exchanger

T (^{0}C)	q_m (mg/ml)	K_d (mg/ml)	k_1 (ml mg^{-1} min^{-1})	k_2 (min^{-1})
10	12.6	0.0058	0.107	0.0006
20	11.9	0.0044	0.135	0.0006

Table.5-1b Adsorption parameters of lysozyme-Cibacron Blue

T (^{0}C)	q_m (mg/ml)	K_d (mg/ml)	k_1 (ml mg^{-1} min^{-1})	k_2 (min^{-1})
17	5.73	0.0019	0.088	0.00017
20	5.19	0.0023	0.087	0.0002
25	4.82	0.0033	0.088	0.0003

5.4 Experimental methods

5.4.1 Point heat source tests

To investigate the sensitivity and response time of the thermistor system , as well as to estimate the thermal properties of the column packing material, point heat source tests were carried out. Heat was input in pulses or continuously by passing a known current through a 1 kΩ resistor implanted in the column.

5.4.2 Thermal monitoring adsorption experiments

Procedures

The column was equilibrated with the buffer, until both thermal and UV detector base lines stabilised (approximately 4 hours). The operation cycle was then initiated under computer control, the loading stage was started by automatically switching the 6 way valve onto the adsorbate solution reservoir, meanwhile the data logging system was started to log thermal and UV responses. After total breakthrough has occurred, the bed was washed with distilled water, then regenerated with 0.1 M NaOH. Finally it was washed with distilled water until the pH value returned to 7 prior to the next experiment.

The cycle control and data processing were performed by the computer using the program, "multlog" (listed in the appendix). For the conditions used the amplifier gain range was set to 200 for ion exchange systems and 1000 for the affinity system, and the PCL-818 analog input range was set to ±1 V.

Initial experiments were carried out using DEAE based beaded resin, and using thermistors with a reference external to the bed. In this system the flow rate was limited to less than 2.5 ml/min (superficial velocity (SV), 0.33 m/h) by the hydrodynamic characteristics of the bed.

In subsequent studies the Productiv™ perfusive resin was used, allowing the experiments to be carried out at a considerably wider range of flow rates (2.2-26.2 ml/min or SV 0.29-3.5 m/h). "In-bed" differential thermistors were also used in experiments conducted with Productiv™ resin in order to assess the advantage of such an approach, especially at high flow rate and under non-thermostatted conditions. Protein adsorption on both ion-exchange and affinity resins was also tested.

Operational conditions

It was expected that thermal signals would depend on flow rate and temperature as well as feed concentration. To study these relationships, a series of breakthrough runs under different conditions were undertaken. The conditions for the experiments are given in Tables. 5-2a and 5-2b.

Table.5-2a Conditions for ion exchange adsorption experiments (external reference thermistor system)

Run No.	bed height(cm)	temp. (°C)	concentration of feed (mg/ml)	flow rate (ml/min)	buffer **
a1	4.0	20	1.00	1.19	1
a2	4.4	20	1.00	1.57	1
a3	4.4	20	1.00	1.53	1
a4	4.4	20	1.00	1.43	1
a5	4.7	21.4*	1.20	2.34	1
a6	4.7	20	1.20	1.21	2
a7	3.6	20	0.50	1.66	1
a8	4.7	20	0.10	4.46	1
a9	4.7	20	1.20	0.80	2
a10	4.7	20	1.20	1.72	2
a11	4.7	22*	1.20	1.98	2
a12	4.7	21.4*	1.20	1.18	2
a13	4.7	17.5*	0.80	1.74	1
a14	4.7	25	1.20	1.00	2
a15	4.7	25	1.60	1.00	2
a16	4.7	25	2.00	1.00	2
a17	4.7	10	2.00	1.02	2
a18	4.7	10	2.00	1.50	2
a19	4.7	20	1.20	1.22	2
a20	4.4	20	1.00	5.00	4
a21	4.4	20	1.00	4.42	3
a22	4.4	20	1.56	4.12	3

* unthermostatted

** buffer code: 1. tris-Hcl, pH=7.2, 2.5 mM; 2. tris-Hcl, pH=7.2, 5mM; 3. Citric, pH=6.2, 5 mM; 4. Phosphate, pH=7.1, 5 mM.

Run No. was coded with axx, indicating that external reference thermistors were used.

Run a1-a7 and a9-a19 using beaded resin, run a8 and a20-a22 using perfusive resin.

Table.5-2b Conditions for ion exchange adsorption experiments (perfusive resin,"in-bed" reference thermistor system)

run No.	concentration of feed (mg/ml)	flow rate (ml/min)	buffer
b1	1.25	2.24	2
b2	1.5	5.59	2
b3	1.25	6.80	2
b4	1.0	16.4	1
b5	1.0	26.2	1
b7	1.25	17.5	1

Run No. was coded with bxx, indicating internal reference thermistors were used.

As, in practice, some biochemical separation processes are carried out at somewhat lower temperatures, a few of the experiments were carried out at 10°C to assess the influence of temperature on sensitivity. Also as in practice, the device should be as simple as possible, so some runs were carried out in a non thermosttated bath to assess the effects of inherent thermal "noise". Operational conditions used in the affinity systems are given in Table. 5-3. Adsorption of BSA onto DEAE based perfusive resin was carried out at a flow rate of 2.3 ml/min with a feed concentration of 5 mg/ml.

Table.5-3 Conditions for affinity adsorption experiments

run No.	concentration of feed (mg/ml)	flow rate (ml/min)	pH	buffer (tris) strength (mM)
1	1.2	1.02	7.2	2.5
2	2.0	0.82	7.2	5
3	5.0	0.82	7.2	5

5.5 Theory of heat transfer in packed beds

5.5.1 General consideration

Theoretical understanding of heat transfer in packed beds is a prerequisite for the successful application of thermal monitoring of packed bed performance. Clearly, the optimisation and scale up of such systems require that the process characteristics including heat and mass transfer and their relationship be well understood. However the immediate requirement is to develop a mathematical model which can provide a basis for the application of state estimation techniques.

Mathematical models for heat transfer in packed beds consist of a set of partial differential equations derived from a heat balance. Various simplifying assumptions have been made to solve these equations, resulting in methods which range from simple plug flow, linear isotherm, equilibrium controlled models, to sophisticated, non-linear isotherm, dispersed flow models. A summary on this topic can be found in Ruthven's text (1984), and a wide range of literature which deals with heat transfer in packed beds with gas flow. Yoshida and Ruthven (1983) obtained an analytical solution to heat and mass balance equations which describe the adsorption of moisture from air using 4A molecular sieve beds. The predicted breakthrough curves and temperature responses compared favourably with those obtained experimentally. Kaguei *et al.*(1985) developed a simple model to describe heat and mass transfer of carbon dioxide uptake on an active carbon bed. Assuming a linear isotherm they obtained an analytical solution. However

in most practical cases analytical solutions are unlikely to be obtained. Despite such extensive research, there are few reports on heat transfer in a packed bed with liquid flows.

5.5.2 Heat Transfer in packed beds with liquid flow

A two dimensional heat transfer model has been developed to describe thermal waves in the adsorption column. The model is based on four main assumptions which are detailed below:

a. The packing material together with the liquid is considered as a homogeneous system, in which the medium and the surrounding liquid are in local thermal equilibrium . This allows the rate of thermal diffusion to be expressed in terms of the overall heat conductivity and the temperature gradient in the medium. The validity of this assumption can be assessed by point heat source experiments, and will be discussed later.

b. Heat transfer due to radiation is negligible.

c. Heat generated by adsorption is uniformly distributed at any cross section of the bed, and temperature profiles in the bed show axial-symmetry. Fluid transport is in dispersed-plug flow.

d. The column wall thickness is negligible.

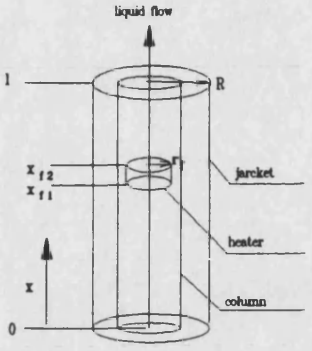

Fig.5-5 Diagram for heat transfer model set up

The heat balance then gives (refer to Fig. 5-5)

$$\frac{\partial T}{\partial t}=\frac{k}{c\rho}\frac{\partial^2 T}{\partial x^2}-v\frac{\partial T}{\partial x}+\frac{k}{c\rho}\left(\frac{\partial^2 T}{\partial r^2}+\frac{1}{r}\frac{\partial T}{\partial r}\right)+\frac{\Delta H}{c}\frac{\partial q}{\partial t} \tag{5-1}$$

with boundary conditions

$$\pm k\frac{\partial T}{\partial x}=h_c(T_0-T) \quad at\ x=0,\ x=l \tag{5-2}$$

$$k\frac{\partial T}{\partial r}=h_w(T-T_0) \quad at\ r=R \tag{5-3}$$

and natural boundary conditions at r=0

$$\frac{\partial T}{\partial r}=0 \tag{5-4}$$

where the adsorption rate, in the last term of Equation (5-1), may be calculated from the adsorption kinetic models which are described in the following section. In the case of a point heat source (in fact a heat source lies on a small region)

the last term in Eq (5-1) takes the following form:

$$\frac{\Delta H \partial q}{c \partial t} = c \frac{p_f}{(x_{f2} - x_{f1}) \pi r_f^2} \qquad x_{f1} < x < X_{f2}\ ,\ r < r_f \tag{5-5}$$

and elsewhere

$$\frac{\Delta H \partial q}{c \partial t} = 0 \tag{5-6}$$

where p_f=power of the fixed point heat source, and x_{f1}, x_{f2}, and r_f are the boundaries of the source (refer to Fig. 5-5).

5.5.3 Mathemetical description of the adsorption process

Stage model

A simple stage model to predict column performance developed by Hubble (1989) was used in conjunction with the above heat transfer model, allowing temperature profiles at any section in the bed, as well as the breakthrough curve, to be numerically calculated. The model takes an empirical approach to the adsorption process and assumes that all the rate limiting processes can be represented by lumped kinetic rate constants. In this model the bed is considered as a series of discrete stages. Each stage can be described as a well-mixed tank with adsorption proceeding for the residence time of the fluid in the stage. Thus the empirical rate equation (in the same form as equation 1-1) can be integrated with respect to time over the residence time in each stage, subsequently the average adsorption rate within this residence time may be calculated.

The empirical parameters k_1, k_2 and q_{max} can be estimated from the adsorption isotherm and rate data obtained in batch experiments, under an assumption that the adsorption equilibrium behaviour can be represented by the Langmuir equation.

A program based on the finite difference method has been written to sole the overall heat transfer model. In the program the step size in column length is set to equal the stage height. The program, coded as "heat transfer", and a sub-program, "sub-model" are given in the Appendix.

Film and pore diffusion model

In the stage model the overall adsorption process is specified by the empirical lumped parameters k_1, k_2 and q_m. While a more detailed consideration of the different steps that occur in a packed bed may lead to a more rigorous approach for modelling the adsorption process, a number of simplifying assumptions are usually made:

i) in-pore diffusion is expressed in terms of effective diffusivity and the gradient of adsorbate concentration in the pores.
ii) the adsorbent particles are uniform spheres with adsorption sites evenly distributed throughout the interior of the particles.
iii) mass transfer to the particle surface is described in terms of a film diffusion coefficient and the concentration difference;

iv) the axial mass diffusion is negligible.

The mass balance equation, *ie.* Eq. 1-3 is then becomes

$$\epsilon\frac{\partial C_i}{\partial t}=\epsilon D(\frac{\partial^2 C_i}{\partial r^2}+\frac{2}{r}\frac{\partial C_i}{\partial r})-(1-\epsilon)\frac{\partial q_i}{\partial t} \qquad (5\text{-}7)$$

where the last term is the surface adsorption rate, taking the same form of Eq. 1-1, however the parameters k_1, k_2 and q_{max} here are not lumped in the same manner as in the stage model. The boundary condition at $r_p=R_p$

$$k_f(C-C_i)=\epsilon D\frac{\partial C_i}{\partial r_p} \qquad (5\text{-}8)$$

and the natural boundary condition at $r_p=0$

$$\frac{\partial C_i}{\partial r_p}=0 \qquad (5\text{-}9)$$

Also the mass balance in the mobile phase gives (note the axial diffusion is neglected)

$$\frac{\partial C}{\partial t}=-v\frac{\partial C}{\partial x}-R_i \qquad (5\text{-}10)$$

where the last term, the rate of mass transfer through the liquid film to the particle surface (*ie* at $r_p=R_p$), may be described by:

$$R_i=k_f D\frac{3}{R}\frac{(1-\epsilon_b)}{\epsilon_b\epsilon}(C-C_i) \qquad (5\text{-}11)$$

To solve these equations 7 parameters have to be estimated, they are k_1, k_2, q_{max}, D, k_f, ϵ, and ϵ_b. For the first three some authors (Chase 1984; Cowan *et al.* 1986) took the values determined in the isotherm and batch uptake experiments as their

initial estimates and then adjusted them to get the best fit for the earlier part of the breakthrough curve. A semi-empirical method (Foo and Rice, 1975) may be used to estimate k_f, however determination of the effective pore diffusivity D is difficult. Horstmann *et al* (1989) treated D as a unknown parameter which was determined by fitting the predicted to the experimental results.

A simple program based on the finite difference method written as a subroutine to the heat transfer program was used to solve the film and pore diffusion model, and is give in the Appendix ("Sub-film and pore diffusion").

5.5.4 Overall heat conductivity and heat transfer coefficient

In view of the high water content (89% approximately) of the packed bed, a reasonable estimation of the heat conductivity, k, is between 89% and 100% of the value of water (0.36 J/cm K min, Cornwell 1977), hence k is given as 0.33 J/cm K min. In this work the column with its jacket is placed in a water bath, which is in forced convection, and for such a case the method to determine the heat transfer coefficient has been well established (Cornwell 1977). The following relations may be applied

$$N=0.027Re^{0.8}Pr^{0.33}\left(\frac{\mu}{\mu_0}\right)^{0.14} \qquad (5\text{-}12)$$

$$h_c=\frac{k}{d}Nu \qquad (5\text{-}13)$$

Taking the velocity of water flow along the jacket wall as 2 m/min, a value of h_c

$= 1.64$ J/cm^2 K min may be obtained.

5.5.5 Estimating adsorption heat

To solve the heat transfer model values for the adsorption heats are required, however the data of adsorption heat for liquid-solid systems are rarely available. Fortunately the good agreement between the calculated and observed temperature profiles in point heat source experiments (described in the later section) allows the estimation of the adsorption heat given the following assumptions:

a. A heat source caused by an adsorption front moving along the column may be approximated by a moving point source, hence the power of the point source can be used as an approximation of that caused by the adsorption.

b. At a certain point the temperature increase caused by a point source nearby is in proportion to its power at steady state. This has been supported by the results of the point source experiments.

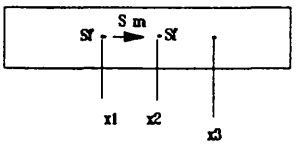

Sf : point heat source with power Pf

Sm : moving heat source with power Pm

Fig. 5-6 Diagram for power estimation of a moving source

Consider a moving point source s_m (refer to Fig. 5-6) with an unknown power p_m which moves from position x_1 to position x_2 in a time interval t, resulting in a temperature increase ΔT_m at a subsequent point x_3. This can be bounded in terms of two separate changes: a fixed point source at x_1 with a power of p_f causes a temperature increase ΔT_1 at x_3, and a second fixed point source at x_2 with the same power resulting in a temperature increase ΔT_2 at x_3. Under these conditions the following relationship is applied:

$$\frac{p_f}{\Delta T_1} < \frac{p_m}{\Delta T_m} < \frac{p_f}{\Delta T_2} \tag{5-14}$$

hence p_m can be estimated, as ΔT_1 and ΔT_2 may be calculated from the model. If x_1, x2, and the time interval are chosen in such a way that the speed of the moving point source equals that of the adsorption front, the adsorption heat may be estimated.

5.6 thermal response in packed beds-results

5.6.1 Temperature profiles in point heat source experiments

A typical example of temperature response to pulse or step heat inputs are shown in Fig. 5-7. It can be seen the response to a step heat input gradually reached a steady state. Fig. 5-7 also shows the model prediction. The good agreement implies that the assumptions for the model and estimations of the thermal parameters are reasonable. Fig. 5-8 shows approximate proportionality between the steady thermal response and the power input.

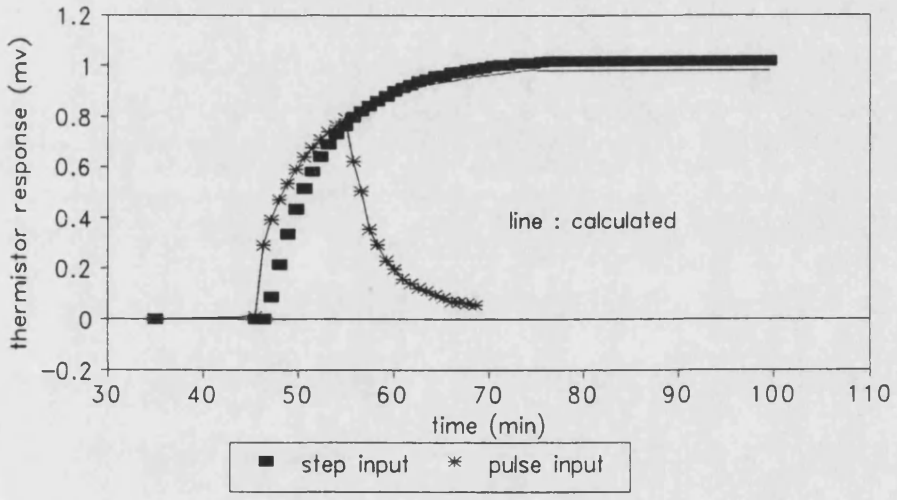

Fig. 5-7 Thermal responses to pulse and step power inputs

heat power : 4 J/min ; thermal response given by thermistor 8
heat source and thermistor positions refer to Fig. 4-3
temperature : 25° C

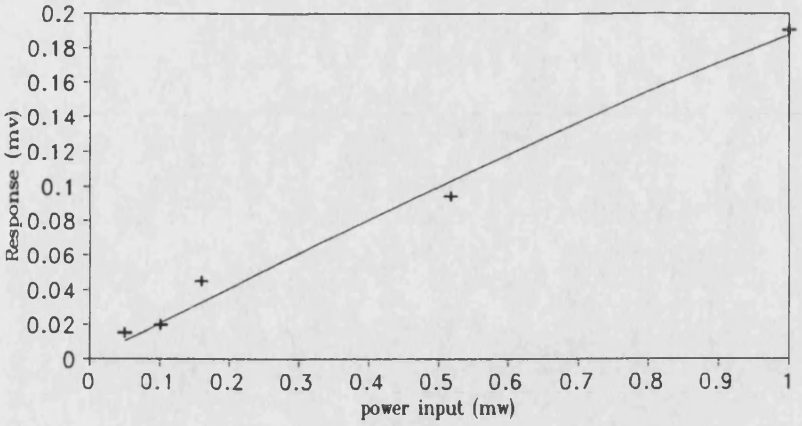

Fig. 5-8 A plot of steady thermal response against input power

heat source: at 2.75 cm ; flow rate : 1 ml/min

5.6.2 Thermal responses to aspartic acid uptake-ion exchange systems

Thermal responses using external reference thermistors

Throughout all the breakthrough experimental runs thermal responses to aspartic acid uptake on the bed were clearly observed. Typical thermal response curves during the loading stages for adsorption experiments conducted using the lowest (0.1 mg/ml), middle, and the highest feed concentrations (2.0 mg/ml) are shown in Figs. 5-9, 5-10a, 5-10b, and 5-11. The adsorption run using the lowest concentration (0.1 mg/ml) was aimed to assess the limitation of the measurable thermal effect. This run was terminated prior to complete bed saturation due to the extended time requirement to saturate the whole bed. Fig. 5-10b shows thermal response profiles at a low operational temperature (10°C). Figs. 5-10a and 5-10b also show the thermal responses to the bed washing. In the washing stage the weakly bound substances was being washed out, and this resulted in a

negative thermal effect.

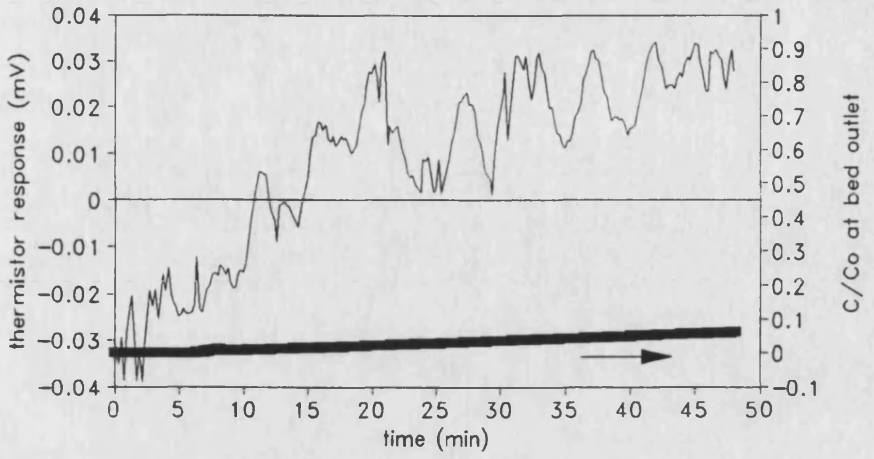

Fig.5-9 Thermal response to aspartic acid uptake
feed concentration: 0.1 mg/ml
flow rate 4.2 ml/min (run a8)

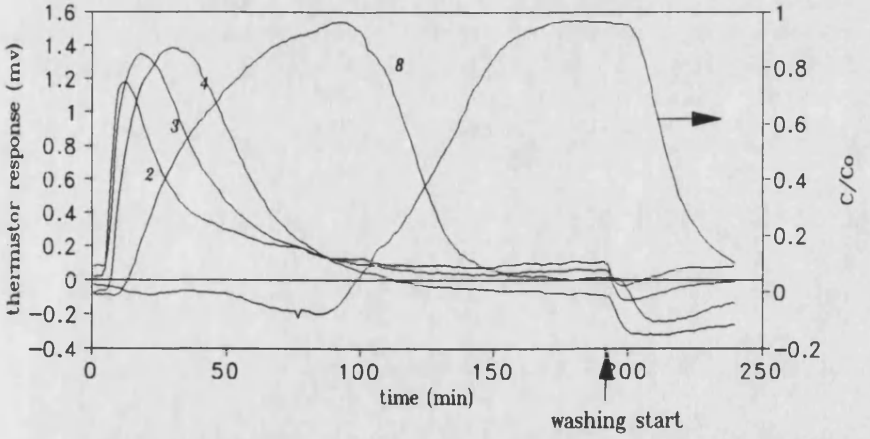

Fig.5-10a Thermal responses in loading and washing stages (run a3)

feed concentration : 1.0 mg/ml ; flow rate : 1.53 ml/min
washing started at 188 min
2, 3, 4, and 8 ; thermal responses sensed by thermistors at given positions
refer to Fig. 4-3

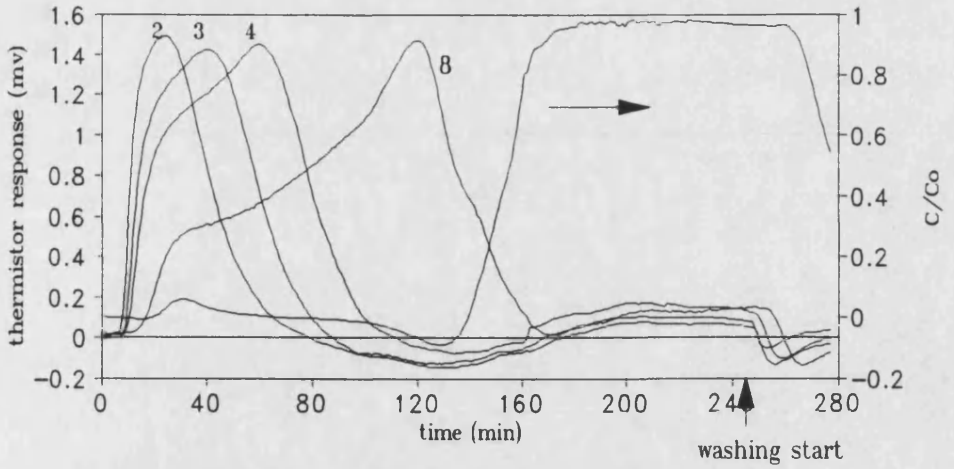

Fig.5-10b Thermal responses in loading and washing stages (run a4)

feed concentration 1.00 mg/ml ; flow rate : 1.43 ml/min
washing started at 244 min Water bath temperature 10 C
2, 3, 4, and 8 : thermal response sensed by thermistors at given position

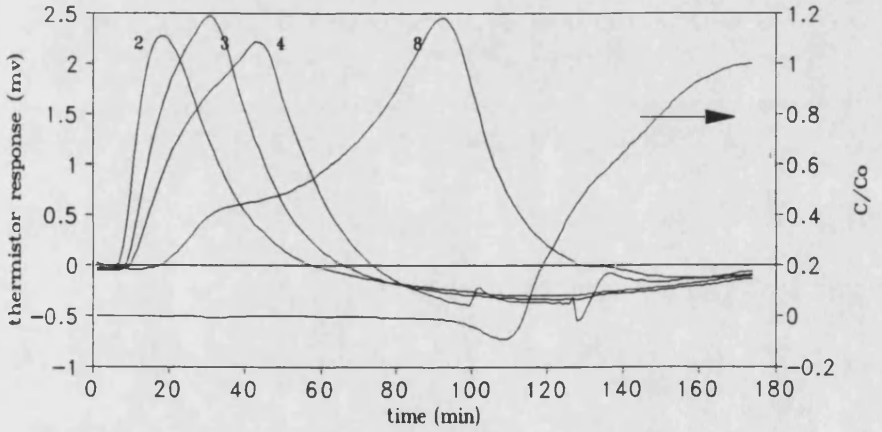

Fig.5-11 Thermal responses in loading stage (run a16)

feed concentration : 2.0 mg/ml; flow rate ; 1.0 ml/min
water bath temperature : 25 C
2, 3, 4, and 8: thermal response sensed by thermistors at given position
refer to Fig. 4-3

Results for experiments conducted using unthermostatted water bath are shown in Fig. 5-12, and for those conducted using citrate and phosphate buffers are

shown in Figs. 5-13, and 5-14. The thermal signal measured in millivolts (mV) results from the temperature increment at the thermistor position within the bed to the common reference external to the bed.

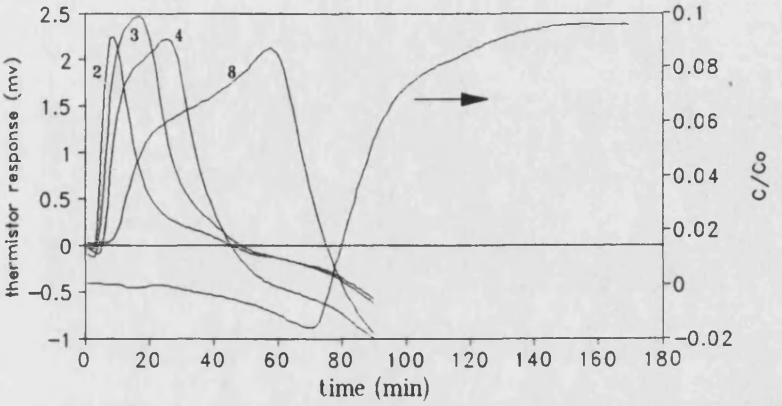

Fig. 5-11 Thermal responses in Loading stage (run a12, unthermostatted)

feed concentration ; 1.20 mg/ml; flow rate : 2.34 ml/min

room temperature : 25 C

2-8 : thermal responses sensed by thermistors at given positions

refer to Fig. 4-3

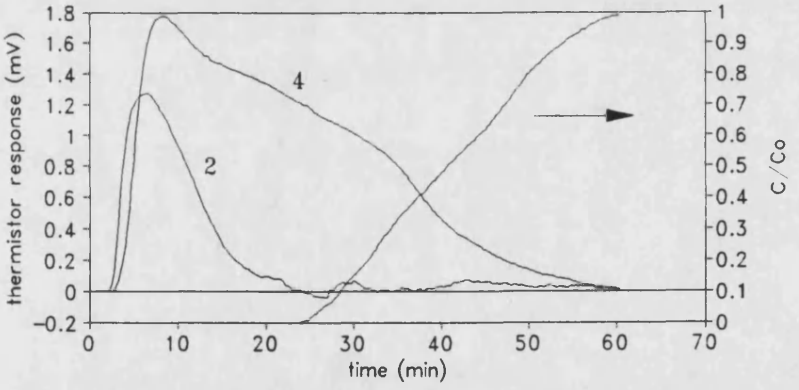

Fig.5-13 Thermal responses in loading stage (run a21, citrate buffer)

feed concentration : 1.5 mg/ml ; flow rate ; 7.32 ml/min

2 and 4 : thermal responses sensed by thermister at positions 2 and 4

refer to Fig. 4-3 for sensor positions

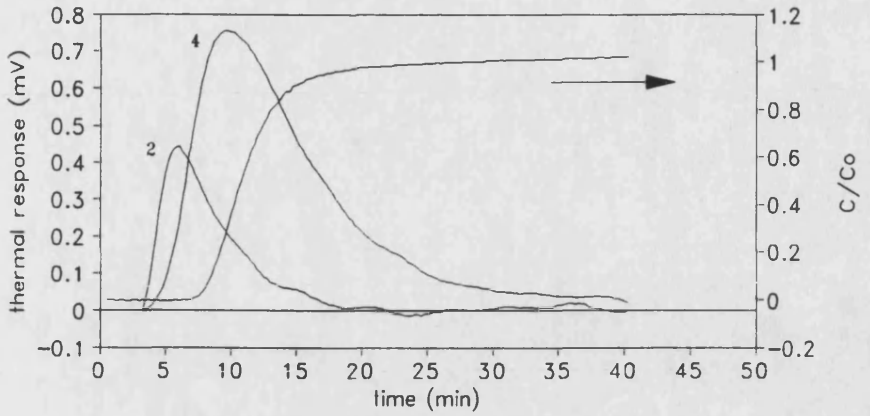

Fig. 5-14 thermal responses in loading stage (run a20, phosphate buffer)

feed concentration : 1.5 mg/ml ; flow rate ; 5.0 ml/min
perfusive resin
sensor positions refer to Fig. 4-3

"In-bed" differential thermal response

Typical results at flow rate values of 2.24 and 26.2 ml/min (0.29 and 3.5 m/h) are shown in Figs. 5-15 and 5-16 indicating that, as expected, the adsorption breakthrough curve follows the thermal profile, *ie.* the temperature difference between two given thermistor positions within the column. Fig. 5-17 shows the results obtained under non-thermostatted conditions. As the adsorption front moves down the column the first thermistor will initially be at a higher temperature than the second, as adsorption proceeds a point will be reached where the second thermistor will reach a higher temperature than the first. The typical trace of a peak followed by a trough can be seen for results at both the highest (26.2 ml/min) and the lowest (2.24 ml/min) flow rate (refer to Figs. 5-15 and 5-16)

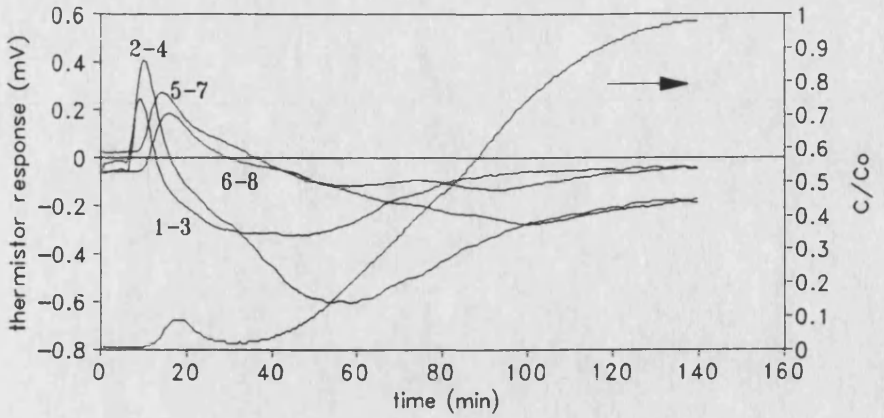

Fig. 5-15 In-bed differential thermal responses in loading stage (run b1)

feed concentration : 1.25 mg/ml ; flow rate : 2.24 ml/min

2-4 et al. : differential thermal responses sensed by the given thermistor pairs

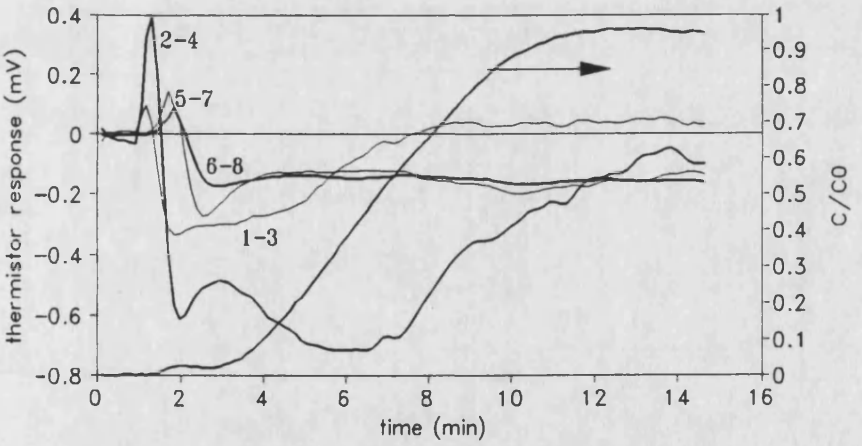

Fig. 5-16 In bed differential thermal responses in loading stage (run b5)

feed concentration : 1.0 mg/ml ; flow rate : 26.2 ml/min

1-3 et al : thermal responses sensed by given thermistor pairs

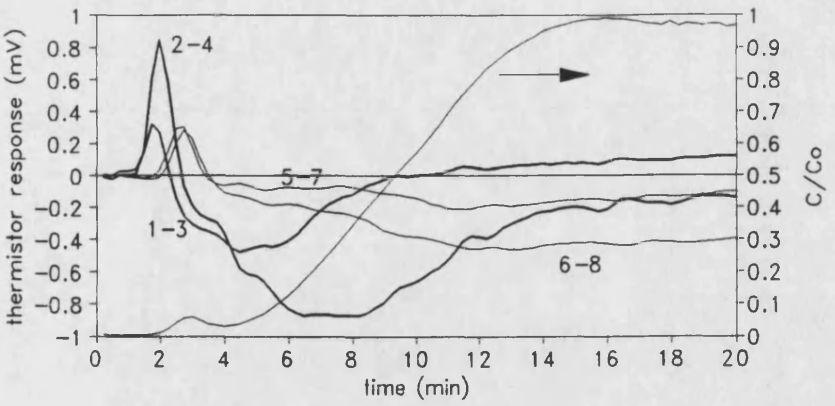

Fig.5-17 In-bed differential thermal responses in loading stage (run b6)

feed concentration : 1.25 mg/ml ; flow rate : 17.3 ml/min

unthermostatted (air filled jacket)

1-3 et al : thermal responses sensed by given thermistor pairs

5.6.3 Protein adsorption systems

Thermal responses to lysozyme uptake onto Cibocron Blue Sepharose were much weaker than in ion exchange processes, only those using the highest feed concentration (5 mg/ml) were vaguely observed, and were shown in Fig. 5-18. The signal and the noise are almost at a similar level. No thermal responses to BSA uptake onto DEAE based ion exchange resin were observed.

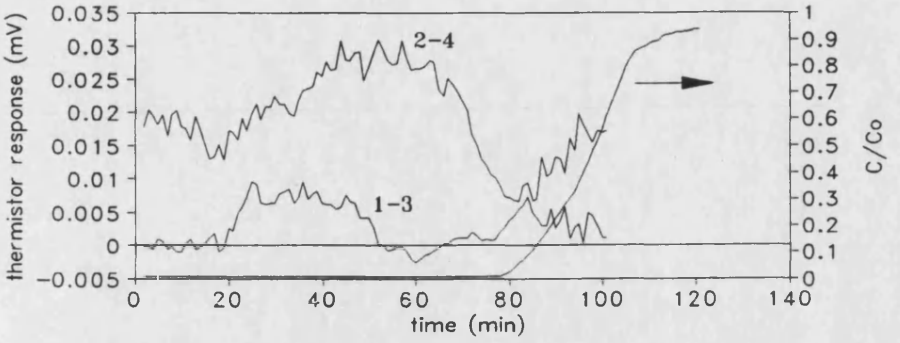

Fig. 5-18 In-bed differential thermal response in loading stage

Lysozyme-Cibacron Blue Sepharose Affinity system

feed concentration : 5.0 mg/ml; flow rate : 0.82 ml/min

1-3, and 2-4 : thermal responses sensed by given thermistor pairs

5.6.4 Adsorption heat

Taking point sources at x1=0 and x2=0.5 cm (refer to Fig. 5-6) the predicted temperature profiles at x=1.0 were calculated and shown in Fig. 5-19. A selected thermal response profile (sensed by thermistor No. 3 in run a6, refer to Fig. 5-10b) is also shown in Fig. 5-19 for comparison. According to the foregoing assumptions, Eq. 5-15 applies until the adsorption front (moving source) passes position x2. After 18.5 minutes the adsorption front reached x=0.5, and the thermal signal sensed by the thermistor at x3=1.0 cm was 1.32 mV. Using this data together with the heat power of the dummy point sources, the adsorption heat is estimated to be 138 J/g (18 KJ/mole). Although no literature data for this adsorption system were found for comparison, the estimated value is at a similar level to that obtained for ion exchange adsorption on Amberlite resin by Groszek (1988) using a micro-calorimeter.

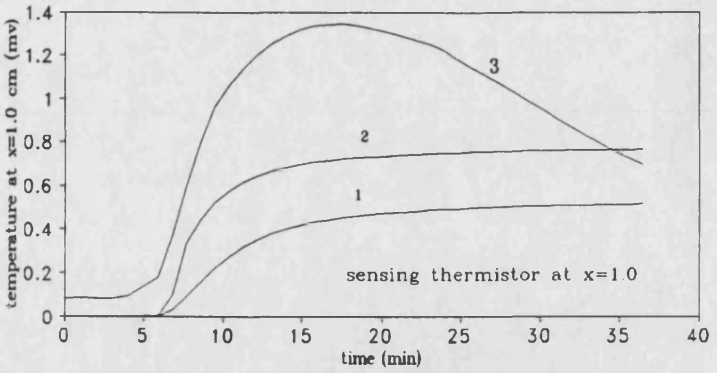

Fig. 5-19 Predicted profiles of thermal responses to point sources

1 : response to a point source at x=0 ; 2 : response to that at x=0.5 (refer to Fig. 5-6)

3 : response to aspartic acid uptake (see Fig. 5-10a)

flow rate : 1.0 ml/min

5.6.5 Comparison of in-bed differential and common reference methods

Performance difference between in-bed differential and external reference systems in baseline stability has been discussed in Chapter. 4. In practice the "in-bed" differential system performs much better than the system with common reference under non-thermostatted conditions. This can be demonstrated by comparison of Fig. 5-12 with Fig. 5-17. Under such operational conditions the thermal responses of the "in-bed" differential system showed significantly lower drift.

5.7 Influences of operational temperature flow rate, feed concentration, and buffer

5.7.1 Operational temperature

A comparison of thermal response profiles obtained at lower operational temperature (Fig. 5-10b) with those at normal room temperature (Fig. 5-10a) shows that no significant influence of temperature changes on sensitivity was

found. This is not surprising given the fact that adsorption heats are usually a weak function of the temperature.

5.7.2 Flow rate and feed concentration

Thermal responses, as expected, were dependent on both feed concentration and the flow rate. These dependencies are shown in Figs. 5-20 and 5-21 using beaded resin, and external reference thermistors. The overall dependence of thermal response on the feed rate, which can be defined in terms of the amount of adsorbate input per unit time, is shown in Fig. 5-22, giving an approximately linear relationship (obtained using the least squares method) under the conditions used (flow rate less than 2.5 ml/min or 0.32 m/h). If 0.1 mV is take as a limit for the resolution of the temperature profiles this implies a minimum practical feed concentration of 0.1 mg/ml for the experimental system in its current form. However, over the range studied, high feed concentrations will result in more precise resolution of the temperature profiles.

For the experiments conducted using perfusive resin and "in-bed" reference thermistors, within a relatively wide range of flow rates, the peak value of thermal responses with respect to the unit concentration in terms of mV/(mg/ml) firstly increases with the flow rate up to 16.2 ml/min and then drops as the flow rate is further increased (Fig. 5-23). This effect may be explained as follows: the temperature rise produced by adsorption is a balance between the rate of heating by adsorption and cooling by conduction and convection. At low feed rate, thermal conduction, which is independent of flow rate, predominates and the

temperature rise is low. As flow rate is increased, and, after a certain value, convection become more significant. Fig. 5-23 also shows the signals obtained from thermistors mounted at a number of axial positions in the bed, and indicates that there is an optimum position for maximum sensitivity.

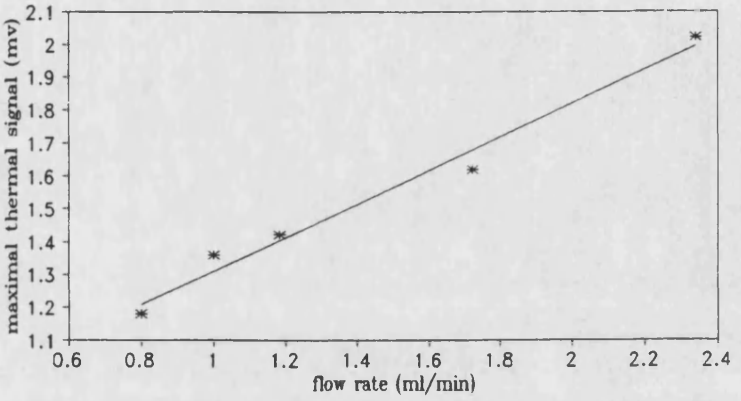

Fig. 5-20 Effects of flow rate on thermal signals
(external reference system)
feed concentration : 1.2 mg/ml

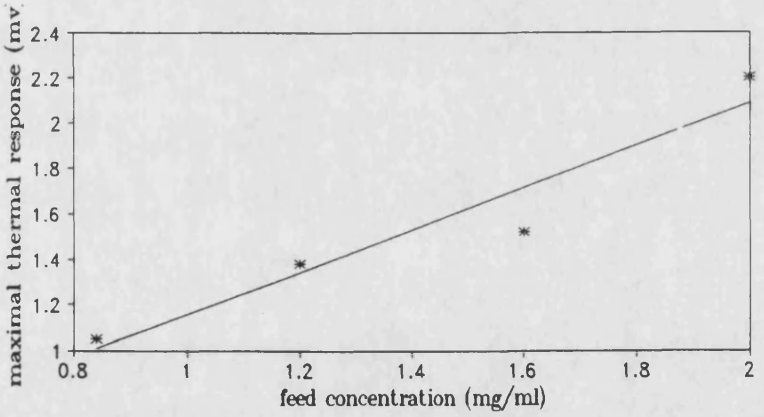

Fig. 5-21 Dependence of thermal responses on
feed concentration
flow rate : 1.0 ml/min ; external reference system

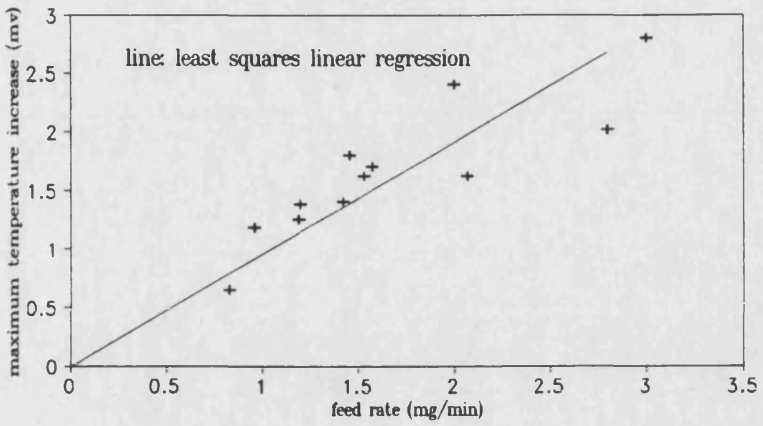

Fig. 5-22 Dependence of the maximum thermal response on Feed Rate

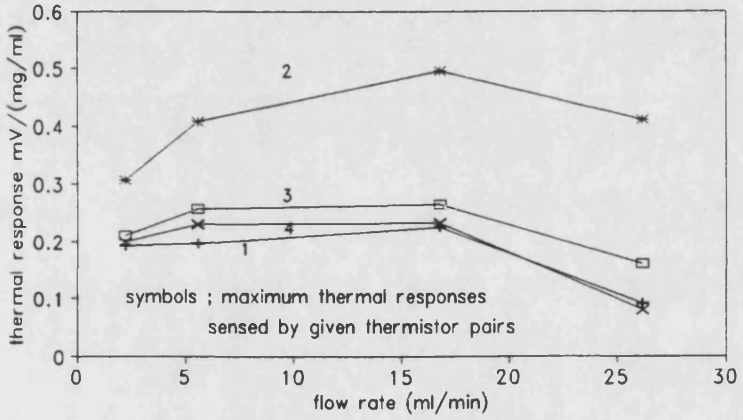

Fig.5-23 Effect of flow rate on in-bed differential thermal responses

1----4: thermistor pairs 1-3, 2-4, 5-7, 6-8 respectively
refer to Fig. 4-3

5.7.2 Buffer

Bed capacity for aspartic acid was found to be highly dependent on the buffer used. In citrate buffer the highest bed capacity was obtained (Fig. 5-13), and the

lowest in phosphate buffer (Fig. 5-14). Despite the difference in bed capacity in different buffers, the thermal response to aspartic uptake is mainly dependent on the flow rate and feed concentration. The reason is that temperature increase in the column is dependent on the heat emission rate which is mainly dependent on the flow rate and feed concentration. Similarly, the pH value influences the bed capacity rather than the heat of adsorption.

5.8 Relationship between thermal responses and the adsorption front

5.8.1 Coincidence of thermal responses and the adsorption front

From the temperature profiles shown in Fig. 5-10 through 5-12 the time (defined as thermal peak time), at which the maximum temperature is measured by a particular thermistor was found to be linearly related to its position, and this linear relationship is shown in Fig. 5-24, and Fig. 5-25. By examining the breakthrough curves, it was found that an extrapolation of this relationship to a point equal to the column length gave a consistent prediction of the time to reach 20% breakthrough. This suggests there is coincidence of the maximum thermal response and the adsorption front. This coincidence can be further demonstrated by a linear plot of the elution volume passed at the thermal peak time against the thermistor position at a unique feed concentration (shown in Fig. 5-26). This gives a simple prediction of the position of the adsorption front from the thermal measurements.

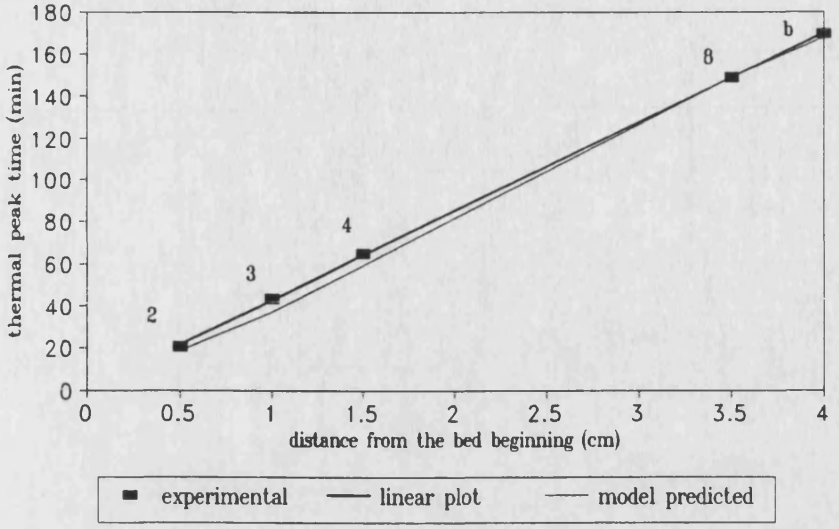

Fig. 5-24 Dependence of thermal peak time on position (run a1)

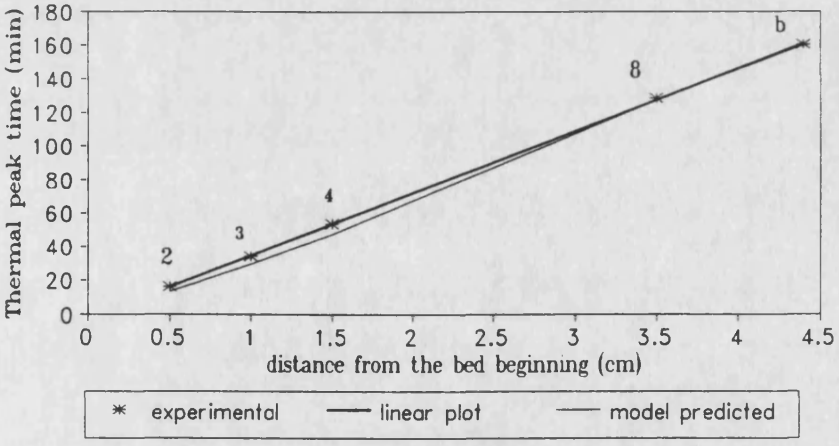

Fig.5-25 Dependence of thermal peak peak time on position (run a4)

2-8 : thermistors ; b : 20% breakthrough

the stage model was used in both Figs. 5-24 and 5-25

refer to Fig 4-3 for sensor positions

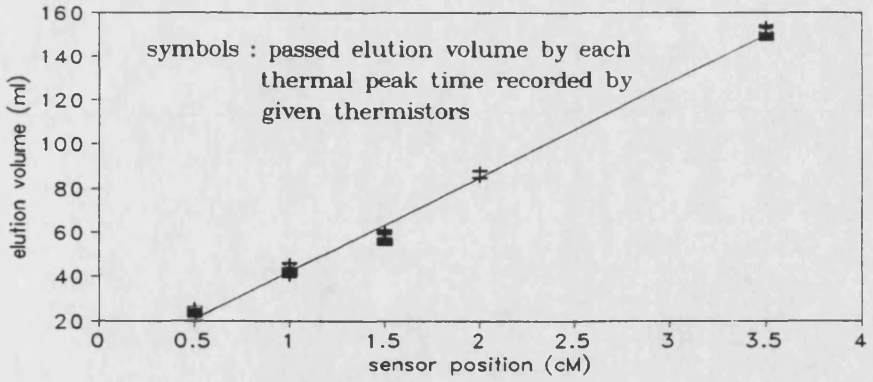

Fig.5-26 Plot of Elution volume passed at thermal peak time against position

fixed feed concentration (1.2 mg/ml) were used
external reference system

5.8.2 A linear correlation of the elution volume ratio

Taking into account the effect of feed concentration, the above relationship can be expressed in terms of elution volume ratio, which can be defined as a ratio of elution volume at the thermal peak time to that at a specified fractional breakthrough. Fig. 5-27 shows a linear plot of elution volume ratio to that of 20% breakthrough against thermistor position, and this can be described as follows:

$$\textit{elution volume ratio} = -0.0185 + 0.2143\,x \qquad (5\text{-}15)$$

Using perfusive resin operated with in-bed differential thermistors similar results were obtained and are shown in Fig. 5-28. The linear relationship between the elution volume ratio and the thermistor location can be written as:

$$\textit{elution volume ratio} = 0.2512 + 0.2106x \qquad (5\text{-}16a)$$

$$\textit{elution volume ratio} = 0.182 + 0.1141\,x \qquad (5\text{-}16b)$$

where Eqs. 5-16a and 5-16b are in respect of 20% and 3% breakthrough

respectively, and x refers to the sensor position.

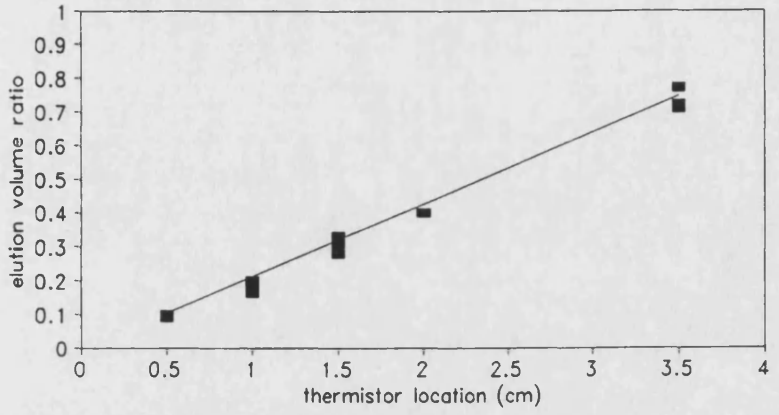

Fig. 5-27 Plot of elution volume ratio against thermistor location
(to 20% breakthrough elution volume)

External reference thermistor system

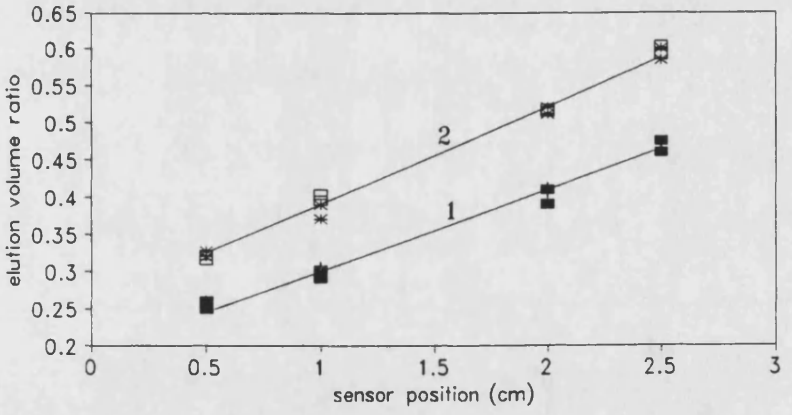

Fig.5-28 Liner plot of the elution ratio against the position
Internal differential thermal sensor system
1: to 3% breakthrough ; 2: to 20% breakthrough

5.9 Comparison of experimental results with theory

5.9.1 Parameter determination

Estimates of adsorption parameters (q_m, k_1, and k_2) obtained in batch experiments were used in the stage model. To use the pore and film diffusion model the value of q_m is required in terms of weight of bounded adsorbate per unit volume of pure resin, which was calculated to be 166 mg/ml. Particle voidage $\epsilon = 0.89$ was estimated from the water content of the wet resin, and bed voidage $\epsilon_b = 0.35$ estimated by consideration of the settled volume and the weight of the resin (wet) added. k_f was estimated as 0.2 cm/min using the approach proposed by Foo and Rice (1975), and finally the value of D (0.0012 cm^2/min for aspartic acid) is taken to be that give the best fit to the observed curve.

5.9.2 Simulation results

Model simulations of thermal responses and breakthrough were carried out using the stage model and the film and pore diffusion model. Thermal response in both in-bed differential form and in terms of temperature increment to an external common reference were simulated.

Thermal response using external reference system

For these cases examples of the calculated temperature and outlet concentration profiles are given in Fig. 5-29 and Fig. 5-30 using the stage model, and in Fig. 5-31 and Fig. 5-32 using the pore and film diffusion model. For the studied system no significant difference is found between the use of the stage and diffusion

models provided the feed concentration is above 1.0 mg/ml, however, the fit predicted using diffusion model was better in the case of a lower feed concentration (run 7)

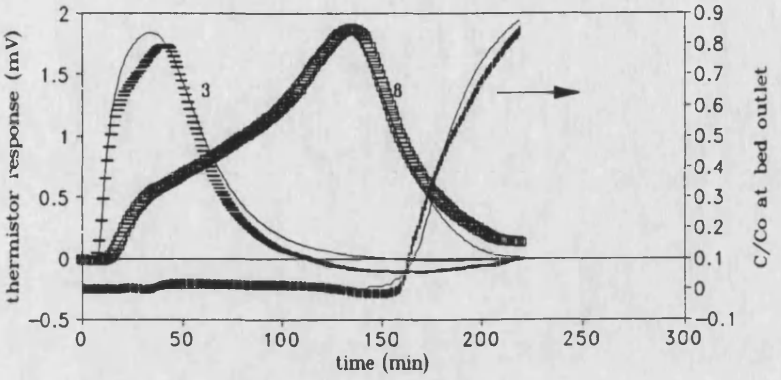

symbols : experimental data ; line : model prediction

Fig. 5-29 Model simulation of thermal and breakthrough profiles (stage model)

feed concentration: 1.2 mg/ml ; flow rate : 1.21 ml/min (run a6)

3 and 8 thermal responses sensed by given thermistors

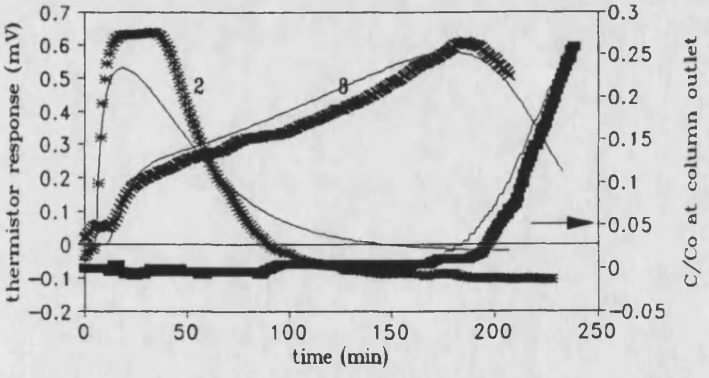

symbols : experimental data ; line : model prediction

Fig. 5-30 Model simulation of thermal and breakthrough profiles (stage model)

feed concentration : 0.5 mg/ml ; flow rate : 1.66 ml/min (run a7)

2 and 8 : thermal responses sensed by given thermistors

refer to Fig. 4-3 for thermistor positions

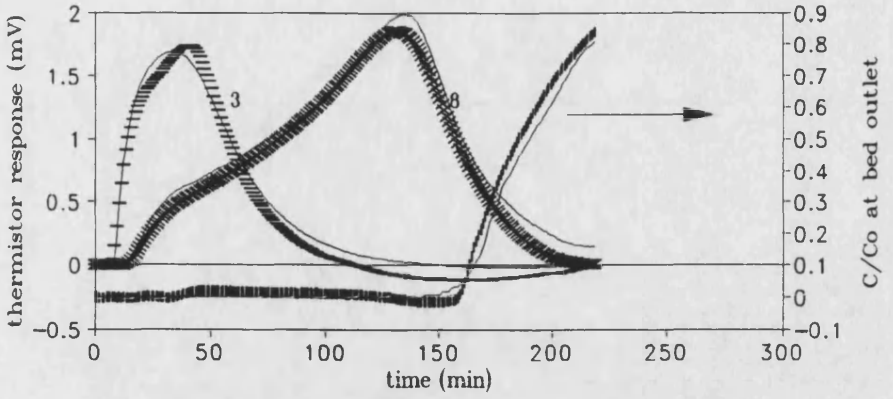

symbols : experimental data ; line : model prediction

Fig. 5-31 Model simulation of thermal and breakthrough profiles

(pore and film diffusion model)

feed concentration: 1.2 mg/ml ; flow rate : 1.21 ml/min (run a6)
3 and 8 : thermal responses sensed by given thermistors
refer to Fig. 4-3 for sensor positions

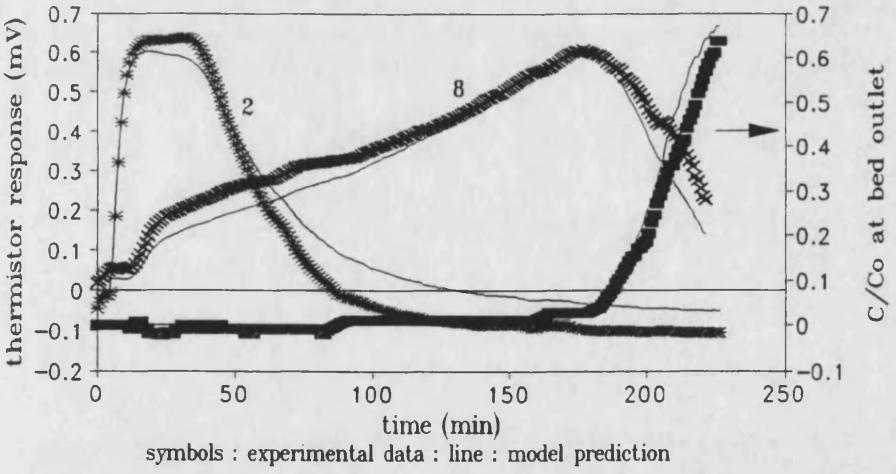

symbols : experimental data : line : model prediction

Fig. 5-32 Model simulation of thermal and breakthrough profiles (pore and film diffusion model)

feed concentration : 0.5 mg/min : flow rate : 1.66 ml/min (run a7)
2 and 8 : thermal responses sensed by given thermistors
refer to Fig. 4-3 for sensor positions

Fig. 5-29 through Fig. 5-32 show that both stage and pore and film diffusion models can give good fits to the thermal response results. This suggests that the overall heat transfer model is acceptable.

For breakthrough curves, a good agreement to the initial region is obtained, however there is a significant deviation in the later part of the curves obtained by using both stage and diffusion models. A similar problem has also been described by Skidmore *et al* (1990), and a possible explanation is the range of the particle size distribution in the resin preparation used.

The thermal response peak times were also determined from the simulation results, and were shown in Figs. 5-24 and 5-25 for comparisons. In the upper region of the column the observed thermal waves are a little slower than the predicted. A possible explanation for this apparent slow movement of thermal waves in the upper region of the column is that the liquid flow may be disturbed by channelling effects resulting from uneven packing. Once a fraction of the liquid flow bypasses part of the adsorbent, saturation in the upper region of the bed would be delayed, and in turn thermal waves in the same region would be slowed.

"In-bed" differential thermal response

Simulations of in-bed differential thermal responses were attempted. The results (Fig. 5-33) show that there are significant fitting errors. These will be discussed in Chapter. 8.

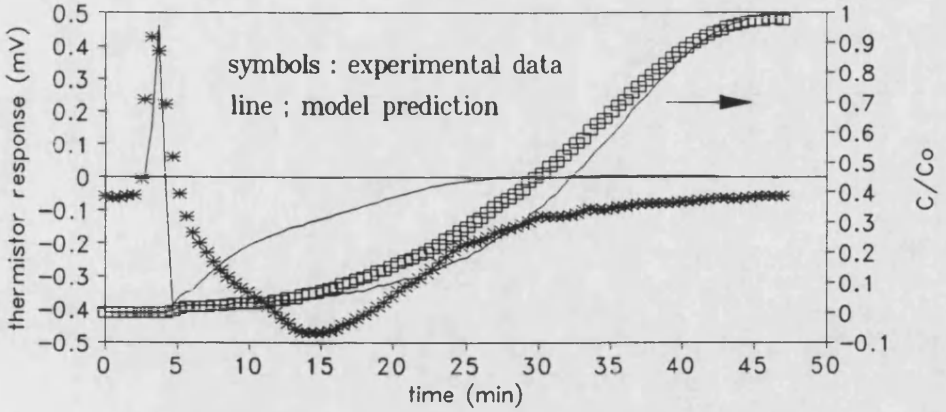

Fig. 5-33 Model simulation of thermal and breakthrough profiles

(internal differential thermal response)

feed concentration : 1.25 mg/ml ; flow rate : 6.8 ml/min

run b3 , thermal responses sensed by thermistor pair 2-4

refer to Fig. 4-3 for sensor positions

5.10 Prediction of breakthrough and optimization of thermistor position

5.10.1 Breakthrough prediction

The prediction of breakthrough is based on the coincidence of the trajectories of thermal waves and the adsorption front. The simplest procedure is to form a linear correlation of the elution volume ratio, *ie* Eq. 5-15 or Eq. 5-16, so that the time when the breakthrough reaches a certain degree (20%) can be directly obtained. This method of prediction, although simple, is subject to significant errors. A more precise prediction could be achieved by using model based estimation techniques such as the Kalman filter. In such an approach process modelling will play a basic role, and simple models with reasonable accuracy will be preferred because of the time limitation in real time computing. Alternatively, a neural network could be used to describe the complex relationship between

thermal signals and adsorption front position. These methods will be presented in later chapters.

5.10.2 Optimization of thermistor positions

Thermistors with a common reference external to the bed

The use of a series of thermistors may permit precise tracking of the adsorption front at the expense of greater complexity. In practice, the fact that the simple linear plot of the thermal peak time against the thermistor position can be extrapolated to give the time taken for 20% breakthrough at the column exit suggests that it is possible to use fewer sensor or even one for breakthrough prediction. The choice is based on a compromise of the following factors: i) extrapolation of a linear plot obtained by using thermistors close to the column entrance may be subject to significant errors; ii) a prediction based on the signal obtained by a thermistor close to the column exit may offer little advantage in terms of the ability to predict ahead. Considering these factors, an appropriate choice of the site for the thermistor installation is in the lower region of the column. Such a choice will also allow model simulation and prediction to be carried out in real time. The optimum position for the thermistor was found to be at a point equivalent to 60% of the column length *ie.* the position of thermistor No.8 which gave a maximum thermal peak in most cases.

"In-bed" differential thermistors

The results shown in Figs. 5-15 through 5-17 clearly indicate that the thermistor pair at the axial mid point of the bed gave signals significantly stronger than

others. Therefore the optimum position of the thermistor pair which gives maximum sensitivity is at No. 2-4.

5.11 The main factors on which the feasibility of the method depends

The approach described in this chapter is based on the fact that a measurable thermal process would occur during the adsorbate uptake in a packed column. According to Eq. 5-1 the shape and magnitude of thermal waves may strongly depend on the rate of adsorption heat evolution, the liquid flow rate, the heat conductivity, and the specific heat. In practice packed columns for biochemical separation are of high water content, so that the heat conductivity and the specific heat of the bed are close to those of water. The most important factor is the rate at which the adsorption heat is evolved. This will be a function of the adsorption heat (ΔH), and the overall adsorption rate which, under most practical conditions, will be limited by the column feed rate. For the studied ion exchange system, taking into account the adsorption heat estimated and the feed rate used, the rate of heat evolution can be calculated to be within the range of 0.11 - 0.62 J/min. This corresponds to maximum thermal response in the range of 0.62-2.8 mV. If 1.0 mg/min is taken as a usual feed rate and 0.1 mV as the limit for thermal wave resolution, the minimum adsorption heat is about 18 J/g for the rig to date. It is interesting to make a comparison with the similar approach in Pressure Swing Adsorption (PSA) (Matz and Knaebel 1987), in which the adsorption heat was about 150 J/g.

CHAPTER. 6 ON-LINE BREAKTHROUGH ESTIMATION USING THERMAL MEASUREMENT - APPLICATION OF EXTENDED KALMAN FILTERS

6-1 Two key problems in application of an EKF for state estimation

EKF techniques have been applied to a variety of chemical engineering systems including both batch and distributed parameter systems as described in Chapter. 3. The theory behind the EKF is well known, however the correct formulation of an EKF to make it effective for applications in real time processes is far less understood. There are two key problems. Firstly the model must be able to describe the system behaviour over the whole range of operational conditions. Secondly, the variation of main parameters should be taken into account. In early studies Kalman Filters were used to deal with processes with white noise characteristics, while in many chemical engineering processes the disturbances comprise both white and non-stationary noise. Neglecting the incorporation of non-stationary disturbances would result in an EKF little different from a fixed parameter model, and lead to non convergent performance of the EKF. This may be a reason why some researchers avoided the use of EKFs. Fortunately, this drawback can be overcome to a significant extent by simultaneous estimation of the model parameters and the state variables (DiMassimo, Lant and *et al.* 1992).

This chapter discusses the use of the EKF for estimation of the adsorbate concentration within the bed, and demonstrates how these two problems were dealt with. Firstly, a state space model is formulated, which, although simplified,

allows the process to be effectively described. This is followed by the formulation of an EKF based on this model, and the results of the model simulation. Finally the results of real time estimation of adsorption states and parameters are presented.

6.2 State space model for the thermal monitoring packed bed adsorption system

6.2.1 Simplified six stage heat and mass transfer model with fixed parameters.

The model development here is similar to that discussed in Chapter. 5, and the main assumptions are as before. However some simplifications were made, and the additional assumption terms are listed as follows:

a) The column consists of six stages, which is shown in Fig. 6-1, with the resin occupying four stages in the middle, and each stage is assumed to be a well stirred tank.

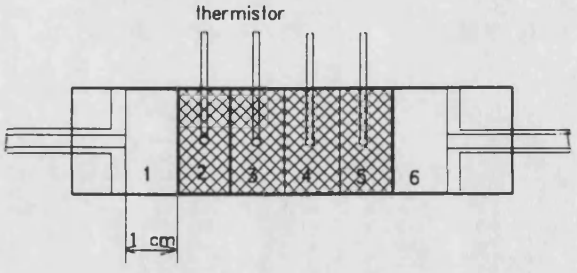

1 and 6 : glass beads
2, 3, 4, and 5 : DEAE ion-exchanger resin

Fig.6-1 Diagram for six stage model

Temperature at each stage is sensed by a centrally placed thermistor with an external reference. Theoretically a finely divided stage model would describe the process more precisely, but this would result in a high order model, and greatly increase the computing requirement. Therefore a compromise between precision and practicality was made. The simulation results which are shown later demonstrate that the six stage model adequately describes the process with acceptable precision.

b) The adsorption rate can be described using

$$R=k_1 c(q_m-q) - k_2 q \qquad (6-1)$$

where c and q are the adsorbate concentrations in the mobile and fixed phase respectively.

c) Heat loss rate through the column wall may be expressed in terms of the temperature difference between the inside and outside of the column. With this assumption the problem is reduced to a simple one dimension heat transfer step. This greatly simplifies formulation of the EKF and the associated computation effort.

The following equations can be derived from the heat balance,

$$\frac{T_i(n+1) - T_i{-}1(n)}{\Delta t} = \frac{k}{c\rho}\frac{T_{i+1}(n) - 2T_i(n) + T_{i-1}(n)}{h^2} - v\frac{T_i(n) - T_{i-1}(n)}{h} - \frac{k_w}{R_c c\rho}[T_i(n) - T_0] + \frac{R\Delta H}{c\rho} \qquad (6-2)$$

where i is the stage number, n the time step number, and R_c the column radius. The continuity of the heat flow gives the boundary condition

$$(T_1-T_o)\,h_c=\frac{(T_2-T_1)}{h}k \qquad (6\text{-}3)$$

$$(T_6-T_o)\,h_c=\frac{(T_5-T_6)}{h}k \qquad (6\text{-}4)$$

where T_o is the ambient temperature, here it was assumed to be 0.

Similarly a mass balance in the mobile phase gives

$$\frac{c_i(n+1)-c_i(n)}{\Delta t}=\frac{v}{v_s}\left[c_{i-1}(n)-c_i(n)\right]-k_1c_i(n)\left[q_m-q_i(n)\right]+k_2q_i(n) \qquad (6\text{-}5)$$

note that the axial diffusion is neglected.

The initial condition is $c_1 = c_o$ when $t>t_o$, and boundary condition $c_6=c_5$.

Whilst in the fixed phase a mass balance gives

$$\frac{q_i(n+1)-q_i(n)}{\Delta t}=k_1\left[q_m-q_i(n)\right]-k_2q_i(n) \qquad (6\text{-}6)$$

where it should be noted that as the resin was packed in the middle four stages, q = 0 in both the first and last stage.

The above equations can be numerically solved using the program, "heat transfer" (listed in the appendix) with a slight modification.

6.2.2 Extended state space model for the EKF

The above model can be modified to a state space form to represent the process by a set of first order difference equations. This modification not only transfers the model to an elegant form, but also provides a practical basis for the EKF formulation.

State vector for a packed bed adsorption system

In the state space model developed in this work all the temperatures, and adsorbate concentrations in both the mobile and fixed phases are treated as state variables. Some important parameters, such as q_m and the adsorption rate constant k_1, which determine dynamic behaviour of the system, could vary with time, consequently resulting in a severe model mismatch if not adjusted. One approach to overcome this problem is to estimate these parameters together with the main target states simultaneously, then to update their values on-line. To do this the parameters, q_m and k_1 are also included in the state variables. The dynamic behaviour of these two variables may be described as follows

$$q_m(n+1) = q_m(n) \; ; \qquad k_1(n+1) = k_1(n) \tag{6-7}$$

where n still refers to the time step number. Thus a state of the system can be represented with an extended state vector

$$\boldsymbol{X} = [x_1, x_2, \ldots\ldots x_{16}]^T \tag{6-8}$$

where x_1.....x_6 refer to the temperature variables in stages 1 to 6; y; x_7.....x_{10} to the concentrations in the mobile phase at stage 2 to 5, while the concentration

variables at stage 1 and 6 have been defined in the initial and boundary conditions; x_{11}.....x_{14} refer to the concentrations in the fixed phase at stage 2 to 5; and x_{15} and x_{16} to q_m and k_1 respectively.

System linearisation and model formulation

In order to apply the EKF technique Eqs. 6-2, 6-5, and 6-6 must be linearized. The equation for each element of the state vector may be simply described in the form of

$$x_i(n+1) = f_i[x_1(n), x_2(n), \ldots\ldots, x_{16}(n)] \qquad i=1,2\ldots16 \qquad (6\text{-}9)$$

where f_1.....f_{16} represent the functions in Eqs. 6-2, 6-5, 6-6, and 6-7, most of which are non-linear. A local linearization is performed by using the following Jacobi matrix (Schultz and Melsa, 1967)

$$\mathbf{A}(n) = \begin{bmatrix} \frac{\partial f_1}{\partial x_1} & \ldots\ldots & \frac{\partial f_1}{\partial x_{16}} \\ \vdots & \ldots\ldots & \vdots \\ \vdots & \ldots\ldots & \vdots \\ \frac{\partial f_{14}}{\partial x_1} & \ldots\ldots & \frac{\partial f_{14}}{\partial x_{16}} \\ 0 & \ldots\ldots & 1 \quad 0 \\ 0 & \ldots\ldots & 0 \quad 1 \end{bmatrix} \qquad (6\text{-}10)$$

where the partial derivatives are calculated at the time step n, hence the 16x16 matrix A is time varying. The state space model can be written in the form

$$X(n) = \mathbf{A}(n-1)X(n-1) + \mathbf{W}(n-1) \qquad (6\text{-}11)$$

where all terms are linearized within the time interval used. The last term in Eq. 6-11 is the process error vector, which is modelled as a zero-mean white noise

process. Therefore Eq. 6-11 represents the real stochastic process.

6.2.3 Measurement formulation

Although it is possible to take all the thermal responses observed by thermistors at different positions as the temperature state measurements, this may lead to excessive complexity for a practical application, and results in an unacceptable computational demand. Hence two thermal responses, which were given by thermistors located at stage 2 and 3 respectively (refer to Fig. 6-1), were chosen as the state measurements. The relationship between the measurement and the state was taken as

$$\boldsymbol{Y}(n) = \boldsymbol{C}\boldsymbol{X}(n) + \boldsymbol{V}(n) \qquad (6\text{-}12)$$

where Y(n) is a two element measurement vector, V(n) is a two element measurement error vector, which is also assumed to be a white noise process, and **C** is a 2x16 measurement matrix

$$\boldsymbol{C} = \begin{matrix} 0 & c_{1,2} & 0 & 0 & \ldots\ldots & 0 \\ 0 & 0 & c_{2,3} & 0 & \ldots\ldots & 0 \end{matrix} \qquad (6\text{-}13)$$

where $c_{1,2}$ and $c_{2,3}$ are the only two non-zero elements whose values depend on the excitation voltage applied to the thermistor bridge. As the temperature change is so small in the adsorption process, thermistors are assumed to give a linear response to the temperature change. When using a 3.5 V excitation voltage, $c_{1,2}$ and $c_{2,3}$ were calibrated to be 34.2 mV/°C.

6.3 Formulation of the EKF

Given Eqs. 6-11 and 6-12, formulating the EKF is straight forward, and the details have been described in Chapter. 3. Following a recursive algorithm, the state estimates are updated through the filter equation

$$\bar{\boldsymbol{X}}(n) = \boldsymbol{A}(n-1)\bar{\boldsymbol{X}}(n-1) + \boldsymbol{K}(n-1)\,[\boldsymbol{Y}(n) - \boldsymbol{C}^{T}\bar{\boldsymbol{X}}(n-1)] \qquad (6\text{-}14)$$

where **K**(n) is the filter gain at the time step n. Given the state and measurement error covariance matrixes **Q** and **R** (refer to section 3.3.2) and the initial states, the gain **K**(n) is determined in such a way that the trace of the state estimate covariance matrix, denoted by

$$Tr[\boldsymbol{P}(n)] = Tr[E[(\boldsymbol{X}(n) - \bar{\boldsymbol{X}}(n))(\boldsymbol{X}(n) - \bar{\boldsymbol{X}}(n))^{T}]] \qquad (6\text{-}15)$$

is minimized. The minimization can be realized by solving a set of three recursive equations (described in Chapter. 3), consequently K(n) and P(n) can be obtained at each time step. According to some authors (Kozub *et al.*, 1992) the main difficulty with the EKF technique is that the filter is derived from the statistics of the added white noise terms in both state and measurement vectors, and quite often the information about their noise characters in unknown. This problem will be discussed in later sections.

The real time calculation was carried out on an OPOS PCSX micro computer using a programm written in QB Basic (Microsoft, 1989), The program is listed in the Appendix, coded as "Kalmanlog". The sample interval used was in the range of 8 to 30 seconds, while it took less than a second to complete one time

step of the EKF calculation. Thus the computational demands would not prevent the on-line use of the EKF in the system described here.

6.4 Simulation studies using fixed parameter model

The main purpose of the simulation work is to minimize the model mismatch by pre- estimating some important model parameters. In this study model parameters are catalogued into two groups: 1) Parameters whose values can be considered to be constant; 2) Parameters whose values may vary with time. Thermal parameters can be classified into group 1, and some thermal parameters, such as effective heat conductivity along the bed and specific heat of the bed can be directly determined by analysis of the system characters. The effective heat transfer coefficient at the column wall (k_w) and the heat of adsorption are either composite terms or difficult to measure, therefore their values will be estimated by model simulation. The values of parameters in group 2, such as the adsorption capacity and adsorption rate constant may vary under different packing and regeneration conditions, hence these parameters will be estimated along with the main state estimation.

To isolate the effect of the thermal parameters the adsorption parameters were preset. Although the initial values of the parameters could be based on those measured in batch experiments, the model assumptions mean that these will be empirical and largely system specific. Hence, the best preset values of theses parameters could be achieved by model simulation of the adsorption

breakthrough, as the adsorption model is essentially independent of heat transfer effects. Fig. 6-2 shows the breakthrough curve fittings obtained using a series of values of q_m and k_1. The experimental data used as the fitting targets were obtained using the perfusive resin, at 20°C. It is seen that given $q_m = 7.2$ mg/ml(bed volume), and $k_1 = 0.088$ ml/(mg.min) the best fit to the measured breakthrough curve (shown with symbols in Fig. 6-2) was obtained using the six stage model. Thermal response profiles were then simulated using these optimized values in order to determine the values of k_w and ΔH. Initially, the estimates of k_w and ΔH were based on those obtained in Chapter. 5 (Yang and *et al.*, 1993), and then these values were adjusted so that the model gave the best fit to the experimental thermal profile as shown in Figs. 6-3 and 6-4. The optimized values of k_w and ΔH were 1.0 J/(min cm^2 K) and 190 J/g respectively. The results shown in Figs. 6-3 and 6-4 also show that the value of k_w affects the amplitude as well as the phase of the temperature profile, whilst the adsorption heat mainly affects the amplitude of the thermal response. Using the optimized set of both adsorption and thermal parameters the model gave the best fit to both temperature and breakthrough profiles as shown in Fig. 6-5.

In view of the very high water content (more than 90%), it is reasonable to take the heat conductivity of water as the effective heat conductivity in the bed. The value of h_c (heat transfer coefficient at column end) was set to be that obtained in Chapter.5.

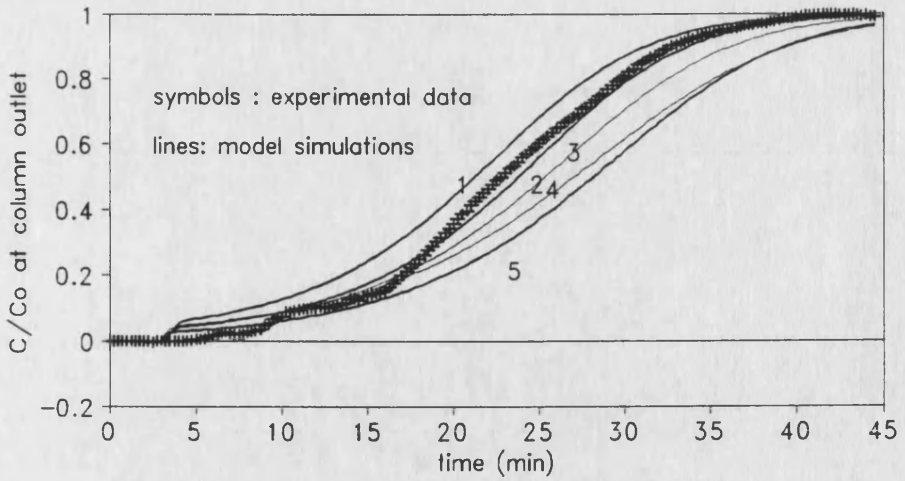

Fig. 6-2 Determination of qm and k1 by breakthrough curve fitting

model simulation with parameter values :

1: qm=6.1 mg/ml, k1=0.08 ml/mg/min; 2. qm=7.2, k1=0.088

3. qm=7.5, k1=0.082; 4 qm=8.5, k1=0.07; 5. qm=9.2, k1=0.082

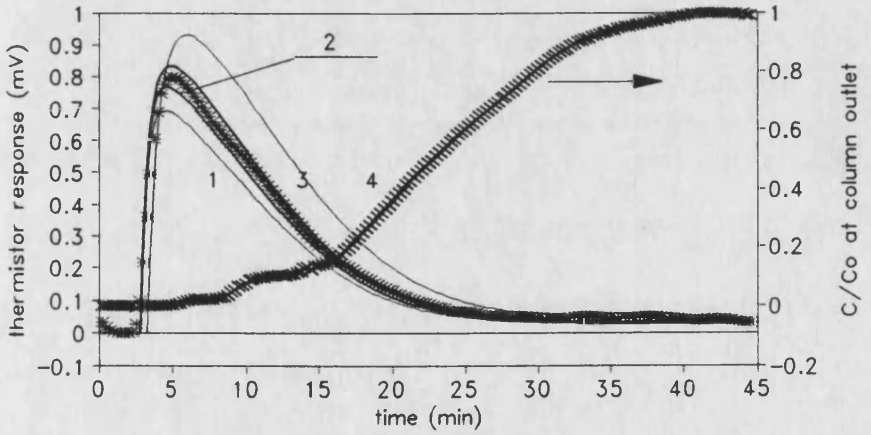

Fig. 6-3 Effects of thermal parameters on temperature profile

Thermal response profile sensed by thermistor at stage 2

(refer to Fig. 6-1)

model simulations with parameter values: (kw J/K. cm .min)

1. kw=1.25 ; 2. kw=1.0 ; 3. kw=0.75 ; 4. kw=0.25

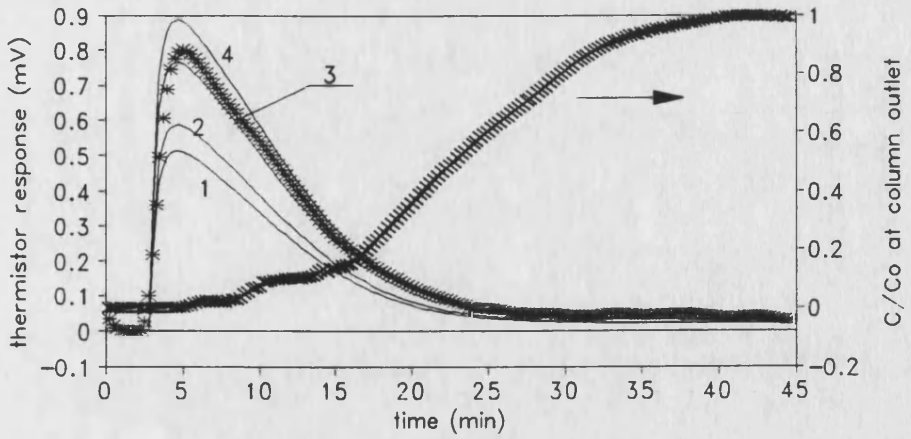

Fig. 6-4 The effect of adsorption heat on temperature profiles

Thermal response profile sensed by thermistor at stage 2 (refer to Fig. 6-1)
temperature profile simulations using the values of adsorption heat :

1: 140 J/g , 2: 160 J/g , 3: 190 J/g , 4: 220 J/g

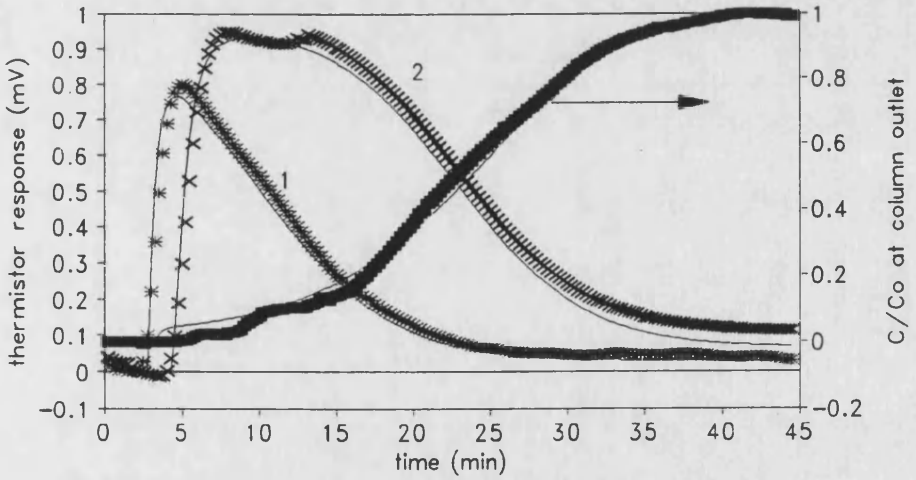

Fig. 6-5 Model fits using optimum parameters
Aspartic acid-DEAE based resin

feed concentration : 1.0 mg/ml ; flow rate : 6.92 ml/min

1 and 2 : thermistor responses at stage 2 and 3 respectively (refer to Fig.6-1)

6.5 Real time estimation of state variables and parameters

All adsorption experiments described in this section were carried out using the perfusive resin. The thermal response profiles (1 and 2) in the figures were sensed by thermistors at stage 2 and 3 respectively. The water bath used was set at 20°C.

6.5.1 Concentration estimation using the EKF with known model parameters

A series of the thermal monitoring adsorption experiments were carried out using regenerated resin under identical conditions, such as pH and ionic concentration, as in previous experiments. This means that the main adsorption parameters q_m and k_1 should be close to the estimates from previous experiments and could be chosen as their initial values in the EKF. In such cases the error terms in the covariance matrix related to these two state variables were reasonably set to rather small values. It was relatively straightforward to preset the measurement error, as considerable information about the measurement noise had been obtained through the base line stability survey, and so the measurement error covariance matrix was set in a diagonal form

$$\boldsymbol{R}=E[(\boldsymbol{Y}-\overline{\boldsymbol{Y}})(\boldsymbol{Y}-\overline{\boldsymbol{Y}})^T]=\begin{matrix}0.014 & 0\\ 0 & 0.014\end{matrix} \qquad (6\text{-}16)$$

where the statistic mean of the measurement should ideally be zero, but where in practice a small offset may exist. Conversely setting the state error covariance matrix elements related to temperature and concentration states is much more difficult, as little knowledge is available about the process state noise characteristics. Fortunately as the model has been fairly well tuned and the

measurement noise characters are well known, the error terms related to the main state variables could be preset by simply regarding the filter performance stability, and the filtering effect, which are highly dependent on the relative values of **R** and **Q**. For simplicity the 16x16 state error covariance matrix **Q** was taken as a diagonal form (see Eq. 6-10 for reference), and the diagonal elements related to the temperature (°C), concentration (mg/ml) in mobile and fixed phases, q_m (mg/ml), and k_1 (ml/mg sec) were set to be 0.0001 (row 1-6), 0.001 (row 7-10), 0.001 (row 11-114), 0.2 (row 15), 0.0004 (row 16) respectively.

Examples of the results are shown in Figs. 6-6, and 6-7. The estimated concentration profiles at the fifth stage are in good agreement with the outlet breakthrough curves measured by the UV detector. In addition, the concentration variation with time at the fourth stage was also estimated, and an example is shown in Fig. 6-7. This would allow the partial loading strategy (Dantigny *et al.*, 1991) to be put into practical use. As described in Chapter. 2, this strategy is aimed at minimising the loss of high value products, and requires the adsorbate concentration within the bed to be determined on-line.

The results also show that the estimated values for q_m and k_1 are fairly close to the preset values, and that the EKF estimates of the thermal responses, *ie.* temperautre states, closely trace the measured profiles albeit with a smoother response.

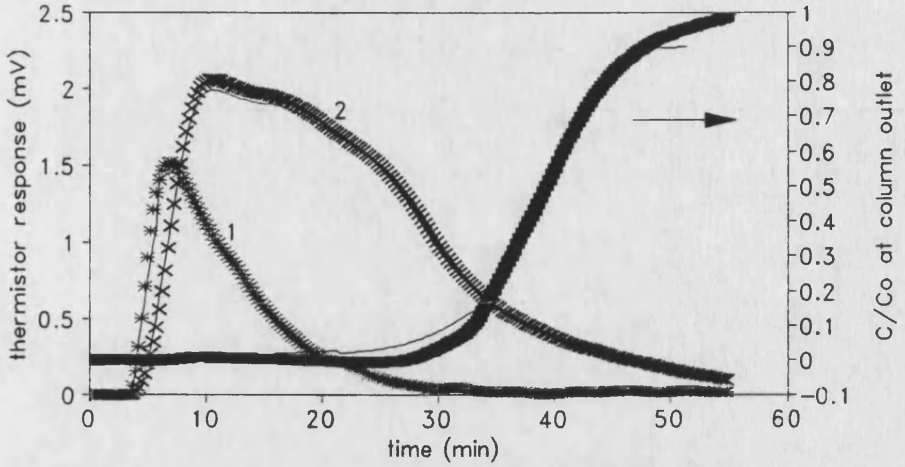

Fig. 6-6 On-line estimation using identical resin conditions

Feed concentration : 1.5 mg/ml ; flow rate : 3.2 ml/min

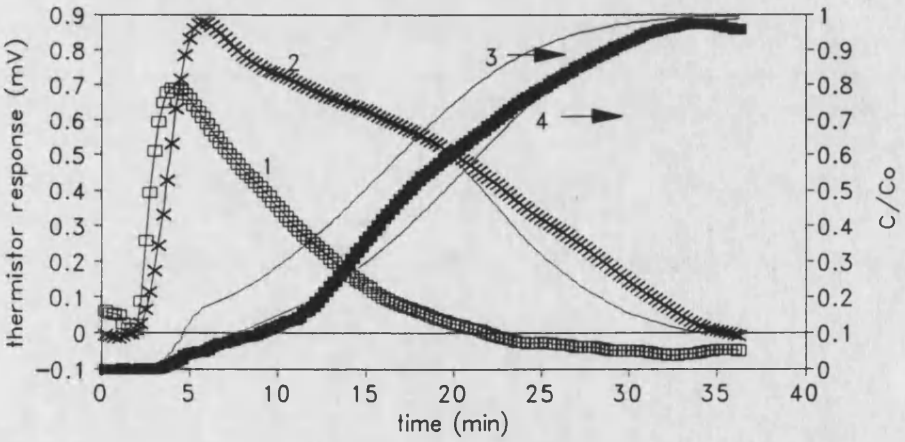

Fig. 6-7 On-line estimation under identical resin conditions

feed concentration : 1.0 mg/ml ; flow rate : 9.23 ml/min
3: estimated breakthrough at stage 4 (refer to Fig. 6-1)
4: measured and estimated breakthrough at bed outlet
converged estimates : qm=7.7 mg/ml, k1=0.09 ml/mg.min

6.5.2 Concentration estimation using the EKF with unknown model parameters

The thermal monitoring adsorption system was run using different buffers with different pH values. In this case the values of q_m and k_1 cannot be assumed to remain unchanged, hence their error terms in the state error covariance matrix were set to be relatively large (*e.g.* 4 and 0.2 when using citrate buffer).

The convergence trajectories of the estimates of these parameters are shown in Fig. 6-8. The estimates converged toward acceptable values regardless of the initial setting. In spite of little prior knowledge regarding these two important parameters the EKF still gave a good prediction of the experimental measurements, as shown in Figs. 6-9, and 6-10. In order to obtain a good filtering effect the error terms related to q_m, and k_1 in the state error covariance matrix were updated with the convergence trajectory. As the uncertainty of the parameters was gradually reduced with the filter performance, the related error terms in the covariance matrix were consequently updated with reduced values. The dynamic response of the EKF, as stated before, is highly dependent on the relative values of **Q** and **R**. If **Q** is set to be considerably large, the gain **K** would also be relatively large, in turn the estimates would be highly determined by the measurements, which means fast convergence of the parameter estimation. This is desirable during the early period. Conversely relatively large values of the **R** elements emphasise the filtering effect, leading to much smoother responses. Hence a covariance matrix element updating strategy enhances the performance of the EKF by allowing both rapid initial convergence coupled with effective filtering ability.

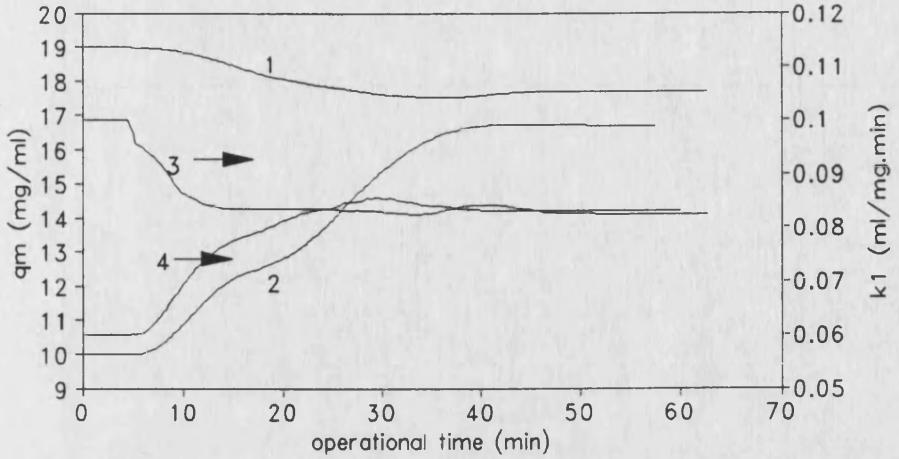

Fig. 6-8 Convergence trajactory of qm and k1 estimation

1 and 2 : initial values of qm , 19 and 10 mg/ml respectively

3 and 4 : initial values of k1, 0.1 and 0.06 ml/mg.min respectively

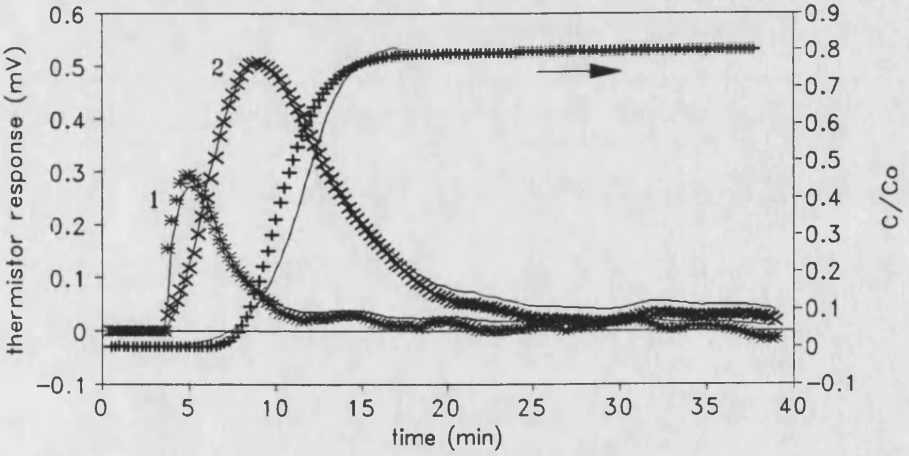

Fig. 6-9 On-line estimation using EKF
(phosphate buffer 0.01 M)

feed concentration : 1.0 mg/ml ; flow rate : 5.1 ml/min
initial values : qm=7 mg/ml, k1=0.09 ml/mg.min
converged estimates : qm=5.2 mg/ml , k1=0.10 ml/mg.min

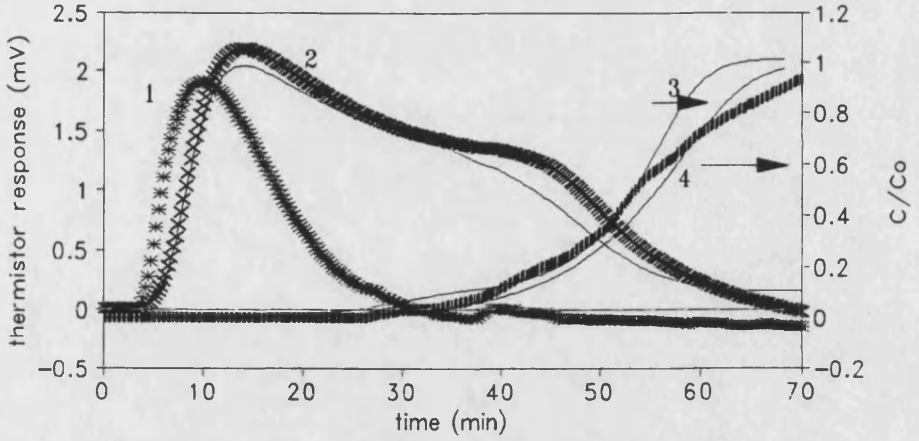

Fig. 6-10 On-line estimation using EKF (citrate buffer 5mM)

feed concentration : 1.6 mg/ml ; flow rate : 4.23 ml/min

3: initial values: qm=10 mg/ml, k1=o.o6 ml/mg.min
converged estimates : qm=16.5mg/ml , k1=0.08 ml/mg.min

4: initial values : qm=19 mg/ml, k1=0.11 ml/mg.min
converged estimates : qm=17.4 mg/ml, k1=0.08 ml/mg.min

6.5.3 Concentration estimation in thermal monitoring system under nonthermostatted conditions

For this case the system was run without any temperature control of the water bath, and the measurement was inevitably corrupted severely by the ambient temperature fluctuation. Hence the error terms in the measurement covariance matrix had to be set much larger. The settings were again based on a base line survey. The EKF responses together with the temperature profiles measured by thermistors and the breakthrough curve obtained by UV detector are shown in Fig. 6-11. The EKF estimates are still acceptable, though some significant deviation appeared during the later period. As the estimation of the early part of the breakthrough is much more important in practice, the EKF estimation achieved in this region is still significant. An attempt was made to improve the

match between the estimated temperature profile and the measured values by simply setting large state error covariance elements. However this led to a significantly greater deviation between the estimated and the measured breakthrough curve. In fact providing artificially large settings for the state covariance elements is equivalent to eliminating the model contribution. Clearly, the thermal measurement noise is not a zero-mean white noise, but a drift caused by the room temperature fluctuation in this case. Thus the measurement became unreliable during the later stages of run period.

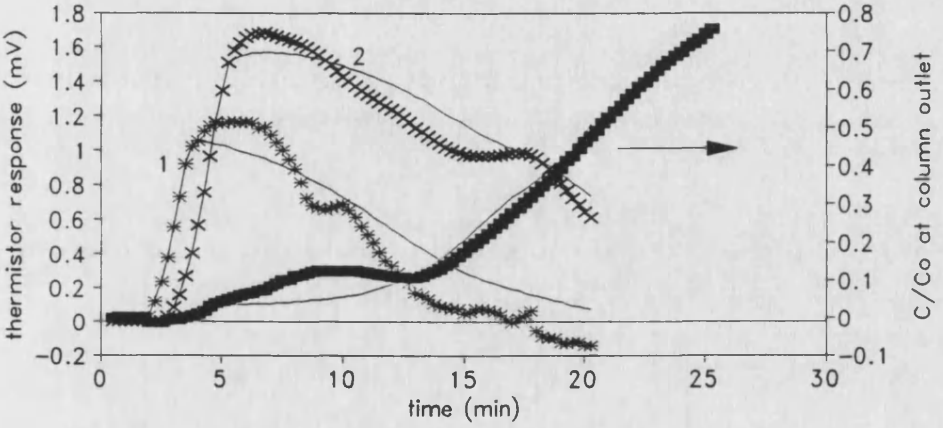

Fig. 6-11 On-line state and paramenter estimation (unthermostatted air filled jacket)

Tris-Hcl buffer, pH=7.2, 5mM
feed concentration : 1.5 mg/ml ; flow rate : 8.72 ml/min
initial values: qm=9 mg/ml, k1=0.08 ml/mg.min
converged estimates: qm=8.7 mg/ml; k1=0.08 ml/mg.min

6.5.4 Concentration estimation when a mixed feed solution is used

For this case the feed solution contained 1 mg/ml of aspartic acid and 0.01 mg/ml of lysozyme. The presence of lysozyme makes it impossible to monitor the breakthrough concentration of aspartic acid using UV detection. However, as

lysozyme is not adsorbed under the conditions used, this will not disturb the thermal monitoring and Fig. 6-12 shows that the concentration of aspartic acid at different stages can still be estimated.

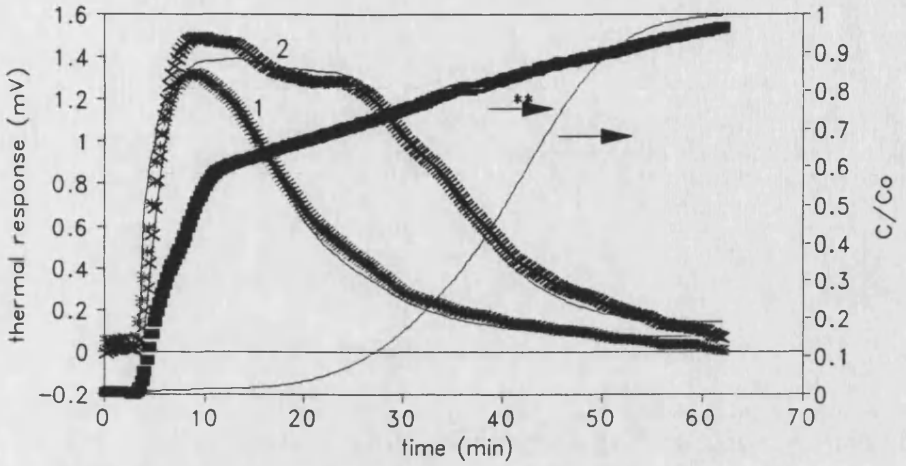

Fig. 6-12 On-line state estimation using EKF
(Mixed feed stock)

feed : 1.2 mg/ml of Aspartic acid and .01mg/ml of Lysozyme
flow rate : 5.88 ml/min
** : recorded by UV detector

6.6 The problem of model mismatch

Generally speaking the Kalman Filter is tolerant to model mismatch given careful settings of the state error covariance matrix. However, as pointed out by a number of authors (Bozub and MacGregor, 1992) (Dimassimo *et al.*, 1992), a Kalman Filter could provide poor and biased estimates if a serious error is made in judging of the state noise characteristics. Although this problem has limited the scope of Kalman filters, a variety of approaches have been proposed to overcome the problem. In addition to model tuning through prior simulation,

simultaneous estimation of parameters and state variables is an effective technique for overcoming this problem (Kozub and MacGregor, 1992; Ramirez, W.F., 1987). Kozub and MacGregor (1992) employed a second EKF to estimate some of the unknown parameters which were then used to update their initial values in the main EKF. This approach performed in an iterative manner was used in the control of a semi-batch polymerization reactor. Similarly, Chattaway *et al.* (1989) developed a separate parameter estimator to do the same job for detecting contaminants in bioreactors. In their systems the parameters which were estimated on-line may vary with time within a long experimental period. These different approaches were all successful, albeit at the expense of model complexity. In packed bed adsorption processes the decline of the bed capacity due to repeated use can be considered as a step variable varying with the run number, and hence could be treated as a constant within each performance period, even though its true value is unknown. Therefore simply by including this unknown parameter in the state vector, the EKF should give good convergent prediction of these parameters. This makes the estimation of bed capacity relatively easy. This approach was also considered by Stephanopoulos and San (1984). In Fig. 6-8 it can be seen that the changes of initial values of q_m and k_1 do not make much difference in the breakthrough estimation. This is because it takes a finite time for the breakthrough curve to reach the column exit, and this gives adequate time for the convergence of the parameter estimates.

6.7 Error covariance matrix

In all the work described in this section the initial setting of the error covariance matrix **P**(0) affected the performance of the filter, however not so much as the state and measurement error covariance matrixes. Unnecessarily large settings, often used in off-line Kalman Filter gain calculations, only led a very slow convergence, which is unacceptable in on-line computer control. In practice this problem can be overcome by using settings based on independent estimates of the range of the state variables.

CHAPTER. 7 ON-LINE BREAKTHROUGH ESTIMATION AND PREDICTION USING THERMAL SIGNALS - APPLICATION OF NEURAL NETWORKS

7.1 Basic consideration

EKFs can be successfully used to solve state estimation problems. However, as has been shown, extensive prior knowledge of the system is required for the design of an effective EKF. Furthermore, an appropriate model which well describes the process is also required. An alternative approach, which avoids this drawback is assessed in this chapter. The method considered uses artificial neural networks (ANNs) and is aimed at estimation and prediction of the breakthrough using rather complex "in bed" differential thermal signals without any prior knowledge of the system. It is expected that by using on-line measured thermal signals a properly trained ANN should be able to give reliable estimation or prediction of breakthrough under various operational conditions. It is also expected that the network should be able to account for the effects of the deterioration of intrinsic parameters, such as the bed capacity due to repeated cycles of use. This chapter is divided into two sections, firstly use of networks for breakthrough estimation is presented, and then a network approach to the long-term prediction of breakthrough is described.

All experiments involved in this chapter were carried out at 20°C using perfusive resin and "in bed" reference system. The symbols, if used, are referring to physical data, and lines the network estimations and predictions if not specified in all Figs. in this chapter.

7.2 Use of networks for breakthrough estimation

7.2.1 Input and target vector, and network structure

The problem to be solved is to relate thermal signals measured on-line to the breakthrough. This clearly specifies that the target vector is just the outlet concentration, but the optimum input vector is not clearly specified, and a number of combinations must be considered. Clearly, some of the thermal signal data must be included, however how much additional information should be supplied is open to question. To seek the most effective network topology a number of input combinations (input vectors) were investigated.

1) The input vector is composed of a thermal signal measured by a specific thermistor pair, and the elution volume, (both of which are time dependent), in addition the feed concentration is input to the network as a bias. This network is coded as Enetd0 .

2) The input vector consists of a thermal signal measured by a specific thermistor pair, together with the same thermal signal with different time delays, (*ie.* three thermal signal inputs) and the elution volume. The network is coded as Enetd2.

In addition to Enetd0 and Enetd2, networks with 1 and 3 time delayed thermal inputs were also attempted for comparison, and they are coded as Netd1 and Netd3. The input vector for Netd1 is an expanded input vector for Enetd0 achieved by adding a time delayed thermal signal input, and that for Netd3 is an

expanded version of Enetd2 achieved by adding another time delayed thermal signal input. Table. 7-1 summarises the structures of the networks used.

Table. 7-1 Characteristics of the networks

Network code	Enetd0	Netd1	Enetd2	Netd3
input node number	3	4	4	5
hidden node number	6	6	4	5
number of inputs with time delay	0	1	2	3
number of weights	24	30	24	30

7.2.2 Sample sets for network training

The sample sets for the network training are selected in such a way that the range of the operational conditions used in the samples is relatively large, so as to cover most of the usual laboratory operational conditions. The range of variation of the intrinsic parameters is similar to that encountered in the laboratory experiments. The details of the four sets of sample data are shown in table 7-2. As the time taken for each training iteration circle is proportional to the number of samples, a small number of samples are desirable. To minimise the number of samples, data at the later stage where the breakthrough has reached over 95% were not taken into account. Sample set 2, in which inactive resin was used, was chosen to give the network sufficient information of the nature of the output when no adsorption takes place. In such a case the fact that no adsorption takes place is specified by the unchanged temperature as measured by the sensing thermistors within the column. This can therefore be used to verify whether the trained

network effectively captures the system behaviour, and thus is able to predict the effect of variation of the bed capacity.

As discussed before, the choice of the network inputs should avoid redundancy of the input information, *ie.* only essential information should be chosen as network input. Clearly zero bed capacity can be only specified by the fact that the breakthrough begins as soon as the elution fills up the dead volume. It is therefore necessary to choose the elution volume as a network input.

Table.7-2 Details of the training sample sets for estimation network

set No.	1	2	3	4
flow rate (ml/min)	5.6	5.6	6.8	26.2
feed concentration (mg/ml)	1.5	1.5	1.25	1.0
regeneration condition	0.1 M NaOH,10 bed volumes	inactive resin	0.1 M NaOH 6 bed volumes	0.1 M NaOH 10 bed volumes
estimated capacity* (mg/ml)	14	0	11	13
sampling interval (min)	0.5	0.5	0.5	0.1337
number of samples	96	60	85	96

* estimated from the breakthrough curve analysis

The variation of one of the main intrinsic characteristics of the system, namely the resin capacity was represented by the inclusion of inactive resin results as one of the sample sets.

7.2.3 Training convergency and network performance

The network training followed the back propagation algorithm described in Chapter. 3, using an "in house" program, which was written in Turbo Basic and is listed in the Appendix, coded as "neural-net". It has been observed that the speed of network training convergence is highly dependent upon the step size of the weight correction, *ie.* the value of μ in Eq. 3-34, and that there is a critical value of the step size at which a steady convergence transfers to a unsteady state. Thus the step size was set close to the critical value which was determined by a trial and error method. The training convergency trajectories against the iteration number are shown in Figs. 7-1a. The convergence is fast for the first 1000 iteration circles, slowing down thereafter. After 50000 iteration cycles, which took 5 hours on a Viglen 486 PC, the error sum (in fact, the total sum of error squares) was reduced to a preset level (9 in this work). Given the total number of the sample sets, the time per iteration is dependent on the structure of the network trained, so that the time taken to complete a certain number of iteration cycles may vary from one to another. Fig. 7-1b shows convergence trajectories against the training time, and may show the efficiency of network training.

It is interesting to note that during the network training work, a mistake occurred such that an incorrect time step was used in the training sample sets. This caused non convergent training, which in turn indicated that the network has the ability to identify whether there is a functional relationship between the data fed to it. A reverse tendency might occur during the training process, *ie.* the error sum

increases with iteration number at some points. This phenomena is also mentioned in the literature (Goodacre and Kell, 1992).

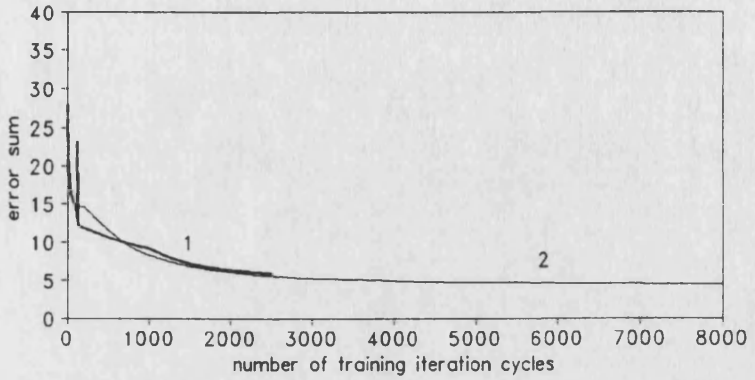

Fig. 7-1a convergency trajactories of the network training

1: Enetd0 ; 2: Enetd2

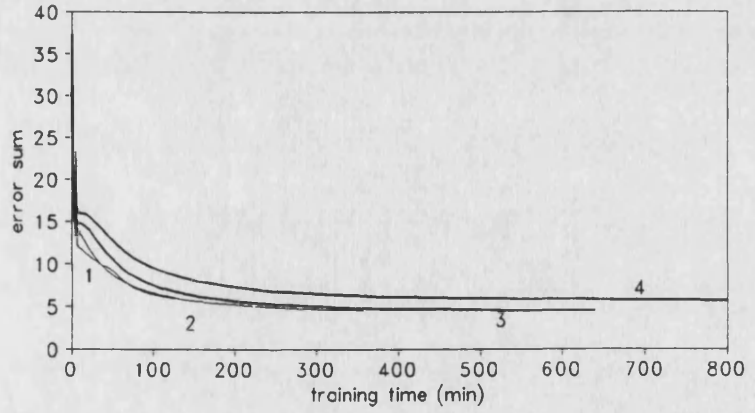

Fig. 7-1b convergency trajactories of the network training

1. Enetd0; 2. Enetd2; 3. Netd1; 4. Netd3

Final fits of the network outputs to the targets are shown in Fig. 7-2 for Enetd0 and in Fig. 7-3 for Enetd2. Both networks gave a good fit to the physical data . It should be noted that the order of the appearance of the breakthrough for the data sets depends on both the resin capacity and the operational conditions. If the predictions were generated by a mechanistic model with preset parameters, the order of the predicted breakthrough curves would be totally different from the experimental ones, unless the factors determining capacity variation were included in the model. However the networks gave correct fits to the experimental curves. This provides further evidence that the networks have effectively recognised the essential features of the system. The figures also show that there are some spikes in the fitting curves, and that this is more evident in the curves given by Enetd0. The spikes correspond to the thermal signal pulse in the input vector, which will be discussed later. The training fitting error sum given by using different networks are shown in Table. 7-3.

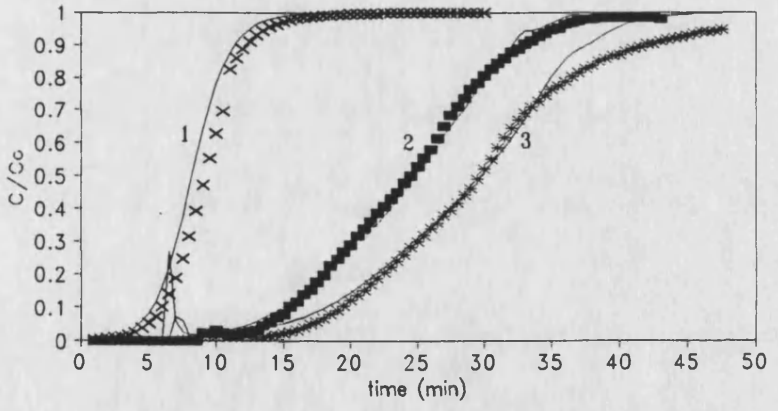

Fig. 7-2 Training fits fiven by Enetd0

1. flow rate : 5.6 ml/min; feed concentration: 1.5 mg/ml; inactive resin
2. flow rate : 6.8 ml/min; feed concentration : 1.25 mg/ml
3. flow rate: 5.6 ml/min; feed concentration : 1.5 mg/ml

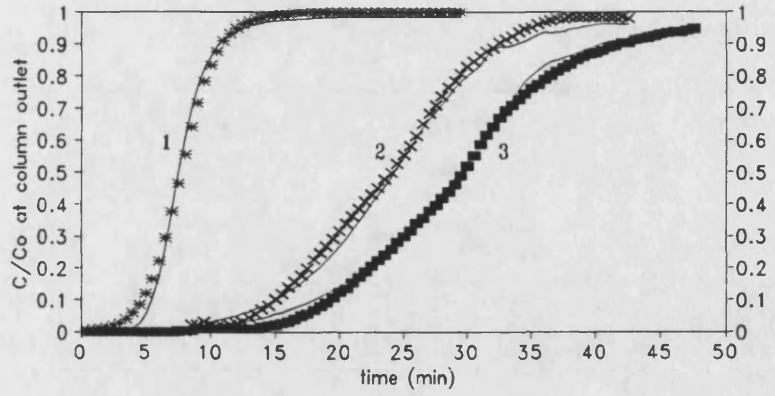

Fig. 7-3 Training fits given by Enetd2

1. flow rate : 5.6 ml/min; feed concentration : 1.5 mg/ml; inactive resin
2. folw rate : 6.8 ml/min ; feed concentration : 1.25 mg/ml
3. flow rate : 5.59 ml/min : feed concentration :1.5 mg/ml

Table. 7-3 Training fitting error sum

network	Enetd0	Netd1	Enetd2	Netd3
number of time delayed thermal signal input	0	1	2	3
error sum	5.2	5.3	4.2	4.1

Using all the four available differential thermal signals in the network input vector is theoretically interesting, and was attempted initially, but this effort was abandoned because of a very slow convergency process. In practice, the use of additional thermal sensors would lead to more complex and expensive systems, and so for both practical and fitting considerations this is undesirable. Thus the thermal signal given by the thermistor pair at the optimized position (see chapter 5) in the column was used as a network input. The use of more than one hidden layer in the network was attempted to minimize the fitting error further, but this also caused problems with training convergence, and no significant improvement was observed. Hornik *et al.* (1989) showed that with one hidden layer and a

sufficient number of nodes any mapping could be achieved to an arbitrary level of accuracy. Accepting his claim, it may be considered that the observed deviation might well represent the experimental errors. One of the possible sources of operational error is the shift of the flow rate, which might occur when the back pressure becomes high, especially at high flow rate.

7.2.4 Comparison of the network estimation and the experimental measurement

Before real time use, the trained networks were tested with three real experimental data sets to check if the trained network recognised the dynamic behaviour of the system. Table. 7-4 shows the details of the experimental conditions for the test data sets.

Table. 7-4 Details of the test data sets

set No.	1	2	3
flow rate (ml/min)	2.24	7.4	16.38
feed concentration (mg/ml)	1.25	1.67	1.0
number of samples	299	70	115
sampling interval (min)	0.5	0.5	0.1667
time lag *	26.5	5.5	1.17

* time lag will be explained later

The test results are shown in Fig. 7-4 given by Enetd0 and Fig.7-5 given by Enetd2. Clearly the estimations given by Enetd2 are in much better agreement with experimental measurements. It is worth mentioning that despite the flow

rate at Set 1 and feed concentration at Set 2 being beyond the ranges used in the training sets, the network still gave reliable estimates. This provides further evidence that the neural network has recognised the behaviour of the system.

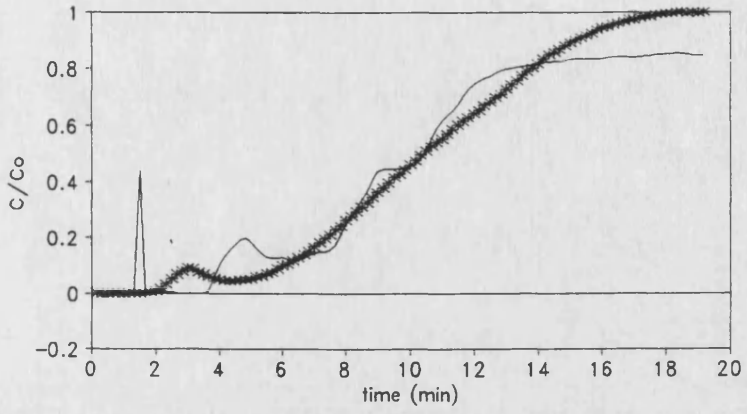

Fig. 7-4 Test fit given by Enetd0

flow rate : 16.4 ml/min ; feed concentration : 1.0 mg/ml

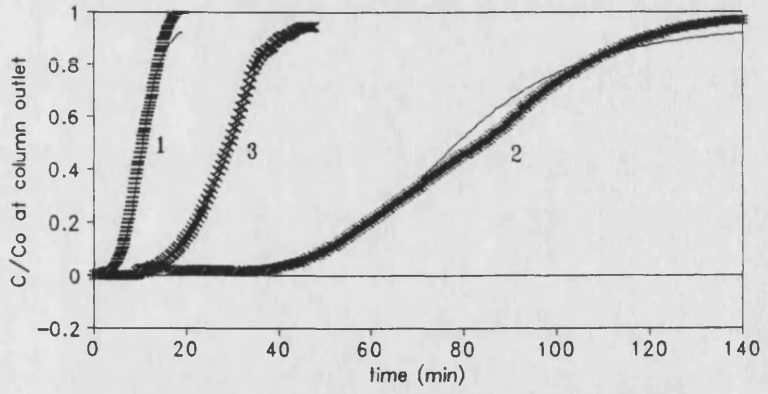

Fig. 7-5 Test fits given by Enetd2

1. flow rate : 16.4 ml/min ; feed concentration : 1.0 mg/ml
2. flow rate : 2.24 ml/min; feed concentration : 1.25 mg/ml
3. flow rate : 7.4 ml/min ; feed concentration : 1.67 mg/ml

Enetd0 gave a poor estimation of the experimental breakthrough curves, although it converged well during training. Furthermore there are some sharp spikes in the estimated curves, similar to those in the training fits shown in Fig.7-2, whose positions correspond to those of the thermal signal pulses. Further training was attempted in order to minimise the error, but no obvious improvement was observed, thus the attempt was abandoned. This may indicate a problem where dynamic relationships exist between the inputs and outputs, and where a dynamic network should be used. A comprehensive discussion of this problem is beyond the scope of this thesis, but a brief analysis is attempted below.

7.1.5 Use of a dynamic network to capture the system dynamic behaviour

As discussed in Chapter.3, a neural network can identify a complex relationship between system variables through a training process, as long as sufficient information about the system behaviour is provided. For Enetd0 only the current thermal signal is provided at each time step, and this signal is not a unique function with respect to time. In addition, another input, the elution volume, can be a weak linear function of time in some cases. This is because the elution volume has to be scaled from the full range, say 0-500 ml to the range of 0-1, so that it may vary only by a small value in the case of a low flow rate. In this situation the input vector space may be imperfect, that is, two input vectors are very close to each other. Therefore one point in the input vector space may correlate to two or more target values. The network may be confused and has to learn the latter by forgetting the former.

Compared with that for Enetd0 the input vector space for Enetd2 is extended by the addition of two thermal dimensions. As pointed out in Chapter 5, such an input vector structure allows the network to account for the system dynamics. In fact this arrangement effectively reduces the risk of the input vector space redundancy. In a physical sense the network is provided with the information not only about the present state of the system but also about the system history. Thus the network can recognise system dynamics through the learning process. The training and estimation results obtained support this argument.

Theoretically, using more inputs of time delayed thermal signals might allow a network to identify the system dynamics more efficiently. However this would inevitably increase the training time, and therefore a compromise must be made. Table. 7-5 shows test fitting error sums given by using networks with different numbers of thermal inputs. The sharp reduction of the error sum from Enetd0 to Netd1 clearly shows that the quality of estimation is greatly improved by introducing a time delayed thermal signal input to the network. It is also seen that using a network with more than 3 thermal signal inputs gives no significant improvement in the test fitting error sum.

The delayed times used for the thermal inputs were determined by a trial and error method, and 2, 4, and 8 sampling intervals were used for the first, second and third additional thermal signals.

Table. 7-5 Test fitting error sum

Network used	Enetd0	Netd1	Enetd2	Netd3
test data 1	56.4	9.2	6.1	5.9
test data 2	37.1	7.4	4.4	4.3
test data 3	41.2	7.1	5.0	4.8

Training convergency trajectories shown in Fig. 7-1b indicate that training a network with small number of nodes is much effective than training a net with a large number of nodes. All of these factors suggest that Enetd2 be an optimum network for the purpose of breakthrough estimation. The weights obtained for Enetd2 are given in Table. 7-6.

Table. 7-6 Weights in Enetd2

hidden node No.(j)	input 1	node 2	number 3	(i) 4	output node
1	-0.0205	-0.1268	-10.567	-.11668	-19.581
2	26.0908	-2.7223	-9.4430	0.25087	23.2944
3	22.0313	8.03493	-45.610	10.6781	-30.371
4	-18.222	-3.1282	20.8767	-5.0240	3.07891

7.2.6 Real time use of the network

Real time use of the trained network is straightforward, as prediction using a trained network is almost instantaneous. An example of the on-line estimation of the breakthrough by using Enetd2 is shown in Fig. 7-6. It should be noted that for breakthrough estimation the information about feed concentration is not required by Enetd2, which suggests that the thermal signal provides the information of feed concentration. In practical applications this is highly desirable, because the feed concentration may vary from batch to batch, and analysis of the

feed solution may be either time consuming or difficult.

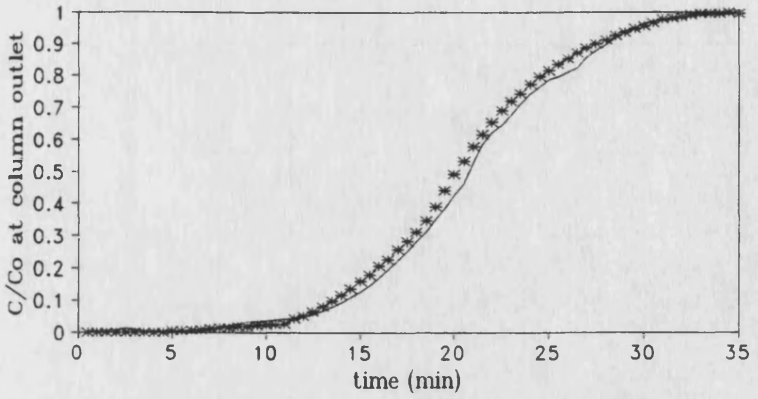

Fig. 7-6 Real time breakthrough estimation using Enetd2
flow rate : 7.1 ml/min ; Co=1.67 mg/ml
operational temperature : 20 C

7.3 Long term prediction of the breakthrough by using dynamic neural network models

7.3.1 Network approach to long-term prediction

In practice predicting of a breakthrough curve before it occurs is desirable. Thus prediction of breakthrough using the thermal signals measured in the early stage is very attractive. This may be achieved by using dynamic modelling techniques. Although the reliability of the long term prediction techniques is often questioned, they do provide potentially valuable information regarding the situation at a future point. In this section two alternative protocols are discussed. Firstly training of a neural network using time shift breakthrough signals as its training target was attempted together with a linear correlation approach. Secondly the

network was trained using time scale compacted rather than time shifted breakthrough signals.

7.3.2 Training sample set assembly

A linear relationship between the relative elution volume and the position of the corresponding thermal sensor has been obtained in Chapter 5. This relationship can also be used to predict the time lag between the peak start of the temperature response and the breakthrough start. This predicted time lag together with the breakthrough profile mapped from the thermal signals measured in the early stage by using a neural network would make a long term breakthrough prediction possible. Training sample sets for such a network were assembled based on those shown in Table. 7-2, however the target time series in each set was set ahead by a time lag equivalent to that between the peak start of the thermal response and the start of breakthrough. The start of breakthrough was determined by producing a tangent at 3% breakthrough to the time axis. Fig. 7-7 shows the position of a shifted breakthrough curve, and the respective relationship (one to one) between thermal and breakthrough signals. The time shift and the number of samples of each training data set are listed in Table. 7-7.

Table. 7-7 Time shift and number of sample set

set No.*	1	2	3	4
time shift(min)	1.2	8	-	7
number of samples	70	70	30	50

set No. refer to that in Table. 7-2

The sample sets were then used for training a network coded as Pnet1 with the same structure as Enetd2.

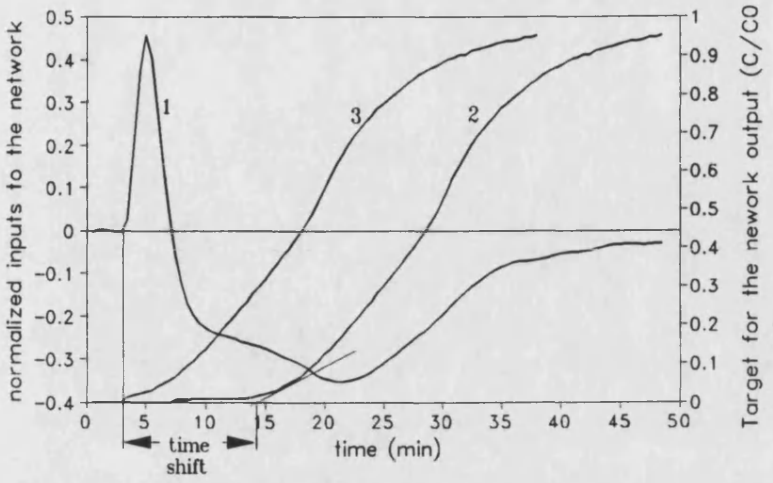

Fig. 7-7 Profiles of training samples using time shifted breakthrough data

1. thermal response ; 2. and 3. original and time shifted breakthrough curve

To form the time scale compact training sample sets the time scale for the breakthrough signals was simply compacted by a factor, so that the breakthrough signals could be related to the temperature signals at an early stage. For example the breakthrough signal at 20 min would be related to the temperature signal at 10 min. The network trained in this way was coded as Pnet2. Compacting the time scale will inevitably reduce the number of samples by a factor equal to the compact factor, thus too big a compaction factor may result in unacceptably small sample set. On the other hand too small a factor leads to a short-term prediction, which is no different from the network estimation described before. To chose an appropriate time scale compaction a compromise is necessary. In addition, a factor in fraction form may greatly reduce the number of sample sets. Taking a

factor of 1.5 for example, the formula, y(i)=y(1.5 i) is used to transfer the initial target data to those in a compacted time scale, thus the unity requirement of 1.5i will exclude all the y(i)s in the series of i=1,3,5,... from the sample set. Therefore 2, and 3 were chosen as the compaction factor. An original breakthrough curve and its transform in a compacted time scale, together with the thermal response profile is shown in Fig. 7-8.

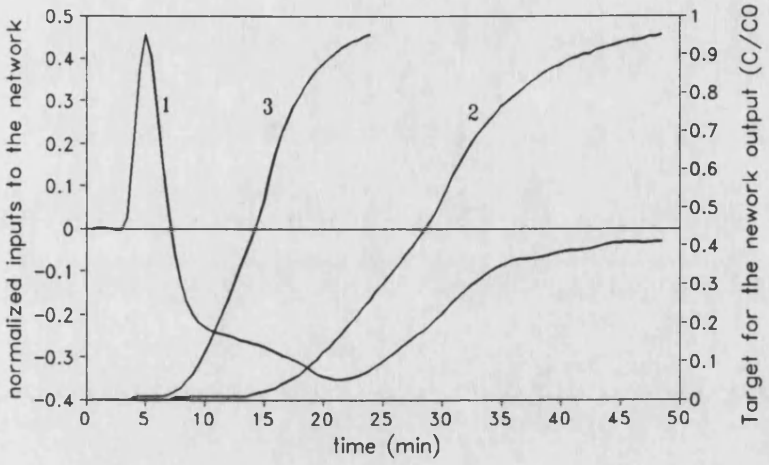

Fig.7-8 Profiles of training samples
using breakthrough data in compacted time scale as the target data
1. thermal response ; 2. original breakthrough curve
3. breakthrough data in compacted time scale

7.3.3 Training fits

Training of the networks for long-term prediction, similarly to the previous network training, required about 50000 training iteration circles to reduce the total error sum to an acceptable level, however the total training time was much less than was required to train Enetd2 due to the considerably reduced sample capacity. The breakthrough curve fits are shown in Fig. 7-9 for Pnet1, and Fig. 7-10 for Pnet2. All the curves were put back to their original position or time

scale. The fits given by both Pnet1 and Pnet2 are acceptable in the whole range.

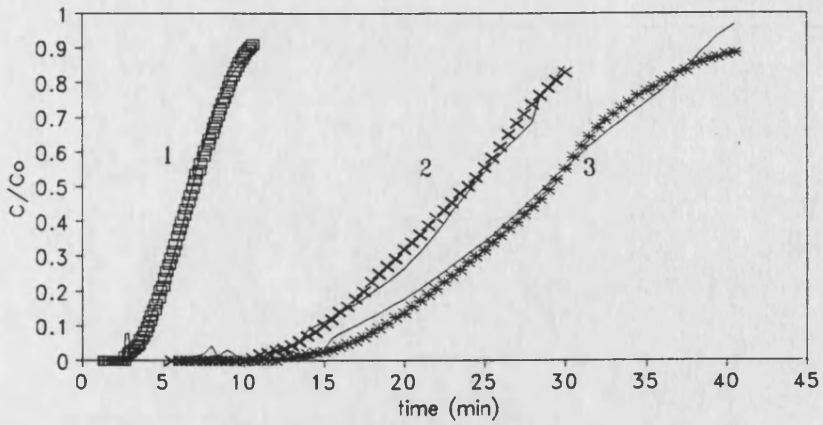

Fig. 7-9 Training fits given by Pnet1

	flow rate (ml/min)	feed concentration (mg/ml)
1	26.2	1.0
2	6.8	1.25
3	5.6	1.5

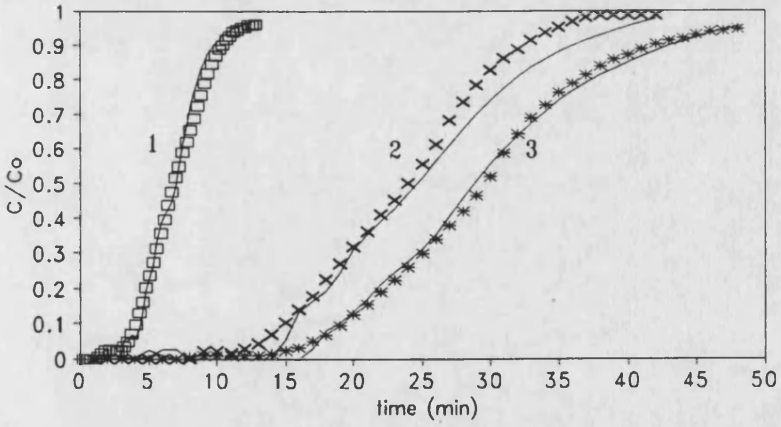

Fig. 7-10 Training fits given by Pnet2

flow rate and feed concentration are as shown in Fig. 7-9

7.3.4 Test of the network prediction

Test data sets were based on the same experimental results as shown in Table.4, however, in this case the time lags used for Pnet1 were calculated using the empirical linear correlation (Eq. (5-16b) with a slight modification, which is

$$elutionvolumeratio=\frac{t_{tp}V}{t_{bs}V}=0.18+0.114x_2 \qquad (7\text{-}1)$$

$$t_{bs}=\frac{t_{tp}}{0.18+0.114x_2}$$

where t_{bs} and t_{tp} are breakthrough start time and thermal peak start time, and x_2 is the position of the sensing thermistor. t_{tp} was determined from the thermal response profiles.

The predicted breakthrough curves together with the measured ones are shown in Fig. 7-11, on which each predicted curve has been moved by the corresponding time lag. The predicted profiles are in good agreement with the measured ones, however small time lags exist. Clearly these small time lags are due to the error introduced by using the empirical linear correlation. Despite these small time lags, the predicted curves are still acceptable. Network Pnet1 is similar to that used by Bhat *et al.* (1990). They developed a backpropagation network dynamic model to predict the response of pH in a stirred tank, using a moving window of pH and NaOH flow rate values as inputs, and outputting the pH one to five time steps (0.4-2 min) into the future. In their approach the time steps into the future were preset artificially. While in this work the breakthrough prediction begins at the time when the pulse temperature response takes place, *ie.* when the

adsorption front reaches the vicinity of the thermal sensor. This indicates that the breakthrough prediction begins as soon as the adsorption front reaches the thermal sensor. Therefore this approach leads to a significant long term prediction.

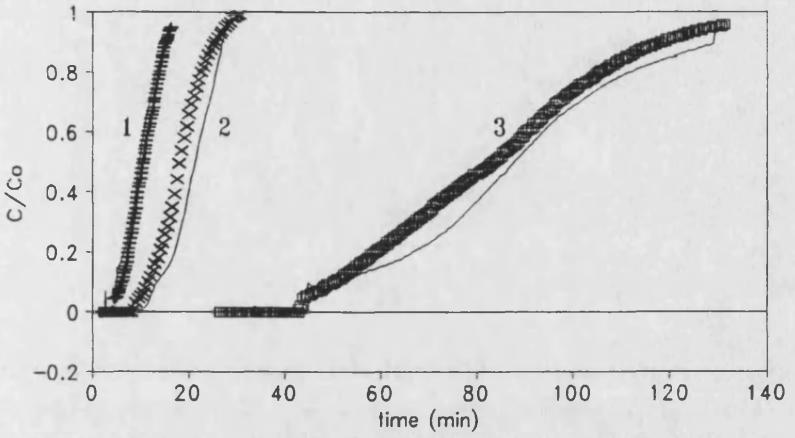

Fig. 7-11 Breakthrough prediction using Pnet1

1. flow rate : 16.4 ml/min ; feed concentration : 1.0 mg/ml
2. flow rate ; 7.4 ml/min ; feed concentration : 1.67 mg/ml
3. flow rate ; 2.24 ml/min ; feed concentration ; 1.5 mg/ml

The test results for Pnet2 are shown in Fig. 7-12, in which predicted breakthrough curves have been translated to the original time scale. There are some deviations between the predicted and measured breakthrough profiles, especially at the later stages, and the deviations are more significant in profile using compaction factor of 3. This implies that errors in the prediction might result from the compression of the time scale, and suggests that a smaller compaction factor, 2 might be a better choice. Despite the deviations, network Pnet2 provides a simple approach to the long term prediction.

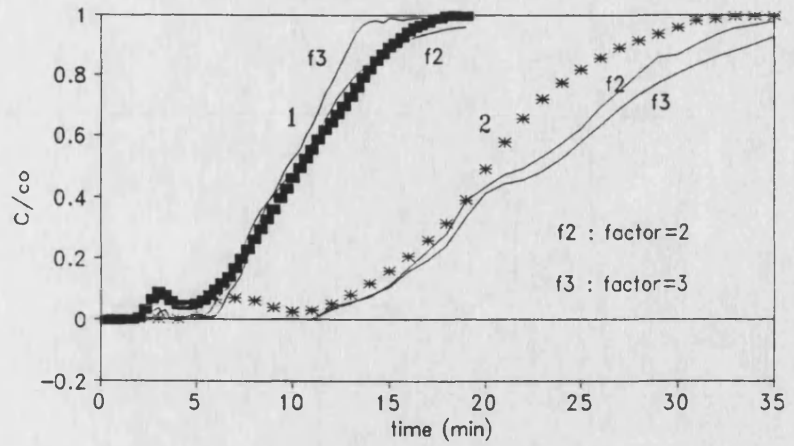

Fig. 7-12 Breakthrough prediction
using Pnet2 with factor, 2 and 3

1. flow rate : 16.4 ml/min ; feed concentration : 1.0 mg/ml
2. flow rate : 7.0 ml/min ; feed concentration : 1.5 mg/ml

CHAPTER. 8 DISCUSSION AND CONCLUSIONS

8.1 Feasibility of the thermal monitoring method

The feasibility of thermal monitoring is dependent on two factors: i) a measurable thermal process occurring during adsorbate uptake in a packed bed; ii) an applicable mapping protocol for use in correlating thermal responses and adsorbate concentration within the bed. Where the thermal signals are large enough to measure, the second factor has been demonstrated by the linear correlation between the elution volume ratio and the sensor position, and confirmed by the successful estimation of adsorbate breakthrough from thermal signals using both Kalman filter and neural network techniques. The generation of a measurable response is highly dependent on the adsorption system itself and will be dictated by the sensitivity of temperature detection and the operational conditions. The current sensitivity for thermal signal detection is 0.005 °C, which is equivalent to a sensor response of 0.1 mV. The results obtained demonstrate that adsorption of amino acids onto ion-exchange columns under normal feed concentrations and flow rates can be monitored by the method developed.

For high molecular weight compounds, such as proteins, the thermal effects of adsorption on ion-exchangers or affinity resins under realistic operational conditions are too small to be detected by the thermistor systems developed to date.

8.2 Choice of reference sensors

In this work sensing configurations using both external and "in-bed" references were used to follow temperature changes. These resulted in two forms of thermal signals: i) a temperature difference between a specific sensing position within the bed and a common reference point outside; ii) a temperature difference between two specific sensing positions within the bed *ie.* an "in-bed" differential thermal signal. Thermal signals obtained from both configurations reflect the system dynamics, and can thus be used to infer the concentration variables within the bed. However their different characteristics lead to differences in system performance and in the data handling methods required. The base line stability achievable using both approaches has already been discussed. The signals with an external reference are clearly more sensitive to outside temperature fluctuations, and so the "in-bed" differential approach is superior in practical application where accurate control of ambient temperature may not be possible. This conclusion is supported by results obtained using DEAE based ion exchange perfusive resins under high flow rates. In addition the sharp maxima of such differential thermal response profiles make identification of the thermal peak position relatively easy. This is particularly desirable when linear correlation is used to predict the initial point of the breakthrough. On the other hand, mechanistic modelling of thermal responses is more complex when using internal differential thermal measurements. It has been shown that there are significant deviations between the measured thermal profiles and those predicted by using the six stage model (see Fig.5-33). These internal differential thermal profiles were actually obtained by a model

simulation of the temperature difference between two positions where the sensing and reference thermistors were located. Therefore, a possible reason for these deviations is the uncertainty of the thermistor position, as the temperature difference is sensitive to the relative position of the two points. As these deviations could not be eliminated, efforts to use an EKF with "in-bed" differential thermal signals were eventually abandoned.

8.3 Advantages and limitations of the EKF approach

8.3.1 Comparison with the empirical correlation approach

In Chapter.5 a simple linear approach was proposed to relate the thermal wave data to the initiation of the breakthrough. The approach was successful, but in each case only a portion of the total thermal information was used as a basis for breakthrough prediction. Clearly the accuracy of this approach is highly dependent on the accurate determination of the maxima of the temperature-time curve, a procedure which is highly error prone (see Fig. 5-11 for example). Furthermore only individual points on the breakthrough curve could be inferred with this correlation. Matz *et al.* (1987) used a polynomial to correlate the trajectories of the thermal and adsorption waves. They also determined the times at which the thermal shift occurred at the thermal sensor's position, and then used these times to infer the time at which the breakthrough occured. Their approach suffers from similar drawbacks with regard to errors in estimation. In general the use of empirical correlations is an approach which may be easier to use but which is also more prone to error in practical applications.

An alternative approach is to use an EKF estimator which is based upon a state space model, in which the intrinsic relationships among the state variables are represented. The model estimation is run in parallel with on-line thermal measurements, and the latter is used to correct the model estimation. Therefore such a breakthrough estimation obtained should be more reliable, and this has been demonstrated by good correlation between the estimated and measured breakthrough profiles shown in Figs. 6-2 through 6-4.

8.3.2 Potential for use in process optimisation

In packed bed adsorption processes it is highly desirable that the adsorbate concentration at different positions within the column be estimated in real time, as a variety of optimisation techniques require such on-line information. An example of such an approach is the partial loading strategy (Dantigny *et al.*, 1991). This uses the information about an adsorption front position within the bed, together with knowledge of adsorption kinetics, to determine the best point at which to stop the loading stage, in order to reduce the loss of high value feed materials. The results described in Chapter. 6 show that adsorbate concentration at different stages of the bed can be estimated on-line by using an EKF enhanced thermal monitoring approach, thus providing a viable sensing system for use with a partial loading protocol.

8.3.3 More understanding of the system and the process

It is also highly desirable that the column adsorption capacity q_m be monitored as it varies due to repeated cycles of use, so that the optimum time to regenerate

or replace the resin can be identified. The EKF offers a potential route to this objective. As the bed capacity is included in the state space, its variation can be directly monitored. Results described in Chapter.6 show that the EKF gave reliable estimation for the bed capacity when different buffers were used.

It should be noted that the temperature and concentrations in both mobile and fixed phases at each stage are all included in the state space for the six stage model. At each sampling time values of all the variables at every stage are estimated, thus a comprehensive description of the process is obtained.

8.3.4 Limitations of the EKF approach

The performance of an EKF is subject to the validation of the model upon which it based. Efforts have been made to use an EKF dealing with in-bed differential thermal measurements. By adjusting the values of covariance matrix elements the EKF could trace the thermal measurements, unfortunately it failed to give convergent estimation for both breakthrough and the bed capacity. Clearly the degradation of performance of the EKF results from the inaccuracies of the model. Therefore use of the EKF is limited to thermal measurements obtained using an external reference in this study.

An EKF approach can be successfully used to solve estimation problems. However prior knowledge of the system is required for the design of such a filter. In this study the dominating equations among state variables can be readily derived by using first principles. However, determination of model parameters is

not straightforward as most are only observable in a lumped form. Efforts had to be made to find effective methods which can be employed to determine the parameters. For example, the effective heat transfer coefficient at the column wall, the adsorption capacity of the resin, and the adsorption rate constant had to be determined by model simulation. This is extremely time consuming.

8.4 Artificial neural networks (ANNs)-a robust approach to state estimation and prediction

8.4.1 Robust approach to state estimation

In many practical cases engineers have to deal with processes about which the information is poor, but where the data are rich. ANNs offer the distinctive ability to learn complex relationships between the state variables without prior knowledge of the processes occurring. Thus they are well suited to state estimation problems. Any mechanistic model with fixed parameters will fail to give correct prediction once some model parameters vary, but a neural network can cater for these parameter variations. The key feature is that the system parameters, such as bed capacity and adsorption rate constants, together with the operational conditions, determine the profiles of the temperature change when adsorption takes place within the column. In other words the thermal responses contain information about both the system parameters and operational conditions. Through the training process a neural network organises itself to form a representation of the system dynamics. Theoretically any consequence of the system parameter variations can be assessed by using a network. However, it was

found that the topology of the input vector space for the network training largely determined the performance of the network. Results described in Chapter. 7 show that even by simply using time histories of the data in the network input, system dynamics can be introduced to the network, and the network performance can be dramatically improved.

8.4.2 Comparison with Kalman filter

The neural network approach, as a "black box" method, does not require any a *priori* knowledge about the system, therefore it is cheap to develop and easy to use. As discussed in the last section, a Kalman filter failed to give correct estimation of the breakthrough by using in bed differential thermal signals, because the model for the filter is not able to describe such a thermal process correctly. However, this problem has been successfully solved by using neural networks. On the other hand, the "black box" feature of neural networks gives rise to their main drawback: at present they cannot be used to improve the understanding of the system. Furthermore, interpreting a network is difficult, as inferred knowledge of the process is spread among its many internal weights. Alternatively, an appropriate Kalman filter can give a comprehensive description of the process, and so widen and deepen our understanding of the system to which it is applied.

System dynamics can be easily introduced to a network in various ways, so that the network can be used to predict ahead, as long as an appropriate target vector is provided in the training process. The target vector can comprise either time

shifted or time compacted measurements of breakthrough. Whilst Kalman filters are rarely used for long term prediction, they can be used to estimate some variables which are not able to be directly measured, for example the concentration within the column.

8.5 Conclusion

8.5.1 A generic and simple approach to packed bed process monitoring

This thesis demonstrates that a generic and simple sensor using thermistors can be used to follow temperature changes in an adsorption column. Using the sensor developed, even very small thermal signals produced by adsorption of amino acids onto ion-exchange column can be detected.

Thermal monitoring is largely unaffected by the presence of non-adsorbing species, as has been demonstrated by the results obtained using a mixed feed consisting of aspartic acid and lysozyme. The presence of lysozyme in the feed solution made it impossible to follow the aspartic acid concentration in the bed outlet flow with a UV detector. However, by using thermal signals measured by the thermistors the adsorption front can be successfully traced.

Thermal signals obtained using an external reference thermistor system are easy to interpret and can be used in conjunction with Kalman filters. Whereas thermal signals obtained using an internal differential thermistor arrangement are less disturbed by the adjacent temperature fluctuations, offering improved sensitivity.

It is also possible to use thermal monitoring without the need of sophisticated ambient temperature control. The results obtained for aspartic acid-DEAE based ion exchange systems indicate that thermal monitoring can be successfully applied to the separation of low molecular weight compounds, including a variety of amino acids, using ion exchanger packed beds under conditions of practical interest.

The adsorption process, together with the accompanying thermal process, can be described by theoretical models derived from mass and heat balances. The existence of functional relationships between thermal and concentration signals was demonstrated by both experiments and theoretical model simulation. The simplest method of representing these relationships is the use of an empirical linear correlation, which can also be used to predict the breakthrough. However this simple approach is prone to error and subject to the location of thermal signal peak values. Model based estimation techniques provide more reliable approaches to breakthrough estimation and prediction using on-line thermal signals.

8.5.2 The model based enhanced thermal monitoring and control approach

Taking advantage of the recursive algorithm, the EKF provides an effective approach to infer non-linear process states, using a limited set of measurements corrupted with additive white noise. In this work, concentration variables at different positions in both mobile and fixed phases within the column were estimated, using on-line measured thermal signals. This allowed the adsorption

and breakthrough waves to be well traced in real time and provides information which can be used in a partial loading strategy (Dantigny *et al.*, 1991). The main drawback of EKF techniques, a performance degradation due to model mismatch, can be effectively overcome by both prior simulation of model parameters and simultaneous estimation of the adsorption parameters and the process state.

Alternatively, neural networks provide reliable inferences of the important, but sometimes difficult to measure, process states. Given an appropriate topology, the network can be trained to characterise the behaviour of the system. Therefore the unknown variations of the bed capacity can be quantified by a network, this being impossible using a simple mechanistic model. The key feature is that the system parameters, such as bed capacity and adsorption rate constants, together with the operational conditions determine the profile of the temperature change within the column.

Trained with either time shifted or time compacted breakthrough data, the neural network can be used to achieve long term prediction. Despite suffering from the time shift error, the network using time shifted data can give an acceptable prediction of the breakthrough, whilst the time compaction approach offers easier application. As it does not require the knowledge of systems, the neural network approach is robust and universal. This suggests that this method can be applied to other on-line monitoring systems, such as the thermal monitoring of pressure swing adsorption.

The conclusions can be summarised as follows: A generic and robust thermal sensor device has been developed, which when integrated with either Kalman filter or neural network techniques can be used for packed bed adsorption process monitoring and control. This approach should be applicable to any thermal monitoring system capable of providing detectable signals.

NOTATION*

A(n) discrete state transition matrix of linearized state space model at time step n

C measurement matrix

C liquid phase concentration (g/ml)

C_i point concentration of liquid inside particles (g/ml)

c specific heat

$c_i(n)$ adsorbate concentration in mobile phase within bed stage i at time step n (mg/ml)

D effective diffusivity (cm/min)

h_c heat transfer coefficient (J/cm^2)

ΔH adsorption heat (J/g)

h stage height (cm) of the bed

k effective conductivity (J/(cm k))

K Kalman filter gain

k_1 forward rate constant for surface adsorption (ml/(g.min))

k_2 reverse rate constant for surface adsorption (min^{-1})

k_f liquid film mass transfer coefficient (cm/min)

k_e heat transfer coefficient through the bed end ($J/min.cm^2$), here taken the same value as k_w

k_w effective heat transfer coefficient through the column wall ($J/min.cm^2$)

Nu Nusselt number

P(n) error covariance matrix at time step n

Q(n) state error covariance matrix at time step n

$q_i(n)$ adsorbate concentration in fixed phase within bed stage i at time step n (mg/ml)

q concentration of adsorbate in adsorbent (g/ml)

q_i point concentration of adsorbate inside particles (g/ml)

q_m Langmuir isotherm constant (g/g or g/ml)

R measurement error covariance matrix

R jacket radius in Chapter. 5, or column radius in Chapter. 6 (cm)

R_i rate of interface mass transfer (g/(ml.min))

R_p particle radius (cm)

r radial co-ordinate (cm)

r_p radial co-ordinate inside particles (cm)

t time (min)

T temperature (K)

$T_i(n)$ temperature in bed stage i at time step n, in fact, the temperature difference from the ambient temperature which assumed to be 0

T_0 temperature of water bath (K)

V excitation voltage

V(n) measurement white noise process vector

v_s stage volume (cm^3)

W(n) white noise process vector of the state

Δt time interval of sampling (min)

v superficial velocity of liquid (cm/min) except in Chapter. 4

v thermistor bridge output (V) in Chapter. 4

x axial co-ordinate in the bed (cm)

x_i element of state vector

X state vector

Y measurement vector in EKF; target vector in ANNs

ϵ, ϵ_b particle and bed porosity

μ viscosity (kg/m.s)

ρ density of the bed (g/ml)

REFERENCES

Ajinkya, M.B., Ray, W.H., and Froment, G.F. (1974), On-line estimation of catalyst activity profiles in packed bed reactor having catalyst decay. *Ind. Eng. Chem., Process Des.* Developm., 13, 107-112

Albery, W.J., Bartlett,P.N., Cass,A.E.G., Craston,D.H, and Hagget, B. G.D. (1986). Electrochemical sensors: theory and experiment, *J. Chem. Soc. Faraday Trans.*, 1, 82 1033-1050.

Anderson, N.G., Willis,D.D., Holladay, D.W., Caton, J.E., Holleman, J.W., Eveleigh, J.W., Attrill, J.E.,Ball, F.L., and Anderson, N.L. (1975) Analytical Techniques for Cell Fractions. XIX The Cyclum: An Automatic System for Cyclic Chromatography. *Anal. Biochem.*, 66, 159-174.

Arnold, F.H.,Blanch, H.W., and Wilke, C.R. (1985) Analysis of affinity separation-1. Predicting the performance of affinity adsorbers. *Chem. Eng. & Biochem. Eng. J.*, 30. B9-B23.

Arve, B.H. and Liapis, I.A., (1987) Modeling and analysis of biospecific adsorption in finite bath. *AIChE. J.*, 33, 179-193.

Bhat, N., Minderman, P., McAvoy, T., and Wang, N. (1989) Modelling chemical process systems via neural computation, *Proc. 3rd Int. Symp.* Control for profit, Newcastle-upon-Tyne.

Bhat, N., Minderman,P., and McAvoy,T. (1989) Use of neural nets for modelling of chemical process systems. Preprints for *IFAC Symp.* Dycord, Maastricht, The Netherlands, Aug. 21-23, pp 147-153.

Bhat, N. and McAvoy, T.J. (1990), Use of neural nets for dynamic modelling and control of chemical process systems. *Computers chem. Engng.* 14(4/5), 573-583.

Bhat, N.V. and McAvoy, T.J. (1992) Determining model structure for neural models by network stripping. *Computers chem. Engng.* 16(4), 271-281.

Birky, G.J. and McAvoy, T.J. (1989) A neural net to learn the design of distillation control. *ibid*, 205-213.

Boitieux, J.L., Desmet, G., and Thomas, D. (1979) An antibody electrode, preliminary report on a new approach in enzyme immunoassay, *Clin. Chem.*, 25, 318-321.

Bonnerjea, J., Stever, Oh., Hoare, M., and Dunnil, P. (1986) Protein purification: the right step at the right time. *Bio/Technology*, No.4, 954-958.

Booth,A., (1992), Ph.D thesis, University of Bath.

Bozic, S.M. (1979) "*Digital and Kalman filtering*", Edward Arnold Ltd, London.

Bremermann, H.J. and Andweson, R.W. (1989), An alternative to back-propagation: a simple rule for synaptic modification for neural net training and memory. Internal report, Department of Mathematics, University of California. Berkeley.

Brogan, W.L. (1991) "Modern control theory", pp72-76. Prentice-Hall International Ltd, New Jersey, USA.

Brown, H.D. 1969. in "Biochemical Microcalorimetry", p 149; Academic Press; New York.

Campbell, D.H., Luescher, E., and Lerman, L.S. (1951), Immunologic Adsorbents (I). Isolation of antibodies by a cellulose-protein antigen. P.N.A.S. U.S., 37, 575-578.

Canavas, C. (1984), Estimation of the dynamic behaviour of a fixed bed reactor through filtering. *IFAC Symposium DYCORD 86*, Bournemouth, U.K., 273-278.

Chase, H.A. (1986) "Automated affinity separation processes", *J. Chem. Tech. Biotechnol.*, 36, 351-356.

Chase, H.A. (1984) Affinity separations utilising immobilised monoclonal Antibodies-a new tool for the biochemical engineer. *Chem. Eng. Sci.* 39, 1099-1125.

Chase, H.A. (1984) Predition of the performance of preparative affinity chromatography. *J. Chromatography*, 297, 179-202.

Chattaway, G. and Stephanopoulos, G. (1989) An adaptive state estimator for detecting contaminants in bioreactors. *Biotech. Bioeng.*, 34, 647-659.

Chibata, I, Tosa, T., and Sato, T. (1985) "Aspartic acid" in Young, M.M. edited Comprehensive Biotechnology, Vol. 3, 633-640. Pergamon Press, Oxford-New York.

Cinar, A. (1984) Controller design for a tubular reactor. *Canad. J. of Chem. Engng.*, 62, 746-754.

Cooney, C.L., Raju, G.K., and Cnnor, G.O. (1991) Expert systems ans neural networks for bioprocess operation. *Int Symp. Bioprocess modelling and control.* Newcastle.

Cornwell, K. (1977) "The Flow of Heat", p237, p160, Van Nostrand Reinhold

Cowan, G.H., Gosling, I.S., Laws, J.F., and Sweetenham, W.P. (1986) Physical and mathematical modelling to aid scale-up of liquid chromatography. *J. Chromatography*, 363, 37-56. Company, New York.

Cuatrecasas, P., Wilchek, M., and Anfinson, C.B. (1968) Selective enzyme purification by affinity chromatography. *Biochem.*, 18, 3039-3045.

Cybenko, G. (1989) Approximation by superposition of a sigmoidal function. *Mathematics of Control, Signals and Systems* 2, 303-314.

Danielsson, B.; Mosbach, K. (1988) Enzyme Thermistors. *Methods in Enzymology*, 137, 181-197.

Dantigny, P., Wang, Y., Hubble, J., Howell, J.A. (1991) Optimisation of frontal chromatography by partial loading. *J. Chromatogr.*, 545, 27-42.

DiMassimo, C., Montague, G.A., Willis, M.J., Tham,.M.T., and Morris A.J. (1992) Towards improved penicillin fermentation via artificial neural networks. *Computers Chem. Engng.*, 16(4), 283-291.

DiMassimo, C., Lant, P.A., Saunders, A., Montague, G.A., Tham,.M.T., and Morris A.J. (1992) Bioprocess application of model based estimation techniques. *J. Chem. Tech. Biotechnol.*, 53, 265-277.

Dimitratos, J.D., Georgakis, M.S., Ei-Aasser, M.S., and Klein, A. (1989) Dynamic modelling and state estimation for an emulsion copolymer reactor. *Comput. chem. engng.*, 28, 121

Enfors, S.O. and Cleland, N (1988) Enzyme sensor for fermentation monitoring: Sample handling. *Methods in enzymology*, 137, 298-307.

Eveleigh, J.W. (1982) Practical considerations in the use of immunosorbents and associated instrumentation. *Anal. Chem. Symp. Ser.*, 9 (Affinity chromatography related techniques), 293-303. Wilmington, DE. USA.

Eveleigh, J.W. and Levy, D.E. (1977) Immunochemical characteristics and

preparative application of agarose based immunosorbents. *J. Solid-phase Biochem.*, 2, 45-78.

Fang Ming and Howell, J.A., 1991. Kinetic behaviour of a novel matrix ion exchanger, carboxymethyl-HVFM operated at high flow rate. *J. Chromatography*, 539, 255-266.

Foo, R.C. and Rice, R.G. (1975) On the prediction of ultimate separation in parametric pumps. *AIChE. J.*, 21, 1149-1156.

Francis, S. (1989) The recent excitement about neural networks. *Nature,* 337, 129-132.

Fulton, S.P., Cooney, C.L., and Weaver, J.C. (1980) Thermal enzyme probe with differetial temperature measurements in a laminar flow through cell. *Anal Chem.*, 52, 505-508.

Geankoplis, C.J. (1983) "Transport Processes and Unit operations" 2nd edition, Allyn and Bacon, Boston.

Gilles, E.D. (1987) Model-based techniques for controlling processes in chemical engineering. *10th World Congress on Automatic Control*, Munich, Germany.

Goodacre, R. and Kell, D. (1992) Rapid Analysis of Bioprocesses using pyrolysis mass spectrometry and neural networks: Application to indole production. *The 4th international symposium on analytical method, system and strategies in biotechnology*, 21-23 September 1992, Noordwikerhout, the Netherlands.

Graves, D.J. and Wu, Y-T. (1979) the rational design of affinity chromatography separation processes. *Adv. Biochem. Eng.*, 12, 219-253.

Graves, D.J. and Wu, Y-T., (1974) On predicting the results of affinity procedures.

Methods Enzymol., 34, 140-163.

Groszek, A.J. (1988) A study of heats of ion exchange processes by flow adsorption calorimetry. In Streat, M. edited "*Ion exchange for industry*" pp286-292, Ellis Horwood Ltd, Chichester.

Guilbault,G.G. (1976) "*hand book of enzymatic methods of analysis*", Marcel Dekker, New York.

Hebb, D.O. (1949) "*Organization of Behaviour*", Weley, New York.

Helfferich, F. (1986) Ion exchange: past, present, and future, in "*Ion exchange: Science and technology*" Edited by Alirio E. Rodrigues, 23-34, Matinus Nijhoff Publishers, Dordrecht/Boston/Lancaster.

Helfferich, F. (1962) "*Ion Exchange*", McGraw Hill, New York & London.

Hernandez, E. and Arkun, Y. (1992) Study of the control-relevant properties of backpropagation neural network model of nonlinear dynamic systems. *Computers Chem. Engng.*, 16(4), 227-240.

Hornik, K., Stichcombe, M., and White, H. (1989) Multilayer feedforward networks are universal approximators. *Neural networks* 2, 359-366.

Horstmann, B.J. and Chase, H.A. (1989) Modelling single-component affinity adsorption of immunoglobulin G to protein A immobilised agarose matrices, *Chem. Eng. Res. Des.*, 67, 243-554.

Hoskins, J.C. and Himmelblau, D.M. (1992) Process control via neural networks and reinforcement learning. *Computer Chem. Engng.*, 16(4), 241-251.

Hoskins, J.C. and Himmelblau, D.M., (1988) Artificial neural network models of

knowledge representation in chemical engineering, *Computers Chem. Engng.* 12.(9/10) 881-890.

Hubble, J. (1989) A simple model for predicting the performance of affinity chromatography column, *Biotechnology. Techniques.*, 3(2), 113-118.

Hubble, J. (1986) "The effect of operating conditions on the response of a differential enzyme thermistor", *J. Chem. Tech. Biotechnol.*, 36, 487-493.

Hudson, J.L., Kube, M., Adomaitis, R.A., Kevrekidis, I.G., Lapedes, A.S., and Farber, R.M. (1990) Nonlinear signal processing and system identification: Application to time series from electrochemical reactions. *Chem. Eng. Sci.*, 45(8), 2075-2081.

Jazwinski,A.H. (1970) *"Stochastic Processes and Filtering Theory"*. Academic Press, New York.

Kaguei, S., Yu, Q., and Wakao, N. (1985) Thermal waves in an adsorption column, *Chem. Eng. Sci.*, 40(7) 1069-1076.

Kalman, R.E. (1960) A new approach to linear filtering and prediction problems. *Trans. ASME. J. of Basic Engineering*, 82D, 35-45, March.

Kavuri, S.N. and Venkatasubramanian, V (1992) Combining pattern classification and assumption techniques for process fault diagnosis. *Computers chem. Engng.* 16(4), 299-312.

Kell, D.B., (1987) The principles and potential of electrical impedance spectroscopy: an introduction. In: Turner, A.P.F., Karube, I. and Wilson, G.S. (Eds.), *"Biosensors: Fundamentals and Applications"*. Oxford Universty Press, Oxford, pp. 427-468.

Kozub,J.D. and MacGregor, F.J. (1992) State estimation for semi-batch polymerizaton reactor. *Chem. Eng. Sci.*, 47(5), 1047-1062.

Kuruoglu, N.R., Ramirez, F.W., and Clough, D.E. (1981) Distributed parameter estimation and identification for systems with fast and slow dynamics. *Chem. Engng. Sci.*, 36, 1695-1712.

Kuruoglu, N.R., Ramirez, F.W., and Clough, D.E. (1982) Steady state sequential distributed parameter filtering. Theoretical developments and applications to packed bed reactors. *IFAC 3rd symposium on control of distributed oarameter systems*, XI. 13-17, 29th Jun.-7th July, Toulouse, France.

Kuruoglu, N.R., Ramirez, F.W., and Clough, D.E. (1985a) Use of a distributed computer system for tubular reactor profile and catalyst activity identification. *AIChE J.*, 31, 339-343.

Kuruoglu, N.R., Ramirez, F.W., and Clough, D.E. (1985b)
Steady state sequential distributed parameter filtering to estimate temperature and concentration profiles of a packed bed tubular catalytic reactor. *Chem. Engng. Sci.*, 40, 1441-1448.

Lewis, F.L. (1986) "Optimal Estimation", John Wiley & Sons, New York.

Liapis, A.I. (1989) Theoretical aspects of affinity chromatography, *J. Biotechnology*, 11, 143-160.

Litz, W., (1983). The thermokinetic reactor TKR and its possible application in chemical research and engineering. *J. Thermal Analysis* 27, 215-228.

Litz,W., (1987). Development and use of a constant flow stirred thermokinetic reactor (steady state TKR). *J. Thermal Analysis* 32, 1991-1999.

Lynch, E.B. and Ramirez, W.F. (1975), Real-time time-optimal control of a stirred tank reactor using Kalman filtering for state estimation. *AIChE J.*, 21, 799.

MacGregor, F.J., Kozub, D.J., Penlidis, A., and Hamielec, A.E. (1986). State estimation for polymerization reactor. *IFAC Symposium DYCORD 86*, Bournemouth, U.K., 147-152.

Mah, R.S.H. and Chakravarthy, V. (1992) Pattern recognition using artificial neural networks. *Computers chem. Engng.* 16(4), 371-377.

Mandenius, C.F. and Danielsson, B., 1988, Enzyme thermistors for process monitoring and control. *Methods in enzymology*, 137, 307-318.

Markx, G.H., Hoppen,H.J.G, Meijer, J.J. and Vinke, K.L. (1991). Dielectric spectroscopy as a novel and convenient tool for study of the shear sensitivity of plant cell in suspension culture. *J. Biotechnol.* 19, 145-158.

Martin, A.J.P. and Synge, R.L.M. (1941) A new form of chromagram employing two liquid phases-I. A theory of chromatography. II. Application to the determination of the high monoamino acids in proteins. *Biochem. J.*, 35 1358-68.

Matz, M.J.; Knaebel, K.S. (1987) Temperature front sensing for feed step control in pressure swing adsorption. *Ind. Eng. Chem. Res.*, 26, 1638-1645.

Microsoft coparation, Quick Basic (1988)

Milsom, P.E. and Meers, J.L. (1985) Gluconic and Itaconic acids in Yuong, M.M. edited *Comprehensive Biotechnology*, Vol. 3, 681-700. Pergamon Press, Oxford-New York.

Minskey M. and S. Papert (1968) *"Perceptrons"*, MIT Cambridge

Montague, G.A., Morris, A.J., and Tham, M.T. (1992) Enhancing bioprocess operability with generic software sensors. *J. Biotechnol.*, 25, 183-201.

Moore, S. (1968) Amino acid analysis: Aqueous dimethyl sulfoxide as solvent for the Ninhydrin reaction. *J. Biological Chemistry*, 243 (23), 6281-6283.

Mosbach, K.; Danielsson, B. (1981) "Thermal bioanalysers in flow streams, enzyme thermistor devices", *Anal. Chem.*, 53, 83A-94A.

Mosbach, K. 1991, Thermal biosensors. *Biosensors & Bioelectronics*, 6, 179-182.

Ramirez, W.F., (1987), Optimal state and parameter identification. An application to batch fermentation. *Chem. Eng. Sci.*, 42(11), 2749-2756

Regenass, W., (1985). Calorimetric monitoring of industrial chemical processes. *Thermochimica Acta* 95, 351-368.

Rialdi, G.; Biltonen, R.L. (1973) Thermodynamics and thermochemistry of biologically important systems, in Skineer, H.A. edited *International Review of Science, Physical Chemistry, Series* 2, 10, 147-189. Butterworth and Co. Ltd. London and Buston.

Rosenblatt, F. (1962) *Principles of Neurodynamics*, Spartan Books, Washington DC.

Rumelhart, D.E. and McClelland (1986) *Parallel Distributed Processing: Exploration in the Microstructure of Cognition,* Vol.1, MIT press, Cambridge

Rumelhart, D.E., Hinton, G.E., and McClelland,J.L. (1986) A general framework for parallel distributed processing. In Rumelhart and McClelland (eds), *Parallel Distributed processing*, MIT press, Cambridge, MA.

Rumelhart, D.E., Hinton, G.E., and Williams, R.J. (1986) Learning representations by back-propagating errors. *Nature* 323, 533-536.

Ruthven, D.M. (1984) "Principles of adsorption and desorption processes", Wiley-Interscience, New York.

RS Data Library, 10209, Thermistors, issued March 1990, RS components, Ltd., London

Said, A.S. (1956) Theoretical-plate concept in chromatography. *AIChE. J.*, 2, 477-481.

Samuelson, O., (1963) "Ion exchange separations in analytical chemistry", John Wiley & sons, New York, London

San, K.Y. and Stephanopoulos, G. (1984a) Studies on on-line bioreactor identification- II. Numerical and experimetal results. *J. Biotech. Bioeng.*, 26, 1189-1197.

San, K.Y. and Stephanopoulos, G. (1984b) Studies on on-line bioreactor identification- IV. Utilization of pH measurements for product estimation. *J. Biotech. Bioeng.*, 26, 1209-1118.

Sapoff, M. (1972) Thermistors for biomedical use, in " Temperature - its measurement and control in science and industry" edited by Plumb, H.H. Vol.4 part 3, 2109-2121. Instrument Society of America.

Schnelle, P.D. and Richards, J.R. (1986) A view of industrial reactor control: difficult problems and workable solutions. *Chem. Process Control* 3, 749-802.

Schuler, H. and Zhang, S. (1985) Real-time estimation of the chain length distribution in a polymerization reactor. *Chem. Eng. Sci.*, 40, 1881-1904.

Schuler,H. and Papadopoulou, S. (1986), Real-time estimation of the chain length distribution in a polymerization reactor- II. Comparison of estimated and measured distributions *Chem. Eng. Sci.*, 41, 2681-2683.

Schultz and Melsa (1967) *"State function and linear control systems"*. pp 112-115, McGraw-Hill.

Skidmore,L., Horstmann, B.J., and Chase, H.A. (1990), Modelling single-component protein adsorption to the cation exchanger S Sepharose FF. *J. Chromatogr.* 498, 113-128.

Slater, M.J. (1991) "The principles of ion exchange technology", Butterworth-Heinemann Ltd, Oxford.

Sorensen. J.P., Jorgensen, S.B., and Clement, K. (1980), Fixed bed reactor Kalman filter and optimal control - I. Computational comparison of discrete vs. continous time formulation. *Chem. Eng. Sci.*, 35, 1223-1230.

Special issue of *Computer & Chemical Engineering* (1992), Vol.16 (4)

Srivastava, A., Roychoudhury, P.R., and Sahai, V. (1992) Extractive lactic acid fermentation using ion exchange resin, *Biotechnology Bioengineering*, 39, 607-613.

Stephanopoulos, G. and San Ka-Yiu (1984), Studies on on-line bioreactor identification- I. Theory. *J. Biotech. Bioeng.*, 26, 1176-1188.

Su Hong-Te and McAvoy, T.J. (1992), Long-term predictions of chemical processes using recurrent neural networks: A parallel training approach. *Ind. Eng. Chem. Res.* 31, 1338-1352.

Thibault, J., Breusegm, V., and Cheruy, A. (1990) On-line prediction of Fermentation variables using neural networks. *Biotechl. Bioeng.*, 36, 1041-1048.

Thomas, H. C. (1944) Heterogeneous ion exchange in a flowing system, *J. Amer. Chem. Soc.*, 66, 1664-1666.

Tsou, H. and Graham, E.E. (1985) Prediction of adsorption and desorption of Protein on Dextran based ion exchange resin. *AIChE. J.*, 31 (12), 1959-1966.

Venkatasubramanian, V. and Chan, K. (1989), A neural network methodology for process fault diagnosis. *J. AIChE.* 35(12), 1993-2002

Venkatasubramanian, V., Vaidyanathan, R., and Yamamoto, Y. (1990), Process fault detection and diagnosis using neural networks-I. Steady state processes. *Computers Chem.Engng.* 14, 699-712

Wankat, P.C., (1974) Theory of affinity chromatography separations, *Anal. Chem.*, 46, 1400-1406.

Wanatabe, K., Matsuura, M.A., Kubota, M., and Himmelblau, D.M. (1989), Incipient fault diagnosis of chemical process via artificial neural networks. *J. AIChE* 35, 1803-1812.

Wang,Z., Tham, M.T., and Morris, A.J. (1992), Multilayer feedforward neural networks: Approximated canonical decomposition of nonlinearity. *Int. J. Cont.*, 56(3), 655-672.

Widrow, B (1962) Generalization and information storage in networks of adaline 'neurons', in "Self organizing systems", Yovitz,M. et al. Eds, Washington, DC, Spartan Books, pp435-461.

Widrow, B. and Lehn, A. (1990), 30 years of adaptive neural networks: Perceptron, Madaline, and Backpropagation. *Proc. IEEE.* 78, 1415-1441.

Willis, M.J., DiMassimo, C., Tham, M.T., and Morris, A.J. (1991), Artificial neural

networks in process engineering, *IEE Proceeding-D*, 138(3), 256-266.

Wood, S.D., Mangum, B.W., Fillben, J.J., and Tillet, S.B. (1987), An investigation of the stability of thermistors. *J. Rew. NBS,* 83, 247-263.

Wu, R.S.H., (1985). Dynamic thermal analysis for monitoring batch processes. *Chem. Engng. Prog.* 57-61

Yang, M., Fang Ming, Hubble, J., Lockett, A.D., Rathbone, R.R., and Howell, J. (1992). On-line thermal monitoring of aspartic acid separation in a high voidage ion-exchange column at high flow rate. *Biotechnol. Biotechniques* 6(5), 409-412

Yang, M., Hubble, J., Fang Ming, Lockett, A.D., and Rathbone, R.R. (1993) A neural network for breakthrough prediction in packed bed adsorption". *Biotechnol. Techniques*, 7(2), 155-158.

Yang, M., Rathbone, R.R., Hubble, J., and Lockett, A.D. (1993) In *situ* thermal monitoring of adsorption column performance. *Analytica Chimica Acta*, 279(1) 95-106

Yang, C.-M. and Tsao, G.T. (1982) Packed-bed adsorption theories and their applications to affinity chromatography in *Advances in Biochemical Engineering* edtied by Fiecher, A., Vol. 25, 1-18.

Yoshida, H. and Ruthven, D.M. (1984) Dynamic behaviour of an adiabatic adsorption column-I Analytic solution for irreversible adsorption, *Chem. Eng. Sci.*, 38(6), 877-884.

APPENDIX

1 The correlation between concentration and UV absorbence (Aspartic acid)

$$c=0.00093+0.0041A+(1.85e-7)A^2+(2.17e-8)A^3$$

2. Programs used in this thesis

Program : heattransfer

```
'Date     : 02/07/1991:  Mengyan Yang

'this program is to solve a partial differential eqaution as follows:
'    T'(t)=k/c/p(T"(x)+T"(r)+t'(r)/r)-vT'(x)+q/c
'with following boundary conditions:
'    ke*T=-k*(dT/dx) at both of the start and end of the column
'    kw*T=-k*(dT/dr) at r=R (eg. the outside surface of the jacket)
cls
input"stage or diffusion model, s or d", mo$

input"loading concentration, C0";C0 :cs=c0
input"total length of the column , cm";tl
input"real length of the column, cm"; rl
input "step size in x, cm";h0
input "start point of the resin, cm";x0
le=tl-x0-rl
si=int(0.5+SQR(1+8*x0/h0)/2)
esi=int(0.5+SQR(1+8*le/h0)/2)
dh1=int(si+2.5/h0): dh2=int(si+3/h0)
m=int(si+esi+rl/h0)
input "total time of breakthrough, min";tt
input"step size in t, min";g
input "How many steps in radius";js
dr0=2.4/js/(js+1)
ej=int((sqr(1+35.2/dr0)-1)/2)
dim t(m+1,ej):dim l(9):dim x(9):dim t1(m+1,ej), d(m)
ro=js+2:re=m-2
input"heat conductivity,w/cm*k";k
input"heat conductivity through  the wall";kw
input"heat conductivity through the column ends, ke";ke
input"heat conductivity through the wire";dwc0
input"specific heat of the front matieral,j/g*k";cg
input"density of the bed, g/cm^3";pb
input"flow rate, cm^3/min";v
input"the voidage";vd

input"adsorption heat, j/g";he
if mo$="s" then 4
input"diffusion coeficient";df
input"film difusity";kf
input "how many steps in pore direction"; ro
input "particle size of the resin, in cm"; r:r=r/2
br=r/ro
v=v/eb
g1=br*br/4/df
```

```
rp=int(g/g1)+1:g1=g/rp
cb=si+1 : ce=si+int(rl/h0)
dim cbu(m),cbu2(m),ci(m,ro),ci2(m,ro),dq(m),q(m,ro),q2(m,ro)

4 t0=x0/v*4.52/1.44
'1.44:  the ratio of empty volume over total volume before the resin
input "name the file";nam$ :input" specify the drive";dr$
nam$=dr$+":"+nam$
input"time of loading end";lend
input"give the interval for loging the data in, min"; wid
tj0=int(wid/g)
ta=int(tt/wid)
input "give the start point where you want to know the temperature";x(0)
input "and the interval in the column , cm";xint
dim tim(ta),d1(ta),d2(ta),d3(ta),d4(ta),d5(ta),d6(ta),d7(ta),d8(ta),c(ta)
l(0)=int(si+x(0)/h0)
intc=int(xint/h0)
for i=1 to 8
x(i)=x(i-1)+xint
l(i)=l(i-1)+intc
next i
y=xint/h0
5 gosub logind1
tim=tim+wid
if tim<t0 then 5
tj=0
tim=t0: gosub logind1

'HUbble's adsorption kenitic model paraments

dim c(2, 500), q(2,500), c0(2,500), dq(500)
input "maximum capacity, qm"; qm
input" adsorption rate constants, k1"; k1
input" and k2"; k2
nstage=int(rl/h0): fr=v/4.04
tfin=h0/fr
cb=si+1 : ce=si+nstage
cb1=si:cb2=si+y:cb3=si+2*y:cb4=si+3*y:cb5=si+4*y:cb6=si+5*y:cb6=si+6*y
cb7=si+6*y:cb8=si+7*y
factor=int(tfin/g)
g=tfin/factor
n=int(tt/g)
ei=int(si+rl/h0)
for tg=0 to n-1
if tim>(t0+lend) then c0=0
c(1,cb-1)=c0*vd
if tg=stept then gosub adsorb
for i=1 to m-1
c=4.18
h=h0
if i<si then h=(si-i+1)*h0: c=cg
if i>ei then h=(i-ei)*h0
vl=v/4.522 :p=pb
dwc=0
if abs(i-dh1)<1 then dwc=dwc0
if abs(i-dh2)<1 then dwc=dwc0
for j=1 to ej
if j>js then vl=0:p=1 :c=4.18
d1=k/c/p:   a1=d1*g :   d=g/c
a3=a1/h/h:  b=1-2*a3:
dr=dr0*j
d2=a1/dr/dr
t(0,j)=t(1,j)/(1+h*ke/k): t(m,j)=t(m-1,j)/(1+ke*h/k)
t(i,0)=t(i,1): t(i,ej)=t(i,ej-1)/(1+dr*kw/k)

if j>js-1 then dwc=0
a2=vl*g/2:a4=a2/h
```

```
a=a3-a4:c1=a3+a4
heat=he*dq(i)
t1i=a*t(i+1,j)+b*t(i,j)+c1*t(i-1,j)+d*heat-t(i,j)*dwc
t1j=d2*((1+1/(1+j))*t(i,j+1)+(1-1/(1+j))*t(i,j-1)-2*t(i,j))
if j=1 then t1j=d2*(t(i,j+1)-t(i,j-1))*2

t1(i,j)=t1i+t1j
next j

next i
for i=1 to m-1
for j=1 to ej-1
t(i,j)=t1(i,J)
next j
d(i)=t(i,0)-t(re,ro)
next i

tim=tg*g+t0
if tim>(tt+t0+4) then 40
if tg=tj then gosub logind1

next tg
40 tim=tim+10
open nam$ for output as #1
print#1, using"###.####"; tim
close #1

50 input "do you want to print the experement conditions out?";p$
if p$="n" then 100
if p$="y" then 60 : else goto 50
60 lprint"length of the column, Lc=";rl
lprint"locations of sensors "
lprint,using"#.##  ";x(0),x(1),x(2),x(3),x(4),x(5),x(6),x(7)
lprint"heat conductivity along the column, k=";k
lprint"heat exchange coef through the jacket wall, kw=";kw
lprint "heat exchange coef through the column ends, ke=";ke
lprint"loading concentration of the adsorbate, C0=";cs
lprint "Liquid flow rate, V=";v
lprint "specific heat , c=";c
lprint "density, d=";p
lprint"q(max)=";qm
lprint"k1,k2";k1,k2
lprint"step size in x and in t";h0,g

open nam$ for output as #1
for i=0 to n
print#1,using"###.##### ";tim(i),d1(i),d2(i),d3(i),d4(i),d5(i),d5(i),d6(i),d7(i) d8(i),c(i)
next i :close #1

100 print:print "**************END*****************"
end

logind1:
tim(n)=tim: d1(n)=d(cb1):d2(n)=d(cb2):d3(n)=d(cb3):d4(n)=d(cb4)
d5(n)=d(cb5):d6(n)=d(cb6):d7(n)=d(cb7):d8(n)=d(cb8):c(n)=c(1,ce)/vd
n=n+1
tj=tj+tj0
return

adsorb:
if mo$="s" then gosub sub-stage
if mo$="d" then gosub sub-diff
return
```

programe: sub-stage model

```
sub-stage:
for i=cb to ce
c0(2,i)=c(1,i-1)+q(1,i)
b=-(k1*(c0(2,i)+qm)+k2)
a=k1*qm*c0(2,i)
x=4*a*k1-b*b
sx=sqr(-x)
q(2,i)=(b-sx)*(2*k1*q(1,i)+b+sx)-(b+sx)*(2*k1*q(1,i)+b-sx)*exp(tfin*sx)
q(2,i)=q(2,i)/((k1*exp(tfin*sx)*(2*k1*q(1,i)+b-sx)-k1*(2*k1*q(1,i)+b+sx))*2)
c(2,i)=c0(2,i)-q(2,i)
next i
stept=stept+factor
for i=cb to ce
dq(i)=(q(2,i)-q(1,i))/tfin
C(1,i)=c(2,i): q(1,i)=q(2,i)
next i
return
```

Program: sub-diffusion

```
sub-diff:

for dg=1 to rp
cbu(si)=c0 : cbu(ce+1)=cbu(ce)   : cbu(si-1)=c0
ci(i,1)=ci(i,2)
ci(i,ro)=(ci(i,ro-1)*e*df/br+kf*cbu(i))/(e*df/br+kf)
cbu2(i)=cbu(i)-v*g1*(cbu(i)-cbu(i-1))/h-3*kf*(1-eb)*g1*(cbu(i)-ci(i,ro))/r/eb/e
q2(i,1)=q(i,1)+g1*k1*ci(i,1)*(qm-q(i,1))-g1*k2*q(i,1)
q2(i,ro)=q(i,ro)+g1*k1*ci(i,ro)*(qm-q(i,ro))-g1*k2*q(i,ro)
for pr=ro-1 to 2 step -1
q2(i,pr)=q(i,pr)+g1*k1*ci(i,pr)*(qm-q(i,pr))-g1*k2*q(i,pr)
ci2(i,pr)=ci(i,pr)+df*g1*(ci(i,pr+1)*(1+1/pr)-2*ci(i,pr)_
+(1-1/pr)*ci(i,pr-1))/br/br-(1-e)*(q2(i,pr)-q(i,pr))/e
next pr
for pr=1 to ro
dq(i)=dq(i)+(q2(i,pr)-q(i,pr))*br*br*br*(2*pr-1)^2
next pr

cbu(i)=cbu2(i)
for pr=1 to ro
ci(i,pr)=ci2(i,pr):q(i,pr)=q2(i,pr) : next pr
next dg
dq(i)=dq(i)/r/r/r*(1-eb)*1.5*(1-e)
return
```

Programe: multlog

```
for data collection and co-orperating with Kalman filter or neural network
Input"delect the data processing, k or n"; pd$
'*****************************************************************
104 '*  Revision : 2.10                                          *
106 '*  Date     : 3/4/92                Mengyan Yang            *
108 'Data logging and program controling the stage conversion
110 CLS

150 LOCATE 20, 5: PRINT "Press any key to start..."
152 DD$ = INKEY$: IF DD$ = "" THEN 152
154 CLEAR , 49152!
158 CLS
160 PRINT : PRINT
162 INPUT "enter p for preparing or e for experiment"; selc$
```

```
164 DIM At(14, 14), p1(14, 14), p(14, 14), tmp(14, 14), tmp1(2, 2), k(14, 2)
166 DIM R(2, 2), q(14), C(2, 14), cY(2), X(14), tX(14), Y(2), tmp2(2, 2)
168 DIM temp(14, 2), tmp3(14, 2), kq2(4), cq1(4)
170 INPUT "Kalman filter or Neural net?"; pro$
172 IF pd$ = "k" THEN 188
174 IF pd$ = "n" then 190 : ELSE 190

188 if pd$="k" GOSUB 2800:  'get data for the model

190 INPUT "How long do you want to run"; period:gosub neuset
194 INPUT "sampling period, in sec"; arm
200 INPUT "do you want to store data in disk"; bd$
202 IF bd$ < > "y" THEN 210
204 INPUT "name the files for orlginal & Estimated data"; nam1$, nam2$
206 INPUT "specify the drive"; DRV$
208 nam1$ = DRV$ + ":" + nam1$: nam2$ = DRV$ + ":" + nam2$

210 SCREEN 0, 0, 0: WIDTH 80: CLS : KEY OFF
212 INPUT "How many channels on board0?"; bon: b0n = bon - 1

221 IF selc$ = "p" THEN perle = period: GOTO 240
222 INPUT "time of loading end"; perle
224 INPUT " time of washing end"; perwe
226 INPUT "time of eluting end"; perele
227 INPUT "time of regenerating start"; peregs
228 INPUT "time of regenerating end"; perege
230 INPUT "time of equilibrium start"; pereq
240 IF bon < 6 THEN aim = 100 * arm:  ELSE aim = 100 * arm
250 nm = INT(perle / arm * 60) + 80
252 dt = arm / 60
254 bl = INT(60 * start / arm)
256 bav = INT(48 * start / arm)
260 '********  STEP 1: LOAD PCL718.BIN DRIVER  ****************************
270 '
320 '********  STEP 2: INITIALIZE DRIVER USING FUNC 0  ********************
330 '
340 DIM DAT%(4), ARY1%(500), ARY2%(500), DATC%(1)
350 port% = &H300          'set I/O port address
360 DAT%(0) = port%        'get I/O port address
370 DAT%(1) = 2            'select interrupt level 2
380 DAT%(2) = 3            'select D.M.A. IRQ3
400 ER% = 0               'error return code
410 FUN% = 0              'driver function 0
420 CALL pcl818(FUN%, SEG DAT%(0), SEG ARY1%(0), SEG ARY2%(0), ER%)
430 IF ER% < > 0 THEN PRINT "Driver initialization failed!": STOP

440 '
450 '********  STEP 3: DEFINE DATA ARRAY AND OBTAIN EACH      ************
460 '********          PCLD-889'S GAIN SETTING                ************
470 '
480 'Initialize a real array D(15) to receive A/D data.
490 DIM d(7)  '16 elements, one for each PCLD-889 channel
500 'Get each of the 5 PCLD-889s'gain setting.
510 DIM AV(4), gain%(4)
520 CLS
530 FOR CH% = 0 TO 1
540 PRINT USING "Enter the # PCLD-889 Gain setting (0.5 TO 1000)"; CH%;
550 INPUT AV(CH%)
555 GOSUB 8000
560 NEXT CH%
neuset:

dim oi(4),wh(4,4), wo(4),ol(4),netl(4)
INPUT "the file is wstore"; wn$
IF wn$ < > "y" THEN wn$ = dr$ + ":tempwe": GOTO 40
wn$ = dr$ + ":" + "wstore"
40 OPEN wn$ FOR INPUT AS #10
```

```
FOR j = 1 TO 4
        FOR i = 1 TO 4
                INPUT #10, wh(i, j)
        NEXT i
        INPUT #10, wo(j)
NEXT j:return

570 DIM DE(2, 8): DIM rde(2, 8), EY1(nm), EY2(nm), MY1(nm), MY2(nm), EC(nm)
574 DIM time(nm), uv(nm), t1(nm), t2(nm), t3(nm), t4(nm), t5(nm),c(nm)
576 IF bon > 6 THEN 578 ELSE 580
578 DIM t6(nm), t7(nm), t8(nm)

580 '********  STEP 4: READ PCLD-889 ANALOG OUTPUTS USING        *********
590 '********          PCL-718 DRIVER FUNCTIONS                  *********
610 'This step is written as a subroutine so you can edit it out and
620 'use it in your own program.
630 '  CH%     - the PCL-718 input channel that PCLD-889 is connected to (0-7).
640 '  D(15)   - real data array to receive data from channels.
645 '  SB%     - the PLCD-889 multiple input channels
648 '  AV(CH%) - gain setting on each PCLD-889.

650 INPUT "initial solution is buffer, isn't it? yes or no or water"; in$
651 IF in$ = "y" THEN DATC%(1) = 7
652 GOSUB 9000
654 IF in$ = "w" THEN DATC%(1) = 6: GOSUB 9000
656 INPUT "press p to survey the baseline or  l  to start loading"; st$
657 IF st$ = "l" THEN DATC%(1) = 3: GOSUB 9000

658 PRINT "********************NOW READ DATA IN**********************"
660 n = 0: pt = TIMER: tsam = perle

663 GOSUB 3200: ' initialise A
665 ct1 = TIMER: FOR i = 0 TO aim
670 FOR CH% = 0 TO 1
680 'Set PCI-818 input scan channel range using driver function 1.
690 FUN% = 1: DAT%(0) = CH%: DAT%(1) = CH%
700 CALL pcl818(FUN%, SEG DAT%(0), SEG ARY1%(0), SEG ARY2%(0), ER%)
710 IF ER% < > 0 THEN PRINT "ERROR IN SETTING PCL-718 INPUT SCAN CHANNEL": END
712 'Set up PCLD-889 sub-multiplexer input channel and gain

714 IF CH% = 0 THEN EI = b0n: UNI = 1000: gain = AV(0)
716 IF selc$ = "p" THEN 725
724 IF iperm > perle THEN gain%(0) = 1: gain = 1

725 GGAIN% = gain%(CH%) * &H10
726 IF CH% = 1 THEN EI = 0: UNI = 1: gain = 1
730 FOR SB% = 0 TO EI
740 DAT%(0) = SB% + GGAIN%: 'sb%, for subchannel setting; ggain%, for gain setting
750 OUT port% + 3, DAT%(0)
760 FOR DD% = 0 TO 140: NEXT DD%
770 'Perform a software triggered single A/D conversion using driver function 3.
780 'Transfer data to corresponding array element D(SB%).
790 FUN% = 3
800 CALL pcl818(FUN%, SEG DAT%(0), SEG ARY1%(0), SEG ARY2%(0), ER%)
810 IF ER% < > 0 THEN PRINT "ERROR IN PERFORMING A/D CONVERSION"
820 '
830 '********  STEP 5: CONVERT A/D DATA TO VOLTS              **********
840 '
850 'Convert A/D data to real volts.
860 d(SB%) = DAT%(0) / 2048 / gain * UNI
862 DE(CH%, SB%) = DE(CH%, SB%) + d(SB%)
864 d(SB%) = 0
870 'Now repeat sequence for all other PCLD-889 channels
880 NEXT SB%

890 '
900 '********  STEP 6: DISPLAY MEASURED DATA  ****************************
```

```
910 '
920 'display measured data of the PCLD-889 16 input channels.
950 '******** STEP 7: REPEAT STEP 4 THROUGH 6 FOR NEXT PCLD-889 *********
960 'Change to next PCLD-889 multiplexer board.
962 NEXT CH%: NEXT i
963 IF n < = 50 THEN ct2 = TIMER

964 FOR IR = 0 TO 1
966 IF IR = 0 THEN EI = b0n:  ELSE EI = 0
974 FOR JR = 0 TO EI
975 rde(IR, JR) = DE(IR, JR) / aim: DE(IR, JR) = 0
976 NEXT JR: NEXT IR
978 GOSUB 2000
979 IF selc$ = "p" THEN perle = period: GOTO 984
982 IF INT(iperm) = INT(perle + 1) THEN DATC%(1) = 6: GOSUB 9000: PRINT "loading end"

984 IF n < 50 THEN ct3 = TIMER: aim = INT((arm - ct3 + ct2) * aim / (ct2 - ct1))

988 IF iperm < perle THEN 665
999 IF bd$ = "y" THEN fin = n: GOTO 1002
990 INPUT "enter c for  continue , n for new start or e for  end "; con$
992 IF con$ = "e" THEN fin = n: GOTO 1000
994 INPUT "how long, in min"; ext: perle = perle + ext
995 perwe = perwe + ext: perele = perele + ext: peregs = peregs + ext: perege = perege + ext
996 pereq = pereq + ext: period = period + ext
997 IF con$ = "n" THEN perle = ext: GOTO 190

998 GOTO 665
1000 IF bd$ < > "y" THEN 1060
1002 IF bd$ = "y" THEN 1120
1010 INPUT "name the file1"; nam1$
1020 INPUT "name the file2"; nam2$
1030 INPUT "which driver"; dr$
1040 IF dr$ < > "a" THEN dr$ = "c"
1050 nam1$ = dr$ + ":" + nam1$: nam2$ = dr$ + ":" + nam2$: GOTO 1120
1060 INPUT "lose all data"; nl$
1070 FOR i = 1 TO bav
1075 uv(i) = 0
1080 NEXT i
1110 IF nl$ = "n" THEN 1010
1112 IF nl$ < > "n" THEN INPUT "are you sure"; sure$
1114 IF sure$ = "y" THEN 1160 ELSE GOTO 1010
1120 IF bon < 6 THEN 1122 ELSE GOTO 1140
1121 fin = n
1122 OPEN nam1$ FOR APPEND AS #1
1124 FOR n = 0 TO fin
1126 PRINT #1, USING " ###.#### "; time(n); uv(n); t1(n); t2(n); t3(n)
1128 NEXT n: CLOSE #1
1130 OPEN nam2$ FOR APPEND AS #2: FOR i = 1 TO fin
1132 PRINT #2, USING "###.#####"; time(i); uv(i); EC(i); MY1(i); EY1(i); MY2(i); EY2(i)
1134 NEXT i: CLOSE #2

1138 IF bon < 6 THEN 1160

1140 OPEN nam1$ FOR output AS #1: FOR n = 1 TO fin
1146 PRINT #1, USING "###.#### "; time(n); uv(n);t2(n);t3(n);c(n)
1148 NEXT n: CLOSE #1

1150 IF slec$ = "p" THEN 1190
1160 GOSUB 6000
1170 IF iperm > period THEN GOTO 1190
1171 IF INT(iperm) = INT(perle + 1) THEN DATC%(1) = 6: GOSUB 9000: PRINT "loading end"
1172 IF INT(iperm) = INT(perwe) THEN DATC%(1) = 5: GOSUB 9000: PRINT "eluetion start"
1174 IF INT(iperm) = INT(perele) THEN DATC%(1) = 6: GOSUB 9000: PRINT "washing start"
1176 IF INT(iperm) = INT(peregs) THEN DATC%(1) = 4: GOSUB 9000: PRINT "regeneration start"
1178 IF INT(iperm) = INT(perege) THEN DATC%(1) = 6: GOSUB 9000: PRINT "regeneration end"
1180 IF INT(iperm) = INT(pereq) THEN DATC%(1) = 7: GOSUB 9000: PRINT "equilibrium start"
```

```
1184 GOTO 1160
1190 PRINT "N="; n: PRINT "***********END***********"

1295 END

2000 '******** SUBROUTINE TO write ANALOG INPUT SIGNALS onto an array ************
2002 '******** and display them on the screen *************
2004 tperm = TIMER: iperm = (tperm - pt) / 60
2006 uv(n) = rde(1, 0): time(n) = iperm
2008 IF bon < 6 THEN 2020
2014 PRINT USING " ###.#### "; iperm; rde(1, 0); rde(0, 0); rde(0, 1); rde(0, 2); rde(0, 3); rde(0, 4); rde(0, 5); rde(0,
6); rde(0, 7)
2015 t1(n) = rde(0, 0): t2(n) = rde(0, 1): t3(n) = rde(0, 2): t4(n) = rde(0, 3)
2016 t5(n) = rde(0, 4): t6(n) = rde(0, 5): t7(n) = rde(0, 6): t8(n) = rde(0, 7)
2018 IF bon > 5 THEN 2050

2020 t1(n) = rde(0, 0): t2(n) = rde(0, 3): t3(n) = rde(0, 2)
2024 t4(n) = rde(0, 3)
2028 IF n = bav THEN 2034
2030 IF n > bav + .2 THEN 2048
2032 PRINT USING "##.####  "; iperm; uv(n); t1(n); t2(n); t3(n): GOTO 2500
2034 FOR i = 5 TO n: basc1 = basc1 + t1(i)
2038 basu = basu + uv(i)
2042 basc2 = basc2 + t2(i): basc3 = basc3 + t3(i): NEXT i
2044 basc1 = basc1 / (n - 4): basc2 = basc2 / (n - 4)
2046 basc3 = basc3 / (n - 4): basu = basu / (n - 4): GOTO 2500
2048 t1(n) = t1(n) - basc1: t2(n) = t2(n) - basc2: t3(n) = t3(n) - basc3
2049 uv(n) = uv(n) - basu
2050 PRINT USING " ####.####  "; iperm; uv(n); t1(n); t2(n); t3(n)


2100 Y(1) = w2 * t2(n) + w1 * t1(n) + w3 * t3(n)
2110 Y(2) = w5 * t2(n) + w6 * t3(n) + w4 * t1(n)
2180 MY1(n) = Y(1): MY2(n) = Y(2)
2190 IF iperm > perle THEN 2600
2200 IF pd$ = "k" THEN GOSUB 4000: GOTO 2300: ' for Kalman filter process
2210 IF pd$ = "n" THEN GOSUB 7000: 'network estimation
2240 GOTO 2500
2300 EC(n) = X(9): EY1(n) = vtp1 * X(1): EY2(n) = vtp2 * X(3)
2400 PRINT USING " ##.####  "; EY1(n); EY2(n); MY1(n); MY2(n)
2500 n = n + 1
2600 RETURN

8000  ' Setting gain for pcl889
8001  IF iperm > perle THEN gain%(CH%) = 1: RETURN

8002  IF AV(CH%) = 1000 THEN gain%(CH%) = 7
8010  IF AV(CH%) = 200 THEN gain%(CH%) = 6
8020  IF AV(CH%) = 100 THEN gain%(CH%) = 5
8030  IF AV(CH%) = 50 THEN gain%(CH%) = 4
8040  IF AV(CH%) = 10 THEN gain%(CH%) = 3
8050  IF AV(CH%) = 2 THEN gain%(CH%) = 2
8060  IF AV(CH%) = 1 THEN gain%(CH%) = 1
8070  IF AV(CH%) = .5 THEN gain%(CH%) = 0
8080  RETURN

9000  'subroutine for 6-way valve control
9010  OUT port% + 11, DATC%(1)
9030  RETURN

6000 'sub after loading
6004  FOR i = 0 TO 10000
64006  NEXT i
6008  tperm = TIMER: iperm = (tperm - pt) / 60
6010  IF iperm > tsam THEN PRINT "time:"; iperm: tsam = tsam + 1
6020  RETURN
```

Program: Kalmanlog

```
2800 ' get data for the model
2820 FOR i = 1 TO 14: X(i) = 0: NEXT i

2900 ' get data for the parameters
2910 INPUT "the flow rate"; v0
2920 INPUT "do you want to update the dead volume before the bed"; vd$
2924 vd = 17
2932 IF vd$ = "y" THEN INPUT "vd"; vd
2934 start = vd / v0
2940 kh = .28: kw = .022: ke = .01
2950 INPUT " feed concentration "; c0

2960 IF selc$ = "p" THEN c0 = c0: ' NOTE this should be repkaced by c0=0

3020 w1 = .6: w2 = .12: w3 = .08: w4 = .075: w5 = .175: w6 = .75
3025 INPUT "Are the following data kh=0.28,kw=0.022,ke=0.01 right"; k$
3030 IF k$ = "y" THEN 3050
3040 INPUT "kh,kw,ke in turn"; kh, kw, ke
3050 INPUT "Are the data w1=0.6, w2=.12, w3=.08, w4=0.075,w5=.175,w6=.75 right"; R$
3055 IF R$ = "y" THEN 3060
3058 INPUT "w1, w2, w3, w4, w5, w6"; w1, w2, w3, w4, w5, w6

3060 INPUT "estimated qm"; qm: X(10) = qm
3070 INPUT "estimated k1"; k1: X(5) = k1
3080 INPUT " estimated k2"; k2
3084 kt = k2 / k1
3090 INPUT "adsorption heat"; heat

3110 INPUT "q(1--4)"; eq
3120 FOR i = 1 TO 4: q(i) = eq: p(i, i) = eq: NEXT i
3125 INPUT "q(6--9)"; eq: FOR i = 6 TO 9: q(i) = eq: p(i, i) = eq: NEXT i
3130 INPUT "q(11--14)"; eq
3135 FOR i = 11 TO 14: q(i) = eq: p(i, i) = eq: NEXT i

3145 INPUT "q(5)"; q(5): p(10, 10) = q(10): INPUT "q(10)"; q(10): p(10, 10) = q(10)
3140 INPUT "R(1,1)"; R(1, 1):  R(2, 2) = R(1, 1)

3150 vtp1 = 24: vtp2 = 24
3160 INPUT "p(5,5)"; p(5, 5)
3172 INPUT "p(10,10)"; p(10, 10)
3174 FOR i = 1 TO 2: FOR j = 1 TO 14
3176 C(i, j) = 0: NEXT j: NEXT i
3180 INPUT "Are vtp1=24,  vtp2=24 right"; vtp$
3182 IF vtp$ = "y" THEN 3200
3184 INPUT "vtp1, vtp2"; vtp1, vtp2
3190 INPUT "fix vtp"; vtp$


3200 ' data for matrix A
3210 vcdt = v0 * dt / 4.54: a1 = kh * dt / 4.18
3215 b1 = 1 - kw * dt - 2 * a1 - vcdt
3220 c1 = a1 + vcdt: d = 1 + ke / kh
3230 dtk2 = k2 * dt
3240 FOR i = 2 TO 5
3250 At(i, i - 1) = c1: At(i - 1, i) = a1: At(i - 1, i + 9) = htk2
3260 At(i, i) = b1: NEXT i: At(5, 4) = 0: At(4, 5) = 0
3270 At(1, 1) = b1 + a1 / d: At(4, 4) = b1 + a1 / d


3280 FOR i = 7 TO 9
3290 At(i, i - 1) = vcdt
3300 NEXT i

3310 At(5, 5) = 1
3330 At(10, 10) = 1
```

```
3400 C(1, 1) = vtp1:  C(2, 3) = vtp2
3410 htc1 = heat * dt / 4.18


3500 RETURN



4000 'sub for Kalman filter

4006 'up to date A(k)
4010 FOR i = 1 TO 4
4012 cq1(i) = X(i + 5) * (X(10) - X(i + 10)) * dt
4014 kq2(i) = X(5) * (X(10) - X(i + 10)) * dt
4016 NEXT i

4020 FOR i = 1 TO 4
4024 At(i, 5) = cq1(i) * heat / 4.18
4030 At(i, i + 5) = kq2(i) * heat / 4.18
4032 At(i, i + 10) = -htc1 * X(5) * X(i + 5) - htk2: 'htc1=heat*dt/4.18
4034 At(i, 10) = -At(i, i + 10) - htk2: NEXT i

4036 FOR i = 6 TO 9
4038 At(i, 5) = -cq1(i - 5)
4040 At(i, i) = 1 - vcdt - kq2(i - 5)
4042 At(i, i + 5) = dt * X(5) * X(i) + dtk2
4044 At(i, 10) = -dt * X(5) * X(i): NEXT i

4046 FOR i = 11 TO 14
4050 At(i, 5) = cq1(i - 10)
4052 At(i, i - 5) = kq2(i - 10)
4054 At(i, i) = 1 - dt * X(5) * X(i - 5) - dtk2
4055 At(i, 10) = dt * X(5) * X(i - 5)
4060 NEXT i

4070 IF vtp$ = "y" THEN 5000

4080 IF 3 + bl < n < bl + 9 GOTO 4100
4090 GOTO 4120
4100 IF ABS(vtp1 - MY1(n) / (X(1) + .000001)) < 14 THEN vtp3 = vtp3 + MY1(n) / X(1): vtn1 = vtn1 + 1
4104 IF ABS(vtp2 - MY2(n) / (X(3) + .000001)) < 14 THEN vtp4 = vtp4 + MY2(n) / X(3): vtn2 = vtn2 + 1
4110 IF vtn1 = 0 OR vtn2 = 0 THEN 5000
4120 IF n > bl + 9 THEN vtp1 = vtp3 / vtn1: vtp2 = vtp4 / vtn2
4130 C(1, 1) = vtp1: C(2, 3) = vtp2

5000 'p1(k)=Ap(k-1)At+q(k-1)

5010 FOR i = 1 TO 14: FOR j = 1 TO 14
5015 FOR s = 1 TO 14
5020 tp = tp + p(i, s) * At(j, s): NEXT s
5025 tmp(i, j) = tp: tp = 0: NEXT j: NEXT i

5030 FOR i = 1 TO 14: FOR j = 1 TO 14: 'A[p(k-1)At]+Q(k-1)
5035 FOR s = 1 TO 14
5040 tp = tp + At(i, s) * tmp(s, j): NEXT s
5045 p1(i, j) = tp: tp = 0
5050 IF j = i THEN p1(i, j) = p1(i, j) + q(i)
5055 NEXT j: NEXT i

5060 'K(k)=P1(k)Ct* inverse[CP1(k)Ct+R(k)]


5065 FOR i = 1 TO 14: FOR j = 1 TO 2
5070 FOR s = 1 TO 14
5075 tp = tp + p1(i, s) * C(j, s): NEXT s
5080 temp(i, j) = tp: tp = 0
5085 NEXT j: NEXT i
```

```
5090 FOR i = 1 TO 2: FOR j = 1 TO 2
5095 FOR s = 1 TO 14
5100 tp = tp + C(i, s) * temp(s, j): NEXT s
5105 tmp1(i, j) = tp: tp = 0: NEXT j: NEXT i
5110 tmp1(1, 1) = tmp1(1, 1) + R(1, 1): tmp1(2, 2) = tmp1(2, 2) + R(2, 2)

5215 DP = tmp1(1, 1) * tmp1(2, 2) - tmp1(1, 2) * tmp1(2, 1)
5220 tmp2(1, 2) = -tmp1(1, 2) / DP: tmp2(1, 1) = tmp1(2, 2) / DP
5225 tmp2(2, 1) = -tmp1(2, 1) / DP: tmp2(2, 2) = tmp1(1, 1) / DP

5230 FOR i = 1 TO 14: FOR j = 1 TO 2
5235 FOR s = 1 TO 2
5240 tp = tp + C(s, i) * tmp2(s, j): NEXT s
5245 tmp3(i, j) = tp: tp = 0: NEXT j: NEXT i

5250 FOR i = 1 TO 14: FOR j = 1 TO 2
5255 FOR s = 1 TO 14
5260 tp = tp + p1(i, s) * tmp3(s, j): NEXT s
5265 k(i, j) = tp: tp = 0: NEXT j: NEXT i
5268 PRINT USING "###.####  "; k(1, 1); k(1, 2); k(6, 1); k(6, 2)

5270 'Estimate X(k)=A(k)X(k-1)+K(k)[Y(k)-CAX(k-1)]

5275 FOR i = 1 TO 14: FOR s = 1 TO 14
5280 tp = tp + At(i, s) * X(s): NEXT s
5285 tX(i) = tp: tp = 0: NEXT i
5290 tX(6) = tX(6) + vcdt * c0


5295 cY(1) = Y(1) - C(1, 1) * tX(1)
5300 cY(2) = Y(2) - C(2, 3) * tX(3)

5305 FOR i = 1 TO 14
5306 X(i) = tX(i) + k(i, 1) * cY(1) + k(i, 2) * cY(2): NEXT i
5308 GOTO 5323
5311 FOR i = 6 TO 9: IF X(i) > X(i - 1) THEN X(i) = X(i - 1)
5312 GOTO 5315: IF X(i) > c0 THEN X(i) = c0: qm = .9 * qm
5314 IF X(i) < 0 THEN X(i) = 0
5315 NEXT i: GOTO 5323
5316 FOR i = 11 TO 14: IF X(i + 1) > X(i) THEN X(i + 1) = X(i): qm = .9 * qm
5317 IF X(i) < 0 THEN X(i) = 0
5318 IF X(i) > qm THEN X(i) = qm
5319 NEXT i

5323 'Up to data P(k)=P1(k)-K(k)*C(k)*P1(k)
5324 FOR j = 1 TO 14: FOR s = 1 TO 14
5325 tp1 = tp1 + C(1, s) * p1(s, j): tp2 = tp2 + C(2, s) * p1(s, j): NEXT s
5330 tmp(1, j) = tp1: tmp(2, j) = tp2: tp1 = 0: tp2 = 0: NEXT j

5335 FOR i = 1 TO 14: FOR j = 1 TO 14
5340 p(i, j) = p1(i, j) - k(i, 1) * tmp(1, j) - k(i, 2) * tmp(2, j)
5345 NEXT j: NEXT i
5400 EY1(n) = vtp1 * X(1): EY2(n) = vtp2 * X(3)

5540 PRINT USING "##.### "; X(10); X(11); X(12); X(13); X(5); X(6); X(7); X(8); X(9): PRINT
5560 PRINT "**********"
5600 RETURN

7000'net prediction
oi(1)=t2(n):oi(2)=t2(n-2):oi(4)=t2(n-4)
oi(3)=v*iperm

FOR j = 1 TO vhn
                FOR i = 1 TO vin
                        net(j) = net(j) + wh(i, j) * oi(i)
                NEXT i
                ol(j, k) = 1 / (1 + EXP(-net(j)))
```

```
        net(j) = 0
        NEXT j

        FOR j = 1 TO vhn
                netl = netl + wo(j) * ol(j, k)
NEXT j
        oo = 1 / (1 + EXP(-netl))
   c(n)=oo
return
```

Program: Neural net

```
'Neural network model thermal monitoring
'training the network using sample sets
'Version 2a.        29th May 1992
'M.y.yang    2b        10th Oct. 1992
'Modified JH 25 June


INPUT "trainning or operating"; t$
'opa for calculation otherwise training

INPUT "name the file for input the trainning data"; train$
INPUT "Drive"; dr$
train$ = dr$ + ":" + train$

INPUT "name the file for output the estimated data"; outp$
INPUT "Drive"; dro$
outp$ = dro$ + ":" + outp$

INPUT "number of the input variables"; vin: vhn = vin
'n1, n2, n3 refer to the sample set boundary
INPUT "sub sample set capacity, n1, n2, n3, n4",n1,n2,n3,n4
n2=n1+n2:n3=n2+n3:n=n3+n4

IF t$ = "opa" THEN n1 = n

INPUT "feed concentration in set1 , set 2 and 3 "; c01, c02, c03
INPUT "flow rate of set 1, 2, 3"; v01, v02, v03
INPUT " time interval"; inte1, inte2

DIM wo(vhn + 1), e(n), y(n), oo(n), oh(vhn, n), oi(vin, n), ol(vhn, n)
DIM net(vhn), netf(vhn), dth(vhn), tn(n)
DIM deo(n), dh(vhn, n), dlh(vhn, n), wh(vin, vhn)

'set the inputs regarding to the operating condition

FOR k = 1 TO n1

        oi(3, k) = v01 * k * inte1
        tn(k) = inte1 * k
NEXT k
IF t$ = "opa" THEN 80

FOR k = n1 + 1 TO n2
        oi(3, k) = v02 * (k - n1) * inte2
        tn(k) = (k - n1) * inte2
NEXT k
FOR k = n2 + 1 TO n3
        oi(3, k) = v02 * (k - n2) * inte2
        tn(k) = (k - n2) * inte2
NEXT k
FOR k = n3 + 1 TO n
        oi(3, k) = v03 * (k - n3) * inte2
        tn(k) = (k - n3) * inte2
```

```
NEXT k

'error criterion

INPUT "error sum limit"; emin
INPUT " max number of over limit"; maxnt
INPUT "error limit for each point"; tmin
INPUT "weight correct step size, mur, and mur1"; mur, mur1

86 'input thermal data to the net input layer and give the targer to the net output

80  OPEN train$ FOR INPUT AS #1

FOR i = 1 TO n
        INPUT #1, oi(1, i), y(i)
NEXT i

CLOSE #1
IF vin < 3 THEN 20
FOR i = 5 TO n
        oi(4, i) = oi(1, i - 4)
        oi(2, i) = oi(1, i - 2)
NEXT i

IF t$ = "opa" THEN 20
IF vin < 4 THEN 20
FOR k = 1 TO 4
        oi(4, k + n1) = 0: oi(4, k + n2) = 0: oi(4, k + n3) = 0
        oi(2, k + n1) = 0: oi(2, k + n2) = 0: oi(2, k + n3) = 0
NEXT k
20 ' preset weights
INPUT " have you got a file to read from"; wg$
IF wg$ = "y" THEN 30
RANDOMIZE TIMER
FOR j = 1 TO vhn: FOR i = 1 TO vin
   wh(j, i) = RND(i * j) - .5
   NEXT i
   wo(j) = RND(j) - .5
   NEXT j
GOTO 10

30 INPUT "the file is wstore"; wn$
IF wn$ < > "y" THEN wn$ = dr$ + ":tempwe": GOTO 40
wn$ = dr$ + ":" + "wstore"
40 OPEN wn$ FOR INPUT AS #10
FOR j = 1 TO vhn
        FOR i = 1 TO vin
                INPUT #10, wh(i, j)
        NEXT i
        INPUT #10, wo(j)
NEXT j


CLOSE #10
GOTO 10
5 INPUT "mur,mur1"; mur, mur1


10 '**********trainning start**********
'output of each layer

FOR k = 1 TO n
        FOR j = 1 TO vhn
                FOR i = 1 TO vin
                        net(j) = net(j) + wh(i, j) * oi(i, k)
                NEXT i
                ol(j, k) = 1 / (1 + EXP(-net(j)))
```

```
        net(j) = 0
        NEXT j
        FOR j = 1 TO vhn
                netl = netl + wo(j) * ol(j, k)
        NEXT j
        oo(k) = 1 / (1 + EXP(-netl))
        netl = 0
        e(k) = ABS(oo(k) - y(k))
        se = se + e(k)
NEXT k
IF t$ = "opa" THEN 200

100 'error test

 FOR k = 1 TO n
        IF e(k) > tmin THEN ntover = ntover + 1
NEXT k
  IF lnum = 260 GOTO 200
IF ntover > maxnt THEN 1000
IF se > emin THEN 1000
200 INPUT "go no or end"; go$
IF go$ = "go" THEN lnum = 1: GOTO 5
 ' store weights in a file
INPUT "update the weights in the file"; upw$
IF upw$ = "n" THEN wstore$ = "c:tempwe": GOTO 210
wstore$ = "c" + ":" + "wstore"
210 OPEN wstore$ FOR OUTPUT AS #2

FOR j = 1 TO vhn
        FOR i = 1 TO vin
                PRINT #2, wh(i, j)
        NEXT i
        PRINT #2, wo(j)
NEXT j
 CLOSE #2

OPEN outp$ FOR OUTPUT AS #3
 FOR k = 1 TO n
         PRINT #3, USING "###.####    "; tn(k); oo(k); y(k)
 NEXT k
 CLOSE #3


 INPUT "print the weights out"; pwe$
 IF pwe$ = "y" THEN GOSUB 300
 PRINT "************END**************"
 END

300 FOR j = 1 TO vin
LPRINT USING "###.#### "; wh(j, 1); wh(j, 2); wh(j, 3); wh(j, 4); wh(j, 5); wh(j, 6)

        PRINT
 NEXT j
FOR k = 1 TO vhn
        LPRINT USING "###.####"; wo(k);
NEXT k
 RETURN

1000 ' back propagation

FOR k = 1 TO n
'error in output layer
        deo(k) = (oo(k) - y(k)) * oo(k) * (1 - oo(k))
'error in the  hidden layer
        FOR j = 1 TO vhn
                dh(j, k) = deo(k) * wo(j) * ol(j, k) * (1 - ol(j, k))
        NEXT j
```

```
 NEXT k
'correct the weights using gradient descent algorithm

FOR k = 1 TO n
        FOR j = 1 TO vhn
                wo(j) = wo(j) - mur * deo(k) * ol(j, k)
        NEXT j
        FOR i = 1 TO vin
                FOR j = 1 TO vhn
                        wh(i, j) = wh(i, j) - mur1 * dh(j, k) * oi(i, k)
        NEXT j
        NEXT i
NEXT k

'monitoring the training procedure

PRINT
PRINT "wo,wh,o,y  "; wo(1), wo(2), wh(2, 1), se
PRINT USING "#.#### "; oo(20); y(20); oo(90); y(90); oo(120); y(120); oo(170); y(170)
PRINT USING "#.####  "; oo(210); y(210); oo(240); y(240); oo(270); y(270); oo(310); y(310)

PRINT "Iteration number"; lnum

lnum = lnum + 1

se = 0
ntover = 0

GOTO 10
```

3. Publications and Presentations of the results contained in this thesis

Publications

Yang, M., Fang Ming, Hubble, J., Lockett, A.D., Rathbone, R.R., and Howell, J. (1992) On-line thermal monitoring of aspartic acid separation in a high voidage ion-exchange column at high flow rate. *Biotechnology Techniques*, 6(5), 409-412.

Yang, M., Hubble, J., Fang Ming, Lockett, A.D., and Rathbone, R.R. (1993) A neural network for breakthrough prediction in packed bed adsorption. *Biotechnology Techniques*, 7(2), 155-158.

Yang, M., Rathbone, R.R., Hubble, J., and Lockett, A.D. (1993) In situ thermal monitoring of adsorption column performance. *Analytica Chmica Acta*. 279(1), 95-106

Yang, M., Rathbone, R.R., Lockett, A.D., and Hubble, J. (1993) Use of an Extended Kalman filter for breakthrough estimation from thermal monitoring of a packed bed adsorption process. *Bioseparation* (submitted).

Presentations

"Thermal monitoring of packed bed adsorption chromatography performance" presented (poster) at *The 1992 ChemE Research Event*, 7-8th, Jan. 1992, UMIST, UK.

"Thermal monitoring of packed bed adsorption chromatography performance using a high voidage resin at high flow rate" presented at *IEX' 92*, 12-17 July, 1992, Churchill College, Cambridge, UK.

"In situ thermal monitoring of packed bed adsorption performance" presented (poster) at *The 4th international Symposium on analytical methods, systems and strategies in Biotechnology*, 21-23 Sep. 1992, Noordwijikerhout, the Netherlands.

"A neural network application in biochemical downstream processing" presented at *Colloquium of neural network and fuzzy logic control*, 12th March, 1993, Liverpool, UK.